The Dissertation Committee for Ashwin Venkatraman
certifies that this is the approved version of the following dissertation:

Gibbs Free Energy Minimization for Flow in Porous Media

Committee:

Larry W. Lake, Supervisor

Russell T. Johns, Co-Supervisor

Kamy Sepehrnoori

Steven L. Bryant

Marc A. Hesse

Gibbs Free Energy Minimization for Flow in Porous Media

by

Ashwin Venkatraman, B. Tech., M. Tech.

DISSERTATION

Presented to the Faculty of the Graduate School of

The University of Texas at Austin

in Partial Fulfillment

of the Requirements

for the Degree of

DOCTOR OF PHILOSOPHY

THE UNIVERSITY OF TEXAS AT AUSTIN

May 2014

Maatru Devo Bhavah,

Pitru Devo Bhavah,

Aacharya Devo Bhavah.

(Salutations to Mother, Father and the Teacher)

- *Taittiriya Upanishad*, commentary on The *Vedas* by Adi Shankara.

.

.

.

I dedicate my dissertation to my late mother-in-law, Mrs. Jeyalakshmi Swaminathan, whose enthusiasm for life continues to be an inspiration.

Acknowledgments

I am grateful to my parents for insisting that I always give my best in all my endeavors. Amma, you have been a great source of inspiration for achieving goals through persistence and discipline. Appa, I have come this far because of your keen interest in my learning that set the ball rolling.

I have been extremely lucky to work and learn from my advisers Drs. Lake and Johns. Thank you for making my graduate student years the most enriching and inspiring years of my life. I have gained immensely from your wonderful insights.

I thank Dr. Lake for his constant encouragement and understanding. Thank you for always believing in me. It was a privilege to learn from you. Your coaching and approach towards research and teaching has been a big influence, one that I endeavor to emulate.

I thank Dr. Johns for his constant support and motivation. Thank you for your commitment even after moving to Pennsylvania State University. I have learnt a lot from your approach towards research.

I thank Dr. Bryant for the wonderful discussions regarding my research and beyond. Thank you for being available to discuss and sharing with me your perspectives on academics.

I thank Dr. Sepehrnoori for the kind support and warmth. I have always enjoyed talking to you. Thank you for sharing your insights.

I thank Dr. Hesse for the warm friendship. It was wonderful to share the mutual joy of analytical solutions.

I have gained from the perspectives of all my committee members that has helped shape this dissertation. Thank you all for serving on my PhD committee. I thank Dr. Roger Terzian for his help and support. I also thank Frankie Hart and Heather Felauer for all the help.

I thank ADNOC, as well as all the companies supporting the gas flooding research in UT Austin and Pennsylvania State University, for funding my research. I thank Dr. Mohanty for his support and encouragement.

I thank my Shell colleagues - Nikhil Agarwal, Mahendra Patel and Henk Vasmel for their encouragement and support. I also thank Shell India for offering me a sabbatical to pursue my PhD.

I am grateful to the libraries of Columbia University, in particular the Butler library, that provided a safe haven for me to work while in New York City.

I am thankful to all my friends for enriching my time in Austin - Amit Paranjape, Gurpreet Singh, Hariharan Ramachandran, Lokendra Jain and Rouzbeh Ghanbarnezhad with whom I shared many beers and laughs. I am thankful to Ryosuke Okuno for his initial guidance when I started as a graduate student.

I am very lucky to have some great friends who have shaped my thinking and have been a big influence in my decision to get back to academics. Abhishek Iyengar, Robert Geary, Rajendran Narayanan, SS Venkateswaran, Srinivas Iyer, Timsy Arora, Saptarshi Guha and Murali Pavithran - thank you all for the encouragement and support.

I thank my grandparents, uncles and aunts in Los Angeles, who ensured I had a home away from home. I thank my younger brother, Pravin, for his encouragement. I am grateful for the constant support and encouragement of my wife's parents - Mr. and Mrs. Swaminathan, during the course of my PhD study.

Most importantly, Neeraja, thank you for your unconditional love, patience and support. You are my biggest strength and the best thing that happened in my life.

Gibbs Free Energy Minimization for Flow in Porous Media

Publication No. _____

Ashwin Venkatraman, Ph.D.
The University of Texas at Austin, 2014

Supervisors: Larry W. Lake
Russell T. Johns

CO_2 injection in oil reservoirs provides the dual benefit of increasing oil recovery as well as sequestration. Compositional simulations using phase behavior calculations are used to model miscibility and estimate oil recovery. The injected CO_2, however, is known to react with brine. The precipitation and dissolution reactions, especially with carbonate rocks, can have undesirable consequences. The geochemical reactions can also change the mole numbers of components and impact the phase behavior of hydrocarbons.

A Gibbs free energy framework that integrates phase equilibrium computations and geochemical reactions is presented in this dissertation. This framework uses the Gibbs free energy function to unify different phase descriptions - Equation of State (EOS) for hydrocarbon components and activity coefficient model for aqueous phase components. A Gibbs free energy minimization model was developed to obtain the equilibrium composition for

a system with not just phase equilibrium (no reactions) but also phase and chemical equilibrium (with reactions). This model is adaptable to different reservoirs and can be incorporated in compositional simulators.

The Gibbs free energy model is used for two batch calculation applications. In the first application, solubility models are developed for acid gases (CO_2/H_2S) in water as well as brine at high pressures (0.1 - 80 MPa) and high temperatures (298-393 K). The solubility models are useful for formulating acid gas injection schemes to ensure continuous production from contaminated gas fields as well as for CO_2 sequestration. In the second application, the Gibbs free energy approach is used to predict the phase behavior of hydrocarbon mixtures - CO_2-n$C_{14}H_{30}$ and CH_4-CO_2. The Gibbs free energy model is also used to predict the impact of geochemical reactions on the phase behavior of these two hydrocarbon mixtures.

The Gibbs free energy model is integrated with flow using operator splitting to model an application of cation exchange reactions between aqueous phase and the solid surface. A 1-D numerical model to predict effluent concentration for a system with three cations using the Gibbs free energy minimization approach was observed to be faster than an equivalent stochiometric approach. Analytical solutions were also developed for this system using hyperbolic theory of conservation laws and are compared with experimental results available at laboratory and field scales.

Table of Contents

List of Tables

List of Figures

Chapter 1

Introduction

This chapter presents description of the research problem and lists the research objectives. The contents of each chapter are also presented to provide an overview of this dissertation.

1.1 Problem Description

CO_2 is used for enhancing oil recovery from reservoirs as it develops miscibility with oil under some circumstances. Compositional simulations use phase behavior calculations (flash and stability calculations) to model the mass transfer between the oil and the injected CO_2 to describe miscibility. The injection of CO_2 in oil reservoirs has the additional benefit of sequestration in underground storage sites, currently being investigated as a mitigation strategy for combating global warming. Hence, the injection of CO_2 in oil reservoirs provides the dual benefit of increasing recovery and sequestration.

The injected CO_2 is also known to react with brine and rock. The geochemical reaction of the fluids, especially with carbonate rocks, can have undesirable consequences. The precipitation reactions around the injection well could lead to an increase in injectivity. The dissolution of rocks could

result in leakage pathways and the opening of cemented fractures, which is undesirable for CO_2 sequestration.

Compositional simulation models must integrate phase behavior computations and geochemical reactions to completely describe such processes. The geochemical reactions change the overall mole numbers of components present in the system and hence, impact the phase behavior computations. In extreme cases, they could also change the number of phases. In this research, we present an approach to integrate reactions with phase behavior computations in compositional simulations.

The phase behavior calculations for hydrocarbon components are performed for components in hydrocarbon phases that are commonly described using an Equation of State (EOS) approach. However, the geochemical reactions between the aqueous phase components and the rock are commonly described using activity coefficient models. One of the challenges in integrating phase behavior computations and geochemical reactions is the use of different thermodynamic phase descriptions - Equation of State and activity coefficient models.

The Gibbs free energy function provides a possible way to combine different component phase descriptions and hence, integrate phase behavior calculations and geochemical reactions. The equilibrium compositions that arise out of both phase (no reactions) as well phase and chemical equilibrium (with reactions) can be obtained by minimization of the Gibbs free energy function. The results of the global minimum of the Gibbs free energy function

for the entire system corresponds to this equilibrium composition.

1.2 Research Objectives

The goal of this research is to develop a framework using the Gibbs free energy function that can integrate phase behavior and geochemical reactions. The capability of this framework to combine different phase descriptions is a distinguishing feature of this research as compared to the other available methods. The research objectives to develop this framework are :-

1. Establish, using a case study, when the Gibbs free energy approach is preferable over the stochiometric approach (the alternative approach) for batch calculations finding equilibrium compositions in a reactive system.

2. Investigate how the Gibbs free energy function can be used to combine different phase descriptions - Equation of State (EOS) models and activity coefficient models.

3. Demonstrate, using applications, how the Gibbs free energy model can be used in batch calculations to predict compositions arising of phase equilibrium (no reactions) as well as phase and chemical equilibrium (with reactions).

4. Establish whether the Gibbs free energy approach or the stochiometric approach is preferable to integrate with flow, using a 1-D case study of cation exchange reactions with three cations.

5. Develop 1-D analytical solution for the above case study of three cations with exchange reactions to compare with the numerical solution and experimental results.

1.3 Dissertation Outline

In the second chapter, a literature survey of available methods to integrate phase equilibrium and geochemical reactions is presented. This survey includes Gibbs free energy models that have been previously used in geochemistry to predict precipitation and dissolution of minerals.

In the third chapter background material from equilibrium thermodynamics, essential for this dissertation, is presented. The two approaches to obtain equilibrium composition for a system with reactive components - the Gibbs free energy approach as well as the stochiometric approach are compared using a case study of a single aqueous phase system with components typically present in a carbonate system. The Gibbs free energy approach was found to be the faster approach to find equilibrium compositions for this case study, when the same number of nonlinear equations are solved using either approache in the case study.

In the fourth chapter, details of the Gibbs free energy model are presented. This chapter lists the underlying equations and assumptions used to combine the different phase descriptions - EOS model and activity coefficient model descriptions. The equations presented in this chapter have been used to obtain equilibrium composition for applications presented in this dissertation.

The fifth chapter covers the first application of using the Gibbs free energy function to calculate the acid gas (CO_2/H_2S) solubility in pure water (phase equilibrium only) as well as brine containing ions (phase and chemical equilibrium). The model predictions are compared to available experimental values. The acid gas solubility model, shown to be accurate at high temperatures and pressures, are particularly useful for production of hydrocarbons from contaminated (hydrocarbons with CO_2/H_2S/mixture) gas fields.

The use of Gibbs free energy function to predict the influence of geochemical reactions on hydrocarbon phase behavior is presented in the sixth chapter. The phase behavior of hydrocarbon mixtures (phase equilibrium calculation only) as well as the change in phase behavior of the mixture in the presence of aqueous phase with ions (phase and chemical equilibrium) are discussed. Two hydrocarbon mixtures - CO_2-CH_4 and CH_4-CO_2-$nC_{14}H_{30}$, have been considered for this illustration as experimental values are available for these mixtures.

In the seventh chapter, a case study of 1-D flow with cation exchange reactions is used to illustrate the integration of the Gibbs free energy model with flow. A similar scheme of integration with the stochiometric approach is also presented to identify which one is faster and hence, preferable.

In the eighth chapter, analytical solutions are developed using the simple wave theory for the case of three cation exchange reactions. These solutions were developed to test the accuracy of predictions from the numerical solution obtained in the previous chapter. A comparison of analytical solutions with

available experimental data, at laboratory and field scales, is also presented in this chapter. Analytical solutions predict the first-order fronts observed during such displacements.

The conclusions from this research are presented in the ninth chapter. This chapter also includes recommendation for future work, highlighting further uses of the Gibbs free energy framework and ways to improve it.

Chapter 2

Literature Review

This chapter presents a review of previous research applicable to this dissertation and is presented in two sections.

The first section summarizes the established approaches for integrating flow, reactions and phase behavior. A review of commonly used reactive and compositional simulators are presented along with their shortcomings in coupling flow, reactions and phase behavior together. The next section reviews the Gibbs free energy minimization function to predict equilibrium compositions in previous research.

A more pertinent literature review, specific to the applications of the Gibbs free energy model discussed in this dissertation, are discussed in Chapters 5, 6 and 8.

2.1 Established Approaches in Simulators

This dissertation focusses on modeling at the continuum scale where system macroscopic properties are obtained by averaging over a macroscopic length. This is also referred to as the REV - Representative Elemental Volume (Bear, 2013) and Darcy's law is applicable at this scale. The choice of REV

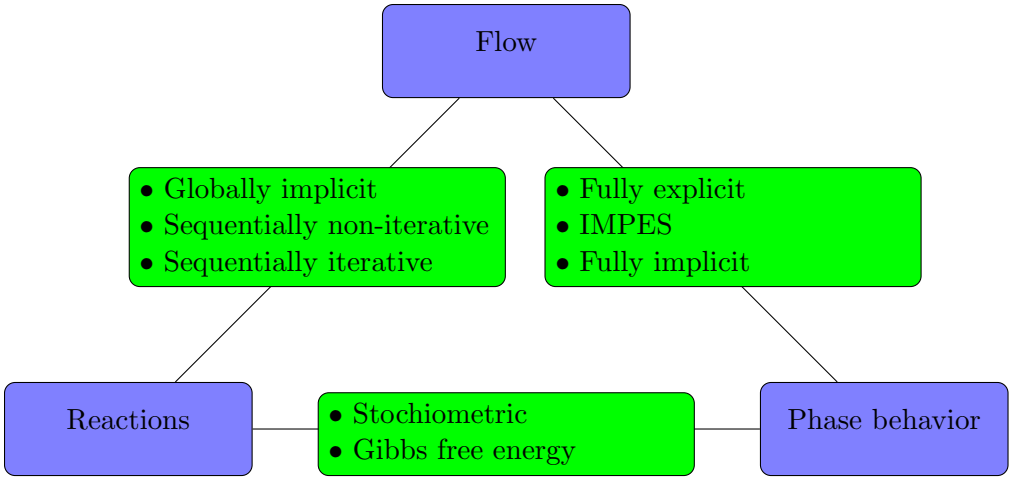

Figure 2.1: Approaches to integrate flow, reactions and phase behavior

scale, however, presents a challenge for reaction rates as these reactions occur at the pore scale and the commonly used volume averaging method for continuum models might not be applicable (Steefel et al., 2005). The upscaling of reaction rates from the pore scale to the macroscopic scale is an active research area (Li et al., 2006a, 2007). In this dissertation, we assume all reactions are at equilibrium.

Figure 2.1 gives an overview of the different approaches used to integrate any two of the three physical phenomena of flow, reaction and phase behavior computations at the REV scale. The stochiometric approach and the non-stochiometric approach, also known as the Gibbs free energy approach, are two ways of finding equilibrium compositions for a reactive system. The advantage of the Gibbs free energy approach and a case study to determine which approach is faster is presented in Chapter 3.

2.1.1 Reactive Simulators

Steefel and MacQuarrie (1996) provide a summary of commonly used approaches in reactive simulators that integrate flow and reactions. In the globally implicit approach, the flow module and reaction module are solved together as one big system implicitly. A sequential computation between the flow and the reactions module and iteration of concentration between the two modules characterizes the other two approaches. The globally implicit method has the disadvantage of having large computational times as compared to the sequential approaches. The sequential iterative approach is more accurate than the non-iterative approach.

Geochemical reactions have been included in some reactive flow simulators like *UTCHEM*, *PHREEQC*, *PFLOTRAN*, *TOUGHREACT* and *STARS*. Among these, only *STARS* has the capability to include a hydrocarbon phase in modeling.

Pope et al. (1978c) presented formulation for a chemical flooding simulator, *UTCHEM*, originally developed to calculate oil recovery. Bhuyan (1989) incorporated reactions in *UTCHEM* primarily associated with high pH chemical flooding. The model presented includes aqueous reaction chemistry, reactions between the acidic components of crude oil and the base components of surfactants injected, precipitation/dissolution of minerals as well as cation exchange reactions (Bhuyan et al., 1990). All reactions are assumed to be at equilibrium and the aqueous phase components are assumed ideal.

PHREEQC is a package for modeling geochemical reactions in the aqueous phase developed by United States Geological Survey (USGS) (Parkhust and Appelo, 2013). The geochemical package can be used to find equilibrium composition for batch calculations for systems with reactions that are kinetically controlled as well as reactions at equilibrium. The manual recommends a careful selection of aqueous species and thermodynamic data as the data in the databases lack internal consistency.

The *PFLOTRAN* code has been used to model variably saturated, nonisothermal and reactive porous media flow in one, two or three spatial dimensions. It consists of two separate modules *PFLOW* (mass and energy flow equations) and *PTRAN* (reactive transport equations) that are coupled together sequentially (Mills et al., 2007). The equations are solved implicitly within each module. The software has homogenous and heterogenous reactions between aqueous and solid phase. It covers all forms of reversible and irreversible reactions - aqueous complexing, oxidation-reduction reactions, mineral precipitation/dissolution reactions as well as adsorption. The irreversible reactions require a kinetic description while the reversible reactions use mass action equations.

PFLOTRAN code has been used for modeling CO_2 sequestration (Lu and Lichtner, 2005) using a Henry's law estimate to calculate CO_2 concentration in water and a pure CO_2 EOS (Duan et al., 1992). The Henry's law estimate is not valid at high pressures and inaccurate initial estimates can lead to error in equilibrium computations.

TOUGHREACT uses the sequential iterative approach and incorporates a gas phase in addition to the aqueous phase and solid phase (Xu et al., 2012). It also has the option of using the sequential non-iterative approach. The aqueous phase components are described using extended Debye-Huckel equation that can deal with ionic strengths from dilute to moderately saline water. The authors do not recommend using this modified model for solutions having ionization constant above four. To handle higher salinities, they implemented Pitzer's ion-interaction model. It is also capable of incorporating changes in porosity and permeability by accouting for the volume change of the fluids in the system.

In summary, the number of phases in *PHREEQC*, *PFLOTRAN* and *TOUGHREACT* are fixed (aqueous and/or gas and solid phase) and cannot include hydrocarbon phases. While *UTCHEM* does include a hydrocarbon phase, a compositional formulation is not used to describe the hydrocarbons and hence, cannot be used to describe the changes in phase behavior occuring during CO_2 injection.

Saaf (1996) has discussed the numerical approaches to integrate flow and reactions in the aqueous phase. In this study, the operator splitting approach was implemented in *PARSim1* simulator (Arbogast, 1998) and a few cases of aqueous phase components and precipitation/dissolution reactions are analyzed. The cases considered do not include hydrocarbons.

The *STARS* simulator model uses the stochiometric approach to find equilibrium composition of reactive systems. Both reversible and irreversible

reactions have been considered in the formulation. It includes a hydrocarbon phase, but the phase equilibrium is calculated by specifying partition coefficients (constant K values) in the aqueous, gas and the oil phase for each component (Computer Modeling Group, 2010).

The partition coefficient approach (constant K values) does not adequately represent the hydrocarbon phase behaviour, especially the case of phase changes accompanying CO_2 injection in oil reservoirs (Okuno et al., 2010) that are more accurately modeled using an EOS description. This is a considerable limitation to model phase and chemical equilibrium in *STARS*.

2.1.2 Compositional Simulators

Compositional simulators integrate flow and phase behavior computations. The fully implicit approach of finding the solution for the pressure and the saturation equations have better accuracy than the fully explicit approach. In the IMPES (Implicit Pressure Explicit Saturation) approach, the pressure equation is solved implicity while the saturation equation is explicit. The IMPES approach is capable of describing the phase changes accompanying CO_2 injection (Chang et al., 1990; Okuno, 2011). The inhouse simulator *UTCOMP* is based on the IMPES formulation (Chang, 1990). Efforts are underway to integrate *PHREEQC* in *UTCOMP* (Kazemi Nia Korrani et al., 2013, 2014).

Nghiem et al. (2010) have also incorporated geochemical reactions in their compositional simulator CMG calling it CMG-GHG . In this formulation, the aqueous phase chemical reactions are assumed fast and hence, at chemical

equilibrium while the mineral reactions (between aqueous ions and solid) are assumed to be slow and rate-dependent. The CO_2 concentration distribution between the aqueous and the gas phase is determined using the Henry's law coefficient with salinity correction using Soriede and Whitson correlation (Soreide and Whitson, 1992). There is no attempt to reconcile the concentration of CO_2 as a result of the aqueous reactions for every gridblock.

Besides, the Soriede and Whitson correlation is valid and useful only at low salinity solutions. For high salinity cases, the CO_2 concentration cannot be determined by Henry's law as this separation of the phase equilibrium from the chemical equilibrium problem (that includes aqeuous phase reactions) is not accurate. CMG-GHG simulator also does not provide for cases where the number of hydrocarbon phases may change.

Fan (2010) implemented reaction modeling in Stanford's compositional simulator *GPRS* (General Purpose Reservoir Simulator). A unified globally implicit approach (GIA) method was implemented with reactions within a EOS compositional simulation framework. The reaction and transport equations are solved simultaneously in the GIA approach. A conservation equation using elements was developed to take advantage of the fact that no reaction terms appear in elemental balance.

The two applications (Fan, 2010) do not consider hydrocarbon phases and geochemical reactions simultaneously. The first one which models the reactive mechanism during the in-situ upgrading of oil shales does not include aqueous phase (reactions occur at temperatures above the boiling point of wa-

ter and no aqueous phase is formed). Similary, the other application discussed on the CO_2 storage in saline aquifers excludes the presence of hydrocarbon phase. The GIA approach is expected to be computationally intensive.

The Implicit Parallel Accurate Reservoir Simulator (*IPARS*) developed at The University of Texas at Austin (Center for Subsurface Modeling, 2000) has the capability to model multiple phases and components. A reaction module *TRCHEM* is integrated with the *IPARS* framework (Peszynska and Sun, 2001) and has the capability to model mineral, adsorption and radionuclide decay reactions. These reactions could either be at equilibrium or governed by kinetic rate laws. The concentrations from pure equilibrium controlled reactions are obtained by using the interior point algorithm to minimize the Gibbs free energy.

However, the mass transfer between the flowing phases are modeled using linear and constant partitioning coefficients (constant K values). The use of partition coefficients do not adequately represent the phase behavior of hydrocarbons as more phases may be present during CO_2 injection in oil reservoirs (Okuno, 2011).

In summary, there is a need to develop a framework that can couple flow, phase behavior and reactions. A framework using the Gibbs free energy function is presented in this dissertation to accurately model flow, phase behavior and reactions. The Gibbs free energy approach used for prediction of equilibrium compositions is discussed in the next section.

2.2 Gibbs Free Energy Minimization Procedure

The Gibbs free energy minimization approach to determine compositions for purely phase (no reactions) as well as phase and chemical equilibrium problems (reacting components) is extensively used for chemical engineering applications like distillation and chemical separation. It is also used to model geochemical reactions. An overview of the important developments in this approach for different applications is presented in this section.

White et al. (1958) developed the RAND algorithm to predict equilibrium concentrations using Newton's method for minimizing the Gibbs free energy function. The system considered was a reactive set of ideal species in a single phase but it was later extended for nonideal systems and to include pure solid, multicomponent solid as well as multicomponent liquid phases (all ideal species).

While the Gibbs free energy function is convex for ideal species in a single phase, convexity need not hold for multiphase systems or even species where nonideality is considered in the form of activity coefficient models (Smith and Missen, 1982b). Hence, the problem in case of multiphase multicomponent system becomes increasingly difficult as the number of phases and the component distribution, in those phases, at equilibrium are unknown.

One approach suggested by researchers is a step-by-step approach of increasing phases and checking if the Gibbs free energy of the system decreases. This methodology of equilibrium computation has been used effec-

tively for problems in reactive distillation and hydrocarbon phase computations in reservoir engineering. This method is also used in geochemical reaction modeling where algorithms does not presume the presence of all components in all phases.

2.2.1 Reactive Distillation

Gautam and Seider (1979a) proposed the phase splitting algorithm to predict equilibrium composition for multicomponent species in multiple phases. This algorithm begins by assuming all components to be present in a single phase and increases phases to check if the Gibbs free energy of the entire system decreases. The addition of phases is continued as long as the Gibbs free energy of the sytem decreases. For cases illustrated in the original paper, this step-by-step approach of increasing phases to find the minimum of Gibbs free energy works well even with poor initial guesses. The presence of many phases at equilibrium drastically increases the computational time.

An alternative to the step-by-step approach is the global minimization approach. Mcdonald and Floudas (1994) presented a global optimization algorithm for liquid components represented using NRTL (even UNIQUAC) and ideal vapor phase components. The overall function was converted into convex sub-problems using transformed variables instead of mole numbers. This approach of partitioning and use of a transformation was developed in the context of only phase equilibrium (no reactions) and has not yet been developed for vapor components defined using EOS. The advances in global optimiza-

tion techniques are useful for finding equilibrium composition, especially for reservoir fluids with changing phases during CO_2 injection in oil reservoirs.

Smith et al. (1993a) proposed the most general criteria for finding equilibrium composition in a multiphase multicomponent system (with each phase containing one or all components). The authors formulate the problem of finding equilibrium composition as one of minimizing the Gibbs free energy of the system with equality (elemental balance) and non-equality constraints (positive mole numbers). The first order necessary conditions for the general form of the equilibrium problem is used to find the KKT points and further derive two new criteria for global optimality. Though the authors indicate their intention of working to develop an algorithm for this global optimality, there have been no further publication from this group.

2.2.2 Reservoir Engineering

In compositional simulation, a step-by-step approach similar to the approach presented in Gautam and Seider (1979a) is used for phase stability calculations. Baker et al. (1982) formulated the tangent plane distance function to separate local and global minima of the Gibbs free energy function. The tangent plane distance function is the distance between the tangent plane, at any extremum point (any identified minimum) in the Gibbs free energy function, and the Gibbs free energy function value of the entire phase at any other feasible point. This distance function is never negative in the composition space if the tangent is constructed at the global minima.

Michelsen (1982) proposed a numerical implementation scheme to compute the tangent plane distance function and use it for phase stability calculations. The central idea is to obtain all stationary points of this tangent plane distance function, a negative value implying an unstable phase and the need to add another phase. A flash algorithm determines the new phase compositions and the stability algorithm is repeated using new composition values in either phase. The disadvantage of this method is that all stationary points of the tangent plane distance function cannot be obtained using this approach. Michelsen suggests using different guesses as starting points to ensure all stationary points are obtained.

Trangenstein (1987) also developed a minimization procedure using the Gibbs free energy function for both flash and stability analysis using the tangent plane distance function. The numerical algorithm proposed was particularly useful for phase behavior calculations near the critical points. Thus, the algorithm provides an advantage over the successive substitution methods (Prausnitz and Chueh, 1968), more commonly used for flash calculations, which can be slow close to critical points.

Wasylkiewicz et al. (1996) used concepts from topology to track the ridges and valleys of the tangent plane distance function to determine the total number of stationary points of the tangent plane distance function. Jalali and Seader (1999) proposed linear homotopy functions to find stationary points of the tangent plane distance function. The use of activity coefficient models for components further increases this nonlinearity (Jalali et al., 2008). These

homotopy functions provide a smooth transition between a linear approximation to a solution and the true solution. Sun and Seider (1995) showed that the Newton-homotopy-continuation method reliably determines multiple stationary points of tangent plane distance function.

2.2.3 Geochemistry

Harvie et al. (1987a,b) use Lagrange multipliers to convert the constrained minimization of Gibbs free energy function to an unconstrained optimization problem. The approach predicts equilibrium composition for the case of aqueous phase with mineralization reactions (Harvie and Weare, 1980; Harvie et al., 1982; Spencer et al., 1990; Møller et al., 1998).

Newton's method is used to find the descent direction to reduce the Gibbs free energy function in this approach. The addition of solid phase (arising out of precipitation) is formulated as a separate optimization problem. The conditions for global minimum of the Gibbs free energy function of the system are established for this system.

2.3 Conclusions

The existing compositional and reactive flow simulators cannot accurately model the coupling of flow with reactions as well as hydrocarbon phase behavior associated with CO_2 injection in carbonate reservoirs. The Gibbs free energy framework is a potential approach to model these processes. The background theory for this framework is presented in chapter 3. The Gibbs free

energy model that integrates different phases descriptions - EOS and activity coefficient models is presented in chapter 4.

The global optimization techniques show promise in obtaining equilibrium composition. However, owing to the large number of phases and components associated with coupling of phase behavior computations and geochemical reactions, these computations may get cumbersome.

A step-by-step approach of increasing the number of phases sequentially, to find the global minimum of the Gibbs free energy function of the entire system, has been used to compute equilibrium composition for all examples presented in this dissertation. A Newton's method is used to find the minimum of the Gibbs free energy function. The minimization method and the constraints used are further discussed for acid gas solubility applications (chapter 5) and hydrocarbon phase behavior applications (chapter 6).

Chapter 3

Geochemical Reaction Modeling

This chapter presents background material from equilibrium thermodynamics drawn from some excellent texts in the area (Sandler, 2006; Denbigh, 1966; Nordstorm and Munoz, 1986; Prausnitz et al., 1998; Garrels and Christ, 1990).

Equilibrium criteria are derived for both closed and open systems and its implication on the Gibbs free energy function is discussed. A case study is presented to highlight the difference between the two approaches (stochiometric and Gibbs free energy minimization) used for obtaining the equilibrium composition for a system with geochemical reactions and determine which approach is faster.

3.1 Equilibrium

All isolated systems, left for adequate time, tend towards a state of equilibrium. Equilibrium systems represent simplification but provide insights into the properties of the system. The criteria for equilibrium are presented in this section. The Gibbs free energy function is introduced and the implication of equilibrium on the Gibbs free energy function is presented.

3.1.1 Multicomponent Systems

The thermodynamic properties for a single component is given in terms of the molar property of the component ($\underline{\theta}$) where the molar property $\underline{\theta} = \theta/N$ and N is the total number of moles. The relation for total internal energy U, volume V as well as entropy S for a single component system can be given as,

$$U = N\underline{U} \quad ; \quad V = N\underline{V} \quad ; \quad S = N\underline{S}. \tag{3.1}$$

The partial molar property $\bar{\theta}_i$ of any thermodynamic variable θ for a component i, in a multicomponent system, is the conditional change in the total system molar property ($\underline{\theta}$) when moles of that component, N_i, are varied while the temperature (T), pressure (P) and other other component moles numbers ($N_{j\neq i}$) are kept constant. The partial molar property for a multicomponent system with N_c components is a derivative of the total molar property and can be written as,

$$\bar{\theta}_i = \left[\frac{\partial(N\underline{\theta})}{\partial N_i}\right]_{T,P,N_{j\neq i}} \qquad \text{where} \qquad N = \sum_{i=1}^{N_c} N_i. \tag{3.2}$$

The thermodynamic properties such as internal energy U, volume V as well as entropy S for such a multicomponent system can also be expressed in terms of their respective component partial molar properties. These relationships are given as,

$$U = \sum_{i=1}^{N_c} N_i\bar{U}_i \quad ; \quad V = \sum_{i=1}^{N_c} N_i\bar{V}_i \quad ; \quad S = \sum_{i=1}^{N_c} N_i\bar{S}_i. \tag{3.3}$$

Eqns 3.3 and 3.1 can be appropriately used to analyze equilibrium as shown in the following sections and are equally applicable to multicomponent and single component systems if P and T are constants.

3.1.2 Entropy and Equilibrium

The mass and energy balance equations, by themselves, do not account for the experimental observation of all systems moving towards equilibrium. This sense of direction is provided by the second law of thermodynamics with the additional thermodynamic variable of entropy.

Clausius (1867) defined entropy as the sum of the *transformation-value* of the heat present in the body and *disgregation*, the exisiting arrangement of particles of the body. He referred to entropy as the *transformational content* of the current state of a system.

The entropy for a system, S_{sys}, at absolute temperature T and with heat content, Q, is given as,

$$S_{sys} = \int \frac{dQ}{T} \tag{3.4}$$

The entropy balance (second law of thermodynamics) for an open system exchanging heat and mass with the surroundings can be written as,

$$\frac{dS}{dt} = \frac{\dot{Q}}{T} + \sum_{i=1}^{N_c} F_i \underline{S}_i + \dot{S}_{gen}. \tag{3.5}$$

Here, S is the entropy of the system, $\dot{Q}$ is the rate of heat exchanged between the system and the surroundings, T is the absolute temperature, $\underline{S}_i$ is the

molar entropy of component i with molar flow rate F_i and $\dot{S}_{gen}$ is the internal rate of entropy generation in the system.

At equilibrium, entropy S is time invariant ($dS/dt = 0$) and for a closed system, $F_k = 0$. Hence, eq 3.5 can be written as,

$$\frac{\dot{Q}}{T} + \dot{S}_{gen} = 0. \tag{3.6}$$

Eq 3.6 incorporates the sense of direction towards equilibrium for natural processes. An axiomatic definition of entropy generation $\dot{S}_{gen}$, being always positive (except zero at equilibrium), can be used to establish the direction of heat flow between the system and the surroundings during thermal equilibrium (Sandler, 2006). Alternatively, the experimental observation of heat flow from bodies with higher degree of "hotness" to lower degrees for thermal equilibrium, can help establish a positive entropy generation $\dot{S}_{gen}$ (Denbigh, 1966). The second law, thus, helps establish how natural processes, left to themselves, are directed towards equilibrium.

The first law and the second law, together, can help make inferences regarding the nature of the Gibbs free energy function at equilibrium.

3.1.3 Open System

An open system is a system capable of exchanging heat and mass from the surroundings. The energy balance equation for an open multicomponent system at constant temperature and pressure can be given as,

$$\frac{dU}{dt} = \sum_{i=1}^{N_c} F_i \bar{H}_i + \dot{Q} - P\frac{dV}{dt} + \frac{dW_s}{dt}; \tag{3.7}$$

Here, $\bar{H}_i$ is the partial molar enthalpy of component i with molar flow rate F_i, $\dot{Q}$ is the rate of heat exchanged between the system and the surroundings while W_s is the shaft work. The entropy balance equation for this system at constant temperature T with entropy generation S_{gen} can be given as,

$$\frac{dS}{dt} = \sum_{i=1}^{N_c} F_i \bar{S}_i + \frac{\dot{Q}}{T} + \dot{S}_{gen}. \tag{3.8}$$

The partial molar quantities, $\bar{H}_i$ and $\bar{S}_i$, are used as P and T are constants. The shaft work is neglected ($W_s = 0$) and the process is assumed reversible ($\dot{S}_{gen} = 0$). Eqns 3.7 and 3.8 can then be simplified and written over a time interval dt to get,

$$dU = TdS - PdV + \sum_{i=1}^{N_c} (\bar{H}_i - T\bar{S}_i) dN_i \tag{3.9}$$

The Gibbs free energy (G) is defined as $G = H - TS$. At constant temperature and pressure, $\bar{G}_i$ is the partial molar Gibbs free energy of component i defined analogous to the definitions in eq 3.2 so that $\bar{G}_i = \bar{H}_i - T\bar{S}_i$. Also, dN_i is the moles of component given by $dN_i = F_i dt$. Eq 3.9 can be written as,

$$dU = TdS - PdV + \sum_{i=1}^{N_c} \bar{G}_i dN_i. \tag{3.10}$$

It can be inferred from eq 3.10 that entropy (S), volume (V) and mole numbers (N) are the independent variables of the total internal energy U for an open system at constant temperature and pressure. Also, the change in internal energy in terms of the independent variables can be given as,

$$dU = \left(\frac{\partial U}{\partial S}\right)_{V,N_i} dS + \left(\frac{\partial U}{\partial V}\right)_{S,N_i} dV + \sum_{i=1}^{N_c} \left(\frac{\partial U}{\partial N_i}\right)_{V,S,N_{j\neq i}} dN_i. \tag{3.11}$$

Using eqns 3.10 and 3.11,

$$\left(\frac{\partial U}{\partial S}\right)_{V,N_i} = T; \qquad \left(\frac{\partial U}{\partial V}\right)_{S,N_i} = -P \qquad \left(\frac{\partial U}{\partial N_i}\right)_{V,S,N_{j\neq i}} = \bar{G}_i. \tag{3.12}$$

The applications discussed in this dissertation are to closed systems with multiple components distributed in different phases. The internal energy of such a multicomponent closed system attaining equilibrium is also a function of these independent variables. The equilibrium analysis for closed systems and the implications on the Gibbs free energy is discussed in the next section.

3.1.4 Closed System

The energy balance equation from the first law of thermodynamics for a closed multicomponent system at constant temperature and pressure is,

$$\frac{dU}{dt} = \frac{dQ}{dt} - P\frac{dV}{dt} = \dot{Q} - \frac{d}{dt}(PV). \tag{3.13}$$

Here, P is the pressure and $\dot{Q}$ is the rate of heat exchanged between the system and the surroundings. A convention of a positive value for heat transferred from the surroundings to the system is used. Also, U and V are the total internal energy and total volume of the multicomponent system respectively, as defined in eq 3.3. The entropy balance for this system can be given as,

$$\frac{dS}{dt} = \frac{\dot{Q}}{T} + \dot{S}_{gen}. \tag{3.14}$$

Using eqns 3.13 and 3.14,

$$\frac{dU}{dt} + \frac{d}{dt}(PV) - \frac{d}{dt}(TS) = \frac{dG}{dt} = -T\dot{S}_{gen} \leq 0. \tag{3.15}$$

In eq 3.15, T is the absolute temperature, always positive. There are two inferences that can be drawn from the axiomatic definition of entropy generation and eq 3.15.

1. Because $\dot{S}_{gen}>0$, the Gibbs free energy, defined as $G = U + PV - TS$, decreases with time ($dG/dt<0$) for all physical processes. This implies that any spontaneous change in a system must be accompanied by a decrease in the Gibbs free energy of the system, making it a decreasing function with time.

2. At equilibrium $\dot{S}_{gen} = 0$, so that $dG/dt = 0$. This implies that the decreasing Gibbs free energy function of the entire system attains its minimum at equilibrium. Thus, the minimum of the Gibbs free energy function of the entire system is the equilibrium criterion for a multicomponent system at constant temperature and pressure in a closed system.

The definitions of molar and partial molar properties (in eqns 3.1 and 3.3) make the two inferences equally applicable to both single component and multicomponent systems.

3.1.5 Equilibrium Criteria

Gibbs (1877) introduced the notion of a free energy in his seminal work on the theory of equilibrium of heterogeneous substances. He introduced the chemical potential, subsequently called the partial molar Gibbs free energy, $\bar{G}$, thus -

"If any homogenous mass we suppose an infinitesimal quantity of any substance to be added, the mass remaining homogenous and its entropy and volume remaining unchanged, the increase of the energy of the mass divided by the quantity of the substance added is the *potential* for that substance in the mass considered." This definition can be written as,

$$\bar{G}_i = \left(\frac{\partial U}{\partial N_i}\right)_{S,V,N_{j\neq i}}. \tag{3.16}$$

The introduction of chemical potential makes the above analysis for open systems (eq 3.9) also applicable for closed systems with varying composition. A multicomponent and multiphase system in the process of attaining equilibrium at constant temperature and pressure is one such example of a closed system with varying composition.

The total Gibbs free energy of a multicomponent and a multiphase system at constant temperature and pressure is a sum of the Gibbs free energy of all components in all the phases. The internal energy for closed system is also a function of the three independent variables - entropy S, volume V and moles of component N_i like the open system.

Using eqns 3.10 and 3.16 and rearranging for a multicomponent (N_c) multiphase (N_p) system,

$$dS = \sum_{j=1}^{N_p} \frac{1}{T_j} dU_j + \sum_{j=1}^{N_p} \frac{P_j}{T_j} dV_j - \sum_{j=1}^{N_p} \sum_{i=1}^{N_c} \bar{G}_{ij} dN_{ij}. \tag{3.17}$$

Here, T_j and P_j are the temperature and pressure of each phase j, while $\bar{G}_{ij}$ is the partial molar Gibbs free energy of component i in phase j. However, for a

closed multicomponent multiphase system with no reacting components, the total number of moles of any component i is a constant. This implies,

$$\sum_{j=1}^{N_p} dN_{ij} = 0 \quad \Longrightarrow \; dN_{iN_p} = -\sum_{j=1}^{N_p-1} dN_{ij} \quad \forall \quad i = 1, 2, \ldots, N_c. \tag{3.18}$$

As the entire system is closed, there are no changes in internal energy and volume of the system. This results in,

$$dU_{N_p} = -\sum_{j=1}^{N_p-1} dU_j \qquad ; \qquad dV_{N_p} = -\sum_{j=1}^{N_p-1} dV_j. \tag{3.19}$$

The total change in entropy for a multicomponent multiphase system can be given as,

$$dS = \sum_{j=1}^{N_p-1} \left(\frac{1}{T_j} - \frac{1}{T_{N_p}} \right) dU_j + \sum_{j=1}^{N_p-1} \left(\frac{P_j}{T_j} - \frac{P_{N_p}}{T_{N_p}} \right) dV_j + \sum_{j=1}^{N_p-1} \sum_{i=1}^{N_c} (\bar{G}_{ij} - \bar{G}_{iN_p}) dN_{ij} \tag{3.20}$$

At equilibrium, the entropy attains a maximum in a closed system at constant internal energy U and volume V. The variables - U_j, T_j and N_{ij} are independent (section 3.1.3) and hence, variation of entropy with respect to all independent variables is zero. This leads to the following conditions for a multicomponent multiphase system at equilbirium,

$$T_j = T_{N_p} \qquad ; \qquad P_j = P_{N_p} \qquad \forall \qquad j = 1, 2, \ldots, N_p - 1. \tag{3.21}$$

$$\bar{G}_{i1} = \bar{G}_{i2} = \ldots = \bar{G}_{iN_p} \qquad \forall \qquad i = 1, 2, \ldots, N_c \tag{3.22}$$

The equality of chemical potentials (eq 3.22) is a necessary, but not a sufficient condition for equilibrium. If the fluid phases are confined in narrow pores, the

equality of pressure between phases does not hold. The difference in pressure between phases is referred to as capillary pressures.

A more direct way to arrive at the equality of chemical potentials is by using the expression for change in the Gibbs free energy of the system. Eq 3.9 can rearranged for a multicomponent multiphase system using the definition of Gibbs free energy ($G = U + PV - TS$) to obtain,

$$dG = VdP - SdT + \sum_{j=1}^{N_p} \sum_{i=1}^{N_c} \bar{G}_{ij} dN_{ij} \tag{3.23}$$

The change in Gibbs free energy of the entire system at constant temperature and pressure can be written as,

$$dG|_{T,P} = \sum_{j=1}^{N_p} \sum_{i=1}^{N_c} \bar{G}_{ij} dN_{ij}. \tag{3.24}$$

As the total number of moles of component i remains constant, eq 3.18 holds. The change in Gibbs free energy of the system can then be given as,

$$dG = \sum_{i=1}^{N_c} \sum_{j=1}^{N_p-1} (\bar{G}_{ij} - \bar{G}_{iN_p}) dN_{ij} = \sum_{i=1}^{N_c} \sum_{j=1}^{N_p} (\bar{G}_{ij} - \bar{G}_{iN_p}) dN_{ij} \tag{3.25}$$

Because the Gibbs free energy function of the system attains a minimum at equilibrium, the change in total Gibbs free energy with respect to independent variables is zero ($dG/dN_{ij} = 0$). This also leads equality of chemical potential of components in all phases (eq 3.22) at equilibrium.

In summary, the temperature and pressure of all phases are equal at equilibrium. The components in a system are distributed among phases so

that the total Gibbs free energy function attains its global minimum at equilibrium. As a consequence, the partial molar Gibbs free energy $\bar{G}$ (also called the chemical potential) of components are equal in each of the phases they are distributed.

3.1.6 Stability Analysis

The phase equilibrium computations by equating chemical potentials in hydrocarbon systems with multiple phases is always followed by stability analysis calculations to identify the global minimum from the extremum (also called stationary states) of the total Gibbs free energy. As the Gibbs free energy function can have multiple minima, the solutions obtained by equating chemical potentials might be any stationary point (local minima, local maxima or saddle point) and not the global minimum (equilibrium composition).

Thus, the equality of chemical potentials of any component in all phase j, $\bar{G}_{ij}$, is a necessary, but not a sufficient condition to find equilibrium composition of a multicomponent and multiphase system. This is especially relevant in cases of CO_2 injection in hydrocarbon reservoirs where miscibility is induced by changing the number of hydrocarbon phases (Okuno, 2011).

Baker et al. (1982) formulated the tangent plane distance criteria using the Gibbs free energy function to identify the global minimum from the stationary points. The Gibbs free energy function of any phase j, G_j, is the

sum of the Gibbs free energy of all components in that phase and is given as,

$$G_j(\mathbf{n}_j) = \sum_{i=1}^{N_c} n_{ij}\bar{G}_{ij}(\mathbf{n}_j) \quad \forall\, j = 1, 2, \ldots, N_p. \tag{3.26}$$

Here, n_{ij} are components of $\mathbf{n}_j = [n_{1j}, n_{2j}, \ldots, n_{N_c j}]$ and are the feasible composition of components (mole numbers) in phase j that satisfy the mass balance and obtained by equating flash calculation. The equation of a tangent plane, $L_j(\mathbf{x})$ at the point $\mathbf{n}_j$ on the Gibbs free energy function G_j can be given as,

$$L_j(\mathbf{x}) = G_j(\mathbf{n}_j) + \sum_{i=1}^{N_c}[x_i - n_{ij}] \left[\frac{\partial G_j}{\partial x_i}\right]_{\mathbf{x}=\mathbf{n}_j} = G_j(\mathbf{n}_j) + \sum_{i=1}^{N_c}[x_i - n_{ij}]\bar{G}_{ij}(\mathbf{n}_j). \tag{3.27}$$

Using eq 3.26,

$$L_j(\mathbf{x}) = \sum_{i=1}^{N_c} n_{ij}\bar{G}_{ij}(\mathbf{n}_j) + \sum_{i=1}^{N_c}[x_i - n_{ij}]\bar{G}_{ij}(\mathbf{n}_j) = \sum_{i=1}^{N_c} x_i\bar{G}_{ij}(\mathbf{n}_j). \tag{3.28}$$

The chemical potentials of components, $\bar{G}_{ij}$, are equal in all phases at all extrema (local minima, local maxima and saddle point) of the Gibbs free energy function of the system (eq 3.22). Thus, if all components are present in all phases, the tangent plane is the same for all the individual Gibbs free energy of different phases ($L_1 = L_2 = \ldots = L_{N_p}$). However, when all components are not present in all phases, the tangent plane equation shall be different and this is further discussed in section 4.4.

The tangent plane distance (D) at any point $\mathbf{z}_j$ is the distance between the tangent plane, drawn at point $\mathbf{n}_j$ on the Gibbs free energy surface (G_j) and extended to point $\mathbf{z}_j$, and the Gibbs free energy value at point $\mathbf{z}_j$, $G_j(\mathbf{z}_j)$.

This can be given as,

$$D(\mathbf{z}_j) = G_j(\mathbf{z}_j) - L_j(\mathbf{z}_j) = G_j(\mathbf{z}_j) - \sum_{i=1}^{N_c} z_i \bar{G}_{ij}(\mathbf{n}_j). \tag{3.29}$$

If $D \geq 0$ for all possible values of $\mathbf{z}_j$, the Gibbs free energy function is always above the tangent plane and the phase j with composition $\mathbf{n}_j$ is stable.

In reservoir simulation, as all components are present in all phases, and all phases are typically described using the Peng-Robinson EOS, the stability of one phase implies the stability of all other phases. Starting with a single phase, the stability of phases can be established by using D. If the minimum is negative, the phase is not stable. An additional phase is accounted in the new flash calculations and the stability test is repeated with the new composition until a nonnegative minimum value for D is obtained.

The tangent plane distance $D(\mathbf{z}_j)$ also helps identify the global minima from other stationary points. Let $\mathbf{n}$ and $\mathbf{m}$ be any two stationary points, each with N_p and $N_{p'}$ phases respectively. Here, $N_{p'} \geq 1$ and can be any number of phases. Also, let $\mathbf{n}_j = [n_{1j}, n_{2j}, \ldots, n_{N_c j}]$ and $\mathbf{m}_j = [m_{1j}, m_{2j}, \ldots, m_{N_c j}]$ represent the mole numbers of components in phase j. The mass balance equation for each component i results in,

$$\sum_{j=1}^{N_p} n_{ij} = \sum_{j=1}^{N_{p'}} m_{ij} = n_i \quad \forall\, i = 1, 2, \ldots, N_c. \tag{3.30}$$

The total Gibbs free energy of the system G^T, using the fact that chemical potentials are equal in all phases and eq 3.30, can be given as,

$$G^T(\mathbf{n}) = \sum_{j=1}^{N_p} G_j(\mathbf{n}_j) = \sum_{i=1}^{N_c} \sum_{j=1}^{N_p} n_{ij} \bar{G}_{ij}(\mathbf{n}_j) = \sum_{i=1}^{N_c} \sum_{j=1}^{N_{p'}} m_{ij} \bar{G}_{ij}(\mathbf{n}_j). \tag{3.31}$$

Using eq 3.28,

$$G^T(\mathbf{n}) = \sum_{j=1}^{N_{p'}} L_j(\mathbf{m}_j). \tag{3.32}$$

The difference in total Gibbs free energy of the system, ΔG between the two states can be given as,

$$\begin{aligned} \Delta G &= G^T(\mathbf{m}) - G^T(\mathbf{n}) & (3.33) \\ &= \sum_{j=1}^{N_{p'}} G_j(\mathbf{m}_j) - \sum_{j=1}^{N_{p'}} L_j(\mathbf{m}_j) = \sum_{j=1}^{N_{p'}} D(\mathbf{m}_j). & (3.34) \end{aligned}$$

Thus, if $D(\mathbf{m_j}) \geq 0$ for all phases $j = 1, 2, \ldots, N_{p'}$, the difference in Gibbs free energy is positive. This implies $G^T(\mathbf{n}) \leq G^T(\mathbf{m})$. If this relationship holds for all stationary points like $\mathbf{m}$, the composition $\mathbf{n}$ is the global minimum of the Gibbs free energy function and hence, the equilibrium composition.

Michelsen (1982) recast the tangent plane distance criteria in terms of fugacity that is easier for EOS phase description and proposed a numerical implementation for stability analysis. The stationary points of the tangent plane distance function are obtained and the phase is stable if all the minimums are nonnegative.

The difference in Gibbs free energy between any two states in eq 3.33 has been shown to be the sum of tangent plane distance functions in all phases. Using the equality of chemical potential of component in each phase and eq

3.30 results in,

$$\begin{aligned}\Delta G = G^T(\mathbf{m}) - G^T(\mathbf{n}) &= \sum_{i=1}^{N_c}\left[\sum_{j=1}^{N_{p'}} m_{ij}\bar{G}_{ij}(\mathbf{m}) - \sum_{j=1}^{N_p} n_{ij}\bar{G}_{ij}(\mathbf{n}_j)\right] \\ &= \sum_{i=1}^{N_c} n_i[\bar{G}_{ij}(\mathbf{m}) - \bar{G}_{ij}(\mathbf{n})]. \end{aligned} \tag{3.35}$$

Multiplying $1/RT$ in eq 3.35,

$$\Delta F = \Delta G/RT = \sum_{i=1}^{N_c} n_i(lny_i + ln\phi_i - h_i) \tag{3.36}$$

where,

$$y_i = \frac{m_i}{\sum_{i=1}^{N_c} m_i} \quad \phi_i = \phi(\mathbf{m}) \quad \& \quad h_i = ln\left(\frac{n_i}{\sum_{i=1}^{N_c} n_i}\right) + ln\phi_i(\mathbf{n}) \tag{3.37}$$

The nonlinear equations obtained by setting $\partial\Delta F/\partial n_i = 0$,

$$lny_i + ln\phi_i - h_i = k \quad i = 1, 2, \ldots, N_c. \tag{3.38}$$

The stationary points are obtained by solving this set of nonlinear equations. A new variable $Y_i = y_i e^{(-k)}$ is defined so that eq 3.38 is,

$$lnY_i + ln\phi_i - h_i = 0 \quad i = 1, 2, \ldots, N_c. \tag{3.39}$$

The phase is stable if the sum of the variables Y_i is less than or equal to one and unstable otherwise (Michelsen, 1982).

Smith and Missen (1982b) have shown that the problem of finding equilibrium composition for a multicomponent single phase ideal system has a unique solution. They proved uniqueness by showing that the Hessian matrix

of the Gibbs free energy function, for an ideal single phase multicomponent system, is always positive. We use this result to find equilibrium composition using the Gibbs free energy minimization approach for the case study described in the next section.

3.2 Reactive System

The general criteria for equilibrium, equal temperatures and pressures of all phases and equal chemical potential of all components in each phase, also hold for a system with reactive components. Additional relationships exist among the partial molar Gibbs free energy of reacting components in the system. These additional relationships are derived using the necessary condition of minimum in the Gibbs free energy function of the entire system. The use of this additional relationship to find the equilibrium composition for a system with reactive components constitutes the stochiometric approach.

Equilibrium compositions can also be obtained without recourse to these additional relationships. The Gibbs free energy function of the entire system attains its global minima at equilibrium, whether components present in the system are reactive or otherwise. The challenge in multicomponent and multiphase systems is the identification of the global minimum from several local minima. The compositions that correspond to the global minimum of the Gibbs free energy function of the entire system are then the equilibrium compositions for a system with or without reactive components. This method of estimating equilibrium compositions is referred to as the Gibbs free energy

minimization approach.

In the next section, the equilibrium criteria for a multicomponent multiphase system with reacting components are presented. The details of a case study is discussed and the two approaches to find equilibrium composition are presented.

3.2.1 Phase and Chemical Equilibrium

A multicomponent multiphase closed system with reacting components at constant temperature and pressure attains phase and chemical equilibrium. The moles of component i in phase j (N_{ij}) can be expressed in terms of reaction extents ϵ_k ($k = 1, 2, \ldots, R$),

$$N_{ij} = N_{ij}^0 + \sum_{k=1}^{R} \nu_{ij,k}\epsilon_k \quad \forall\, i = 1, 2, \ldots, N_c;\ j = 1, 2, \ldots, N_p. \quad (3.40)$$

Here, $\nu_{i,k}$ is the stochiometric coefficient of the component in k^{th} reaction and N_{ij}^0 is the initial moles of component in phase j. Eq 3.40 can be summed over all phases to obtain,

$$\sum_{j=1}^{N_p} N_{ij} = N_i^0 + \sum_{k=1}^{R} \nu_{i,k}\epsilon_k \quad i = 1, \ldots, N_c. \quad (3.41)$$

Here, N_i^0 is the total initial moles of component in all phases. Eq 3.41 is the additional constraint in a reactive system that separates it from a system where no reactions occur. The equilibrium composition for this reactive system can then be obtained by minimizing the Gibbs free energy function of the system subject to the reaction constraint in eq 3.41.

A Lagrangian approach is used to obtain the equilibrium composition for such a reactive system. In this approach, a new objective function $\mathcal{G}$ is defined using Lagrange multipliers, α_i, that includes the reaction constraint in addition to the total Gibbs free energy of the system. There are a total of N_c Lagrange multipliers, one for each component. The function $\mathcal{G}$ can be given as,

$$\mathcal{G} = \sum_{j=1}^{N_p}\sum_{i=1}^{N_c} N_{ij}\bar{G}_{ij} + \sum_{i=1}^{N_c}\alpha_i\left(\sum_{j=1}^{N_p} N_{ij} - N_i^0 - \sum_{k=1}^{R}\nu_{i,k}\epsilon_k\right) \tag{3.42}$$

Here, ϵ_k, N_{ij} and α_i are independent variables and the necessary condition of minimum is used to obtain the equilibrium criteria. The equations obtained using the necessary condition for the independent parameter N_{ij} are,

$$\left(\frac{\partial \mathcal{G}}{\partial N_{ij}}\right)_{T,P,\epsilon_k,N_{i\neq i}} = 0 \implies \underbrace{\sum_{j=1}^{N_p}\sum_{i=1}^{N_c} N_{ij}\frac{\partial \bar{G}_i}{\partial N_{ij}}}_{\text{Gibbs-Duhem equation}} \overset{0}{\cancel{}} + \bar{G}_{ij} + \alpha_i = 0. \forall s = 1, 2, \ldots, N_c. \tag{3.43}$$

Eq 3.43 is obtained for the component i in every phase j. This implies,

$$\bar{G}_{i1} = \bar{G}_{i2} = \ldots = \bar{G}_{iN_p} = -\alpha_i. \quad \forall\, i = 1, 2, \ldots, N_c. \tag{3.44}$$

Also, the equations obtained from the necessary condition for the independent parameter ϵ_k results in the following equations,

$$\left(\frac{\partial \mathcal{G}}{\partial \epsilon_m}\right)_{T,P,\epsilon_{k\neq m},N_{ij}} = 0 \quad \implies \sum_{j=1}^{N_p}\sum_{i=1}^{N_c}\nu_{i,m}\alpha_i = 0; \quad \forall\, k = 1, 2, \ldots, R.$$

Using eq 3.44,

$$\sum_{i=1}^{N_c}\nu_{i,k}\bar{G}_{ij} = 0; \quad \forall\, k = 1, 2, \ldots, R. \quad j = 1, 2, \ldots, N_p. \tag{3.45}$$

In summary, in addition to the equality of chemical potentials, additional relationship among all reacting components (eq 3.45) exist for a system with reactive components. Eqns 3.44 and 3.45 together, constitute the phase and chemical equilibrium criteria for a closed system at constant temperature and pressure.

3.2.2 Case Study

In this example, the equilibrium compositions have been estimated using the Gibbs free minimization approach and the stochiometric approach for a case of single phase aqueous components. The components are assumed ideal, and are those expected in a carbonate system (See Table 3.1). The equilibrium compositions have been obtained for a specific case of initial mole numbers (Table 3.1) at standard conditions (temperature, $T_0 = 25°C$ and pressure, $P_0 = 1$ atm). The nonlinear equations solved in either approaches are presented and the objective is to identify the faster approach to obtain equilibrium composition.

3.2.2.1 Gibbs free energy approach

In this approach, equilibrium composition of a system, with or without reactions, is the solution of a minimization problem. The Gibbs free energy function of the entire system is the objective function that is to be minimized. The elemental balance constraint is the equality constraint while the positive mole number requirement constitutes the inequality constraint for this mini-

No, i	Components, n_i	Stadard state, $\underline{G}_i^0$ (KJ/mol)	Initial moles n_i^0
1	Ca^{2+}	-132.18	1
2	HCO_3^-	-140.31	0
3	H^+	0	0
4	OH^-	-37.6	0
5	H_2O	-56.69	1
6	CO_3^{2-}	-126.22	1
7	H_2CO_3	-149.00	0
8	CO_2	-92.31	0.5
9	$CaCO_3$	-262.76	0

Table 3.1: Case study with components and initial moles used in case study. The standard state Gibbs free energy values, $\bar{G}_i^0$, are from Rossini et al. (1952)

No. (k)	Elements	Total moles (b_k)
1	Ca	1
2	C	1.5
3	O	5
4	H	2

Table 3.2: Elemental balance from initial mole numbers used in case study.

mization problem.

The case study consists of aqueous phase components with initial number of moles as listed in Table 3.1. The standard state Gibbs free energy for aqueous component, $\bar{G}_i^0$, is the hypothetical aqueous solution of unit molality of the solute component i in the Lewis-Randall convention (Lewis and Randall, 1961). The Gibbs free energy values at standard state conditions for each component, $\bar{G}_i^0$, are also listed in Table 3.1. The standard state values are from Rossini et al. (1952).

The partial molar Gibbs free energy, $\bar{G}_i$, of a component i in an ideal aqueous phase mixture, with mole fraction x_i and moles n_i can be given as (Denbigh, 1966),

$$\bar{G}_i(T_0, P) = \bar{G}_i^0(T_0, P_0) + RTlnx_i = \bar{G}_i^0(T_0, P_0) + RTln(\frac{n_i}{\sum_{i=1}^{N_c} n_i}) \qquad (3.46)$$

As seen in Table 3.1, there are a total of nine components ($N_c = 9$) and four elements ($M = 4$) in this single phase case study. Equilibrium compositions are obtained by minimizing the Gibbs free energy function for the entire system, G^T. The objective function along with the equality and nonequality contraints can be written as,

$$\begin{aligned} Minimize \quad G^T = \sum_{i=1}^{9} n_i \bar{G}_i &= \sum_{i=1}^{9} n_i \left[\bar{G}_i^0 + RTln(\frac{n_i}{\sum_{i=1}^{9} n_i}) \right] \qquad (3.47) \\ Subject \quad to \quad \sum_{i=1}^{9} a_{ki} n_i &= b_k \quad \forall \quad k = 1, 2 \ldots 4. \\ \text{and} \quad n_i &\geq 0. \end{aligned}$$

In this case study, there are four elements Ca, C, O and H with initial moles b_k given in Table 3.2. In eq 3.47, a_{ik} is the coefficient of particular element k in the molecular formula of any component i. As an example, for component CO_2 where $i = 8$, $a_{81} = 0$, $a_{82} = 1$, $a_{83} = 2$ and $a_{84} = 0$.

The minimization of the Gibbs free energy function of the single phase system with ideal components, results in a unique solution (Smith and Missen, 1982b). Hence, the necessary condition for the minimum is used to obtain equilibrium composition.

A Lagrangian approach is used to convert the constrained minimization problem to an unconstrained minimization problem. The Lagrangian function ($\mathcal{L}$) using Lagrangian parameters, λ_k for constraints in eq 3.47 is,

$$\mathcal{L} = \sum_{i=1}^{9} n_i \bar{G}_i + \sum_{k=1}^{4} \lambda_k (b_k - \sum_{i=1}^{9} a_{ki} n_i). \tag{3.48}$$

The necessary conditions for minimum of the function are,

$$\frac{\partial \mathcal{L}}{\partial n_i} = 0 \quad \Longrightarrow \bar{G}_i - \sum_{k=1}^{4} \lambda_k a_{ki} = 0 \quad \forall i = 1, 2, \ldots 9. \tag{3.49}$$

$$\frac{\partial \mathcal{L}}{\partial \lambda_k} = 0 \quad \Longrightarrow b_k - \sum_{i=1}^{9} a_{ki} n_i = 0 \quad \forall k = 1, 2 \ldots 4. \tag{3.50}$$

The equilibrium composition is obtained by solving equations resulting from the necessary conditions of minimum of the Lagrangian function, $\mathcal{L}$ (eqns 3.49 and 3.50). For this case study, the total number of nonlinear equations solved in the Gibbs free energy minimization approach is $N+M=13$, that simplifies to $M+1=5$ for ideal components (See Appendix A). The solution obtained

Reaction	Reaction extent	Reaction constant
$H^+ + OH^- \Leftrightarrow H_2O$	ξ_1	$K_1 = 0.0077$
$HCO_3^- \Leftrightarrow H^+ + CO_3^{2-}$	ξ_2	$K_2 = 0.9943$
$HCO_3^- + H^+ \Leftrightarrow H_2CO_3$	ξ_3	$K_3 = 1.0035$
$HCO_3^- \Leftrightarrow OH^- + CO_2$	ξ_4	$K_4 = 0.9958$
$Ca^{2+} + HCO_3^- \Leftrightarrow H^+ + CaCO_3$	ξ_5	$K_5 = 0.9961$

Table 3.3: Linearly independent reactions in the case study and the equilibrium constants at standard conditions.

by solving this minimization problem is the equilibrium composition and is presented in Table 3.5.

In summary, only a list of components and their standard state values are required to determine the equilibrium composition for a system with or without reacting components.

3.2.2.2 Stochiometric approach calculation

The calculation of equilibrium composition in the stochiometric approach follows from the additional relationships between reacting components. The additional relationships are derived using the necessary condition arising out of a minimum in the Gibbs free energy function of the entire system. The stochiometric formulation, in constrast to the Gibbs free energy approach, requires a knowledge of all reactions occuring between the components in the system.

There are five linearly independent reactions ($R = 5$) in this case study. These reactions are listed in Table 3.14. The knowledge of reactions helps

No, (i)	Component,	Initial moles (n_i^0)	Equilibrium composition (n_i)
1	Ca^{2+}	1	$n_1^0 + \xi_5$
2	HCO_3^-	0	$n_2^0 + \xi_2 - \xi_3 - \xi_4$
3	H^+	0	$n_3^0 - \xi_1 + \xi_2 - \xi_3 + \xi_5$
4	OH^-	0	$n_4^0 - \xi_1 + \xi_4$
5	H_2O	1	$n_5^0 + \xi_1$
6	CO_3^{2-}	1	$n_6^0 + \xi_2$
7	H_2CO_3	0	$n_7^0 + \xi_3$
8	CO_2	0.5	$n_8^0 + \xi_4$
9	$CaCO_3$	0	$n_9^0 + \xi_5$

Table 3.4: Equilibrium component mole numbers in terms of reaction extents.

determine the stochiometric coefficient, ν_{ij}, of each component i in the different reactions j. Hence, component mole numbers n_i can be expressed in terms of the reaction extents, ξ_j. The component mole numbers can be given as,

$$n_i = n_i^0 + \sum_{j=1}^{R=5} \nu_{ij}\xi_j \qquad \forall \qquad i = 1, 2, \ldots 9. \tag{3.51}$$

The Gibbs free energy function of the entire system can then be written as,

$$Minimize \quad G^T = \sum_{i=1}^{9} n_i \bar{G}_i = \sum_{i=1}^{9} \left(n_i^0 + \sum_{j=1}^{R} \nu_{ij}\xi_j \right) \bar{G}_i \tag{3.52}$$

Again, the necessary condition for a minimum in the Gibbs free energy leads to the following equations,

$$\frac{\partial G^T}{\partial \xi_j} = 0 \quad \Longrightarrow \quad \underbrace{\sum_{i=1}^{N=9} n_i \frac{\partial \bar{G}_i}{\partial \xi_j}}_{\text{Gibbs-Duhem equation}} \overset{0}{\nearrow} + \sum_{i=1}^{N=9} \nu_{ij}\bar{G}_i = 0 \qquad \forall j = 1, 2, \ldots 5.$$

$$\Longrightarrow \quad \sum_{i=1}^{N=9} \nu_{ij}\bar{G}_i = 0 \qquad \forall j = 1, 2, \ldots 5. \tag{3.53}$$

Eq 3.53 is simplified using the Gibbs-Duhem equation and represents the additional relationship that exists among the reactive components. The equilibrium mole numbers of all components in terms of the reaction constants are given in Table 3.4. The expression for partial molar Gibbs free energy $\bar{G}_i$ is similar to that given in eq 3.46 where n_t is the total number of moles at equilibrium. Rearranging eq 3.53 for the first reaction in Table 3.4 results in,

$$\begin{aligned} \frac{x_{H_2O}}{x_{H^+}x_{OH^-}} = exp\left[\frac{-(\mathrm{G}^0_{H_2O} - \mathrm{G}^0_{H^+} - \mathrm{G}^0_{OH^-})}{RT}\right] &= K_1 \\ \implies \left[\frac{n_5^0 + \xi_1}{(n_3^0 - \xi_1 + \xi_2 - \xi_3 + \xi_5)(n_4^0 - \xi_1 + \xi_4)}\right]\left(\frac{1}{n_t}\right) &= K_1 \quad (3.54) \\ \text{where} \quad n_t = (\sum_{i=1}^{9} n_i^0) - \xi_1 + 3\xi_2 - \xi_3 + \xi_4 + 3\xi_5 & \end{aligned}$$

The four similar equations for other reactions in Table 3.4 are,

$$\left[\frac{(n_3^0 - \xi_1 + \xi_2 - \xi_3 + \xi_5)(n_6^0 + \xi_2)}{n_2^0 + \xi_2 - \xi_3 - \xi_4}\right](n_t) = K_2 \quad (3.55)$$

$$\left[\frac{(n_7^0 + \xi_3)}{(n_3^0 - \xi_1 + \xi_2 - \xi_3 + \xi_5)(n_2^0 + \xi_2 - \xi_3 - \xi_4)}\right]\left(\frac{1}{n_t}\right) = K_3 \quad (3.56)$$

$$\left[\frac{(n_8^0 + \xi_4)(n_4^0 - \xi_1 + \xi_4)}{n_2^0 + \xi_2 - \xi_3 - \xi_4}\right](n_t) = K_4 \quad (3.57)$$

$$\left[\frac{(n_3^0 - \xi_1 + \xi_2 - \xi_3 + \xi_5)(n_9^0 + \xi_5)}{(n_1^0 + \xi_5)(n_2^0 + \xi_2 - \xi_3 - \xi_4)}\right] = K_5 \quad (3.58)$$

The constants K_i $(i = 1, 2, \ldots 5)$ can be directly obtained from the Gibbs free energy standard state values of components (eq 3.54) and are listed in Table 3.3.

The number of nonlinear equations solved to obtain equilibrium composition using the stochiometric approach is equal to the number of linearly

No, (i)	Components,	Initial moles (n_i^0)	Stochiometric approach	Gibbs free energy approach
1	Ca^{2+}	1	0.4017	0.4017
2	HCO_3^-	0	0.7962	0.7962
3	H^+	0	2.56E-08	2.56E-08
4	OH^-	0	5.60E-07	5.60E-07
5	H_2O	1	0.5825	0.5825
6	CO_3^{2-}	1	0.0036	0.0036
7	H_2CO_3	0	0.0194	0.0194
8	CO_2	0.5	0.0825	0.0825
9	$CaCO_3$	0	0.5983	0.5983

Table 3.5: Equilibrium composition for the case study using both approaches

independent reactions (R). Eqns 3.54-3.58 form a set of five equations formed by the five linearly independent reactions of this system to obtain the five unknown reaction extents (ξ_j). The equilibrium mole numbers can be further obtained from these reaction extents.

3.2.3 Conclusions

The same number of nonlinear equations are solved to obtain equilibrium compositions using both methods. Identical results have been obtained using either approaches (Table 3.5). The computational times taken to obtain equilibrium composition using either approach was compared for this example case study. The Gibbs free energy minimization approach was about 30% faster than the stochiometric approach (0.2143 sec versus 0.0573 sec) and is due to the nature of the nonlinear equations solved in either cases.

The choice of approach to calculate equilibrium composition is gov-

erned by the number of nonlinear equations that is solved in each approach. For an ideal single phase system, the number of reactions in the system, R, corresponds to the number of nonlinear equations solved in the stochiometric approach. The number of nonlinear equations solved in the Gibbs free energy minimization approach is $N + M$ which simplifies to $M + 1$ for the ideal case.

When the number of nonlinear equations being solved using either approaches is the same, the Gibbs free energy algorithm is faster. In addition, since no equilibrium constant need to be specified, the Gibbs free energy approach is the preferred method of finding equilibrium composition for reactive system. This algorithm is further investigated for integrating phase equilibrium computations with geochemical reactions in the next chapter.

Chapter 4

Gibbs Free Energy Model

In this chapter, the Gibbs free energy expressions used for different components are presented. These expressions together with the reference states constitute the Gibbs free energy model that is used to calculate equilibrium compositions. The Gibbs free energy function for applications discussed in this dissertation are also presented in this chapter.

4.1 Gibbs Free Energy Expression

The expressions developed for Gibbs free energy in chapter 3 measure changes rather than absolute values of free energy. Eqn 3.23 gives the change in Gibbs free energy for a multicomponent system. The expression for change in Gibbs free energy for a single component system where mole number is not an independent variable, is given as,

$$d\underline{G} = \underline{V}dP - \underline{S}dT \tag{4.1}$$

Here, $\underline{G}$, $\underline{V}$ and $\underline{S}$ are the molar properties - Gibbs free energy, volume and entropy respectively, of the pure component. The change in Gibbs free energy

at constant temperature can then be given as,

$$\left(\frac{\partial \underline{G}}{\partial P}\right)_T = \underline{V} \tag{4.2}$$

The change in Gibbs free energy at constant pressure can be given as,

$$\left(\frac{\partial \underline{G}}{\partial T}\right)_P = -\underline{S} = \frac{\underline{G} - \underline{H}}{T} \tag{4.3}$$

Multiplying eq 4.3 by $(1/T)$ on both sides,

$$\begin{aligned} -\left(\frac{\underline{G}}{T^2}\right) + \frac{1}{T}\left(\frac{\partial \underline{G}}{\partial T}\right)_P &= -\left(\frac{\underline{H}}{T^2}\right) \\ \implies \left(\frac{\partial (\underline{G}/T)}{\partial T}\right)_P &= -\left(\frac{\underline{H}}{T^2}\right) \end{aligned} \tag{4.4}$$

Eq 4.4 is also referred to as the Gibbs-Helmholtz equation. Eqns 4.2 and 4.4 can also be used to obtain an equivalent expression for a change in Gibbs free energy for a mixture. Multiplying eq 4.2 by total number of moles N and differentiating with respect to N_i, the moles of component i results in,

$$\left.\frac{\partial}{\partial N_i}\right|_{N_j \neq i} \left[\frac{\partial (N\underline{G})}{\partial P}\right]_T = \left.\frac{\partial}{\partial N_i}\right|_{N_j \neq i} [N\underline{V}]. \tag{4.5}$$

The order of differentiation can be interchanged and the definitions of partial molar properties (eq 3.2) are used to obtain,

$$\left.\frac{\partial \bar{G}_i}{\partial P}\right|_{T^r, N_j} = \bar{V}_i. \tag{4.6}$$

The same technique is employed for the Gibbs free energy change for a mixture at constant pressure (eq 4.4). The resulting expression for change of partial

molar Gibbs free energy at constant pressure is,

$$\left.\frac{\partial(\bar{G}_i/T)}{\partial T}\right|_{P,N_j} = -\left(\frac{\bar{H}_i}{T^2}\right). \tag{4.7}$$

Eqns 4.6 and 4.7 are the expressions for change in Gibbs free energy for mixtures. The reference states, discussed in the next section, are used to obtain the absolute values of Gibbs free energy for different components.

4.2 Reference States

The expression for the absolute value of Gibbs free energy of a pure component at any pressure P is obtained by integrating eq 4.2 at constant temperature T^r. This results in,

$$\underline{G}(T^r, P) = \underline{G}^r(T^r, P^r) + \int_{P^r}^{P} \underline{V} dP. \tag{4.8}$$

Here, $\underline{G}^r$ and $\underline{G}$ are the Gibbs free energy values of the pure component at reference pressure, P^r, and desired pressure, P, respectively. If the component is assumed ideal,

$$\underline{G}(T^r, P) = \underline{G}^r(T^r, P^r) + RT^r ln\frac{P}{P^r}. \tag{4.9}$$

The equivalent expression for the Gibbs free energy for any component in a mixture at pressure P is obtained by integrating eq 4.6 at constant temperature to obtain,

$$\bar{G}_i(T^r, P) = \bar{G}_i(T^r, P^r) + \int_{P^r}^{P} \bar{V}_i dP. \tag{4.10}$$

This can be further simplified for an ideal gas mixture to obtain,

$$\bar{G}_i(T^r, P) = \bar{G}_i(T^r, P^r) + RTln\frac{x_i P}{P^r}. \tag{4.11}$$

In eq 4.11, the reference state for the Gibbs free energy is the partial molar Gibbs free energy of the component ($\bar{G}_i$) at T^r and P^r. One can also choose the pure component property ($\underline{G}_i$) at T^r and P^r as the reference state. The choice of pure component property as reference state for an ideal gas mixture results in,

$$\bar{G}_i(T^r, P) = \underline{G}_i(T^r, P^r) + RTln\frac{x_i P}{P^r}. \tag{4.12}$$

Here, x_i is the mole fraction of component i in the ideal gas mixture while P is the total pressure of the system. While any values for P^r and T^r may be chosen, it is important to note that $\underline{G}$ at pressure P and obtained using eq 4.9 is at the chosen reference temperature, T^r.

Lewis and Randall (1961) defined fugacity for consistency with the corresponding equation for an ideal gas (eq 4.11). The general expression for chemical potential of any component i in a non-ideal phase mixture is measured from a reference state (Prausnitz et al., 1998) and is given as,

$$\bar{G}_{ij} = \bar{G}_i^r + RTln\left(\frac{\bar{f}_{ij}}{\bar{f}_{ij}^r}\right) \tag{4.13}$$

Here, $\bar{G}_{ij}$ is the chemical potential of component i in phase j at the pressure and temperature conditions of interest, $\bar{f}_{ij}$ is the fugacity of component i in phase j at the state of interest, $\bar{G}_i^r$ is the chemical potential of the component at reference state and $\bar{f}_{ij}^r$ is the fugacity at that reference state. The temperature is constant, both, at the reference state and the state of interest while the pressure may vary.

The chemical potential can also be defined in terms of activity (a_{ij}) of the component (Nordstorm and Munoz, 1986), the reference state being implicit in the definition of activity.

$$\bar{G}_{ij} = \bar{G}_i^r + RTln\, a_{ij} \tag{4.14}$$

The convention for the reference state for components varies and depends on the nature of the component (solute or solvent) as well as the thermodynamic description (activity coefficient model or EOS description) of the phase in which the component is present. The Lewis-Randall convention for reference states for different components are listed in Table 4.1.

The NIST database (Rossini et al., 1952) lists the Gibbs free energy reference state values for different components in the Lewis-Randall convention. These values of reference state values from the NIST database listed in Table 3.1 were used to estimate equilibrium compositions in the case study of chapter 3. The specific Gibbs free energy expressions for components in gas phase, hydrocarbon phase, aqueous phase and solid phase are presented in Appendix A.

4.3 Gibbs Free Energy Model

In the Gibbs free energy approach for computing equilibrium composition, the Gibbs free energy function of the entire system is the objective function that is minimized using an elemental balance constraint. The solution to the minimization problem is the equilibrium composition. The advantage of

Table 4.1: Reference states for components as reported in the Lewis-Randall convention in NIST database (Rossini et al., 1952). The reference state is at standard conditions of temperature, $T_0 = 25°C$ and pressure, $P_0 = 1$ atm.

Component type	Reference state (at standard conditions)
Gas phase component	Hypothetical ideal gas
Hydrocarbon phase component	Hypothetical ideal gas
Aqueous phase component	Hypothetical ideal solution of unit molality
Water	Pure liquid
Solid	Pure solid

the Gibbs free energy model is that it is equally applicable to both systems with or without reactive components. In this section, the formulation for this model is presented.

The Gibbs free energy function of the entire system is a sum of the appropriate Gibbs free energy expressions for different components in the system. These components may be present in different phases and hence, have different reference states as discussed in the previous section. It is possible to combine components that use different reference state descriptions and/or components with reference states at different pressure and temperature conditions. This combination constitutes the Gibbs free energy function for the entire system that is minimized to obtain the equilibrium composition at a fixed temperature and pressure.

4.3.1 Combining Reference States

As discussed in section 4.2, the Gibbs free energy expression for different components in the system are based on different reference states. However,

the reference states of a component in different phases may be related by a standard expression. As an example, the aqueous and gas phase reference states at standard conditions for a component i are related by the following equation,

$$\bar{G}_s^0(T_0, P_0) = \underline{G}_s^{IG}(T_0, P_0) + (\Delta G)_{hyd}(T_0, P_0). \tag{4.15}$$

Here, $\underline{G}_s^{IG}$ is the reference state for the component in the gas phase, $\bar{G}_s^0$ is the reference state property for the component in the aqueous phase, while $(\Delta G)_{hyd}$ is the Gibbs free energy of hydration of the component ; all properties at standard conditions of temperature and pressure. The hydration energy is defined as the energy required to convert the component from a hypothetical ideal gas to an aqueous solute at a concentration of unit molality.

More generally, the components with reference states at different pressure but same temperature can also be related. Consider the case of component i, present in two phases (I and II) that use different reference states - $\bar{G}^I$ (T, P^I) and $\bar{G}^{II}$ (T, P^{II}) for their Gibbs free energy expression. Using eq 4.13, the partial molar Gibbs free energy (chemical potential) of the component in the two phases, $\bar{G}_i$ and $\bar{G}_{i2}$, at any pressure P and system temperature T can be given as,

$$\bar{G}_{i1}(T, P) = \bar{G}_i^I(T, P^I) + RTln\left(\frac{\bar{f}_{i1}}{\bar{f}_i^I}\right); \tag{4.16}$$

$$\bar{G}_{i2}(T, P) = \bar{G}_i^{II}(T, P^{II}) + RTln\left(\frac{\bar{f}_{i2}}{\bar{f}_i^{II}}\right). \tag{4.17}$$

In the above equation, $\bar{f}_i^I$ and $\bar{f}_i^{II}$ are the fugacity of component i at reference pressures P^I and P^{II} respectively, while $\bar{f}_{i1}$ and $\bar{f}_{i2}$ are the fugacity of the

component in the two phases at pressure P. Eq 4.13 can also be used to relate the reference states (Prausnitz et al., 1998) to obtain,

$$\bar{G}_i^{II}(T, P^{II}) = \bar{G}_i^{I}(T, P^{I}) + RTln\left(\frac{\bar{f}_i^{II}}{\bar{f}_i^{I}}\right). \tag{4.18}$$

Eqns 4.16-4.18 imply that the chemical potentials of the component, $\bar{G}_{i1}$ and $\bar{G}_{i2}$ are equal at equilibrium (a necessary condition for equilibrium) even though different reference states might be used for the same component in different phases. This also implies that the fugacities of the component in these phases, $\bar{f}_{i1}$ and $\bar{f}_{i2}$, are also equal. Hence, the equality of chemical potential criteria of a component present in different phases at equilibrium also extends to the equality of fugacity of the same component in different phases irrespective of the reference state. However, the activities of the component (defined in eq 4.14) are equal at equilibrium only if the same reference states are used for the component in both the phases.

In summary, as shown for component in aqueous and gas or hydrocarbon phase, the Gibbs free energy function of the entire system is additive if all the different reference states for components are at standard conditions of temperature and pressure (eq 4.15). Also, the reference states at different pressures but same temperatures can also be related using appropriate corrections (eqn 4.18) to make the Gibbs free energy function additive. If the reference states of components are at different pressures and temperatures, appropriate corrections can be made to make the system Gibbs free energy function additive. The details of the corrections to the Gibbs free energy expressions for different components used in this model is explained below.

4.3.2 Combining States at Different Pressure and Temperature

The system pressure (P) and temperature (T) condition can be chosen as a reference state instead of the standard conditions (P_0 and T_0). This choice of system T and P as reference state results in the following expression for the partial molar Gibbs free energy for components in gas/hydrocarbon phase ($\bar{G}_{ig}$ in eq A.8),

$$\bar{G}_{ig}(T,P) = \underline{G}_i^{IG}(T,P) + RTln(y_i\hat{\phi}_i). \tag{4.19}$$

For component in the aqueous phase (eq A.10) the partial molar Gibbs free energy ($\bar{G}_{iw}$) is,

$$\bar{G}_{iw}(T,P) = \bar{G}_i^0(T,P) + RTln(x_i\gamma_i). \tag{4.20}$$

The expression for the partial molar Gibbs free energy for the solid phase component ($\bar{G}_{is}$ in eq A.12) is,

$$\bar{G}_{is}(T,P) = \underline{G}_i{}^0(T,P) + RTln(z_i\delta_i) \tag{4.21}$$

The partial molar Gibbs free energy for solvent water ($\bar{G}_w$) that has pure water as reference state (eq A.11) is,

$$\bar{G}_w(T,P) = \underline{G}_w{}^0(T,P) + RTln(x_w\gamma_w) \tag{4.22}$$

The second term of on the right side in eqns 4.19-4.21 represents deviation from ideality ($\hat{\phi}_i$, γ_s/γ_w, δ_i) with this choice of reference state. Using the change in Gibbs free energy for pure components (eqns 4.2, 4.4) as the change for

components in mixtures (eqns 4.6 and 4.7), the new reference state values at any system T and P can be related to the NIST tabulated values at standard conditions of T_0 and P_0. This results in the following equations for components,

$$\underline{G_i}^{IG}(T,P) = \underline{G_i}^{IG}(T_o,P_o) + RTln(\frac{P}{P_o}) + T\int_{T_o}^{T} -\left(\frac{\underline{H_i}}{T^2}\right)_P dT \quad (4.23)$$

$$\bar{G}^0_{iw}(T,P) = \bar{G}^0_i(T_o,P_o) + \int_{P_o}^{P}(\bar{v}_i)_{T_o}dP + T\int_{T_o}^{T} -\left(\frac{\bar{H}_{iw}}{T^2}\right)_P dT \quad (4.24)$$

$$\bar{G}^0_{is}(T,P) = \underline{G_i}^0(T_o,P_o) + \int_{P_o}^{P}(\underline{v_i})_{T_o}dP + T\int_{T_o}^{T} -\left(\frac{\underline{H_i}}{T^2}\right)_P dT \quad (4.25)$$

$$\bar{G}^0_w(T,P) = \underline{G_w}^0(T_o,P_o) + \int_{P_o}^{P}(\underline{v_w})_{T_o}dP + T\int_{T_o}^{T} -\left(\frac{\underline{H_w}}{T^2}\right)_P dT \quad (4.26)$$

Here, y_i is the mole fraction in the gas phase, $\hat{\phi}_i$ is the fugacity coefficient, $\bar{v}_s$ is the molar volume of solute, $\underline{v_w}$ is the molar volume of water, $\underline{v_i}$ is the molar volume of pure solid phase component while $\underline{H_i}$ is the molar enthalpy of component i in the gas phase and solid phase, $\underline{H_w}$ is the molar enthalpy of pure water and $\bar{H}_{sw}$ is the partial molar enthalpy of solute component in the aqueous phase.

Helgeson and co-workers (Shock et al., 1989; Helgeson and Kirkham, 1976; Johnson et al., 1992) have developed EOS models for the partial molal volumes $\underline{v_s}$ as well as expressions for partial molal enthalpies $\underline{H_s}$ for aqueous solutes (CO_2, H_2S as well as ionic solutes) to evaluate the reference state values at high temperatures and pressures (upto 1000°C and 5000 bars). The applications considered in this dissertation are in the pressure range 20-80

MPa. In this model, the molar volumes and enthalpies at T_0 and P_0 (tabulated in NIST database (Rossini et al., 1952)) are assumed to be constants over the pressure and the temperature range of acid gas injection. We can then simplify eqns 4.23-4.26 to obtain,

$$\underline{G}_i^{IG}(T,P) = \underline{G}_i^{IG}(T_o,P_o) + RTln(\frac{P}{P_o}) + [\underline{H}_i]_{P_o,T_o}\left(1-\frac{T}{T_o}\right) \quad (4.27)$$

$$\bar{G}^0_{iw}(T,P) = \bar{G}^0_i(T_o,P_o) + (\bar{v}_1^{\infty})_{T_o}(P-P_o) + [\bar{H}_{iw}]_{P_o,T_o}\left(1-\frac{T}{T_o}\right) \quad (4.28)$$

$$\bar{G}^0_{is}(T,P) = \bar{G}^0_i(T_o,P_o) + (\bar{v}_1)_{T_o}(P-P_o) + [\bar{H}_{sw}]_{P_o,T_o}\left(1-\frac{T}{T_o}\right) \quad (4.29)$$

$$\bar{G}^0_w(T,P) = \underline{G}_w{}^0(T_o,P_o) + (\underline{v}_2)_{T_o}(P-P_o) + [\underline{H}_w]_{P_o,T_o}\left(1-\frac{T}{T_o}\right) \quad (4.30)$$

The Gibbs free energy function of the system is the sum of all components in all the phases. The Gibbs free energy expression for corresponding components in gas phase, aqueous phase and solid phase are used to construct the total system Gibbs free energy function G^T. The resulting function for a system with N_c components and N_c phases (sum of gas/hydrocarbon, aqueous phase as well as solid phase) is,

$$\begin{aligned} G^T(T,P) &= \sum_{i=1}^{N_c}\sum_{j=1}^{N_p} n_{ij}\bar{G}_{ij}(T,P) \\ &= \sum_{i=1}^{N_c} n_{ig}\bar{G}_{ig}(T,P) + \sum_{i=1}^{N_c} n_{iw}\bar{G}_{iw}(T,P) + \sum_{i=1}^{N_c} n_{is}\bar{G}_{is}(T,P) + n_w\bar{G}_w \end{aligned}$$

Here, n_{ig}, n_{iw} and n_{is} are the number of moles of component i in the gas/hydrocarbon phase, aqueous phase and solid phase respectively. Also, n_w is the moles of solvent water in the aqueous phase. Using eqns 4.19-4.22 in the above equa-

tion,

$$G^T(T,P) = \sum_{i=1}^{N_c} n_{ig}[\underline{G_i}^{IG}(T,P) + RTlny_i\hat{\phi}_i] + \sum_{i=1}^{N_c} n_{iw}[\bar{G}^0_{iw}(T,P) + RTlnx_i\gamma_i] + \sum_{i=1}^{N_c} n_{is}[\bar{G}^0_{is}(T,P) + RTlnz_i\delta_i] + n_w[\bar{G}^0_w(T,P) + RTlnx_w\gamma_w]. \quad (4.31)$$

The reference states $\underline{G_i}^{IG}$ for gas phase as well as hydrocarbon phase components, $\bar{G}^0_{iw}$ for aqueous phase components, $\bar{G}^0_{is}$ for solid phase components and $\bar{G}^0_w$ for pure water are at system T and P. The model eqns 4.27-4.30 are used to relate these reference state values at system T and P to the NIST database values.

As discussed in section 3.1, the global minimum of the Gibbs free energy function (G^T in eq 4.31) at any temperature and pressure is the equilibrium composition of the system at those conditions. The Gibbs free energy minimization approach can be used to find equilibrium composition of not just pure phase equilibrium but also phase and chemical equilibrium. The Gibbs free energy function, G^T, specific to the applications discussed in this dissertation are presented below.

4.3.2.1 Gas solubility computations

Several industrial processes require computation of gas solubility in water at high temperatures and pressures. The Gibbs free energy minimization approach can be used to obtain the mole fraction of the gas component in the aqueous phase. The gas phase can be a mixture of components or just a single

component. The Gibbs free energy function used for such applications is,

$$\begin{aligned} G^T(T,P) &= \sum_{i=1}^{N_c} n_{ig}[\underline{G}_i^{IG}(T,P) + RTlny_i\hat{\phi}_i] + \sum_{i=1}^{N_c} n_{iw}[\bar{G}_{iw}^0(T,P) + RTlnx_i\gamma_i] \\ &+ n_w[\bar{G}_w^0(T,P) + RTlnx_w\gamma_w]. \end{aligned} \tag{4.32}$$

The standard state values for different components are required for this computation. The standard states can be related to the reference state value at system T and P using eqns 4.27 and 4.28. The acid gas solubility model developed in chapter 5 have been developed using the Gibbs free energy function in eq 4.32. This is a case of pure phase equilibrium computation as only the acid gas component and pure water are in the aqueous phase.

If, in addition to the gas phase components, ions are present in the aqueous phase that are capable of reacting with solid, the Gibbs free energy function for system can be given as,

$$\begin{aligned} G^T(T,P) &= \sum_{i=1}^{N_c} n_{ig}[\underline{G}_i^{IG}(T,P) + RTlny_i\hat{\phi}_i] + \sum_{i=1}^{N_c} n_{iw}[\bar{G}_{iw}^0(T,P) + RTlnx_i\gamma_i] \\ &+ n_w[\bar{G}_w^0(T,P) + RTlnx_w\gamma_w] + n_s[\underline{G}_s(T,P)]. \end{aligned} \tag{4.33}$$

In the above equation, the solid is assumed as a pure component, n_s are the moles of the solid and $\underline{G}_s$ is the reference state of the pure component solid. The gas solubility models for such cases of phase and chemical equilibrium are also presented in chapter 5.

4.3.2.2 Hydrocarbon phase equilibrium computations

Compositional simulators routinely perform phase equilibrium computations to calculate the distribution of components in phases and estimate

recovery. Multiple hydrocarbon phases may exist, especially, during CO_2 injection in oil reservoirs. The equilibrium composition for such phase equilibrium computations can also be calculated using the Gibbs free energy minimization approach.

The minimization can be performed assuming different number of phases to find the number of phases that gives the lowest Gibbs free energy. The reference state Gibbs free energy values for hydrocarbon phase components is the hypothetical pure component ideal gas value $\underline{G_i}^{IG}$ (Table 4.1). However, these reference states are not required for these equilibrium computations of involving only hydrocarbon systems. This is explained below.

Consider a hydrocarbon system with N_c components distributed in N_p phases. Let the initial moles of each component be z_i these moles are distributed in the hydrocarbon phases at equilibrium so that $z_i = \sum_{j=1}^{N_p} n_{ij}$ where n_{ij} is the number of moles of component i in phase j. Also, x_{ij} is the corresponding mole fraction. The Gibbs free energy function of the system using the partial molar Gibbs free energy expression for hydrocarbon phase component is,

$$\begin{aligned} G^T(T,P) &= \sum_{i=1}^{N_c}\sum_{j=1}^{N_p} n_{ij}\bar{G}_{ij}(T,P) \\ &= \sum_{i=1}^{N_c}\sum_{j=1}^{N_p} n_{ij}[\underline{G_i}^{IG}(T,P) + RTln(x_{ij}\hat{\phi}_i)] \end{aligned} \tag{4.34}$$

Relating the reference state to NIST database in eqn 4.27 results in,

$$G^T(T,P) = \sum_{i=1}^{N_c}\sum_{j=1}^{N_p} n_{ij}\left[\underline{G}_i^{IG}(T_0,P_0) + RTln(\frac{P}{P_0}) + [\underline{H}_i]_{P_o,T_o}\left(1-\frac{T}{T_o}\right)\right] + \sum_{i=1}^{N_c}\sum_{j=1}^{N_p} n_{ij}[RTln(x_{ij}\hat{\phi}_i)] \quad (4.35)$$

Expanding and rearranging,

$$G^T(T,P) = \sum_{i=1}^{N_c} \underbrace{z_i\left[\underline{G}_i^{IG}(T_0,P_0) + RTln(\frac{P}{P_0}) + [\underline{H}_i]_{P_o,T_o}\left(1-\frac{T}{T_o}\right)\right]}_{\text{a constant}} + \sum_{i=1}^{N_c}\sum_{j=1}^{N_p} n_{ij}[RTln(x_{ij}\hat{\phi}_i)]. \quad (4.36)$$

A new function H can be defined as below,

$$H(T,P) = \sum_{i=1}^{N_c}\sum_{j=1}^{N_p} n_{ij}[RTln(x_{ij}\hat{\phi}_i)] \quad (4.37)$$

Both functions, G^T (eq 4.36) and H (eq 4.37) have the same minimum as the first term on the right side in eq 4.36 is a constant. Also, the function H is devoid of reference state values and hence, preferable over G^T for minimization to obtain equilibrium composition. This is, of course, true for only phase equilibrium computations involving only hydrocarbon components. However, the challenge of finding the global minimum from local minima persists.

4.3.2.3 Hydrocarbon and aqueous phase equilibrium computations

If the aqueous phase with their components are combined with the hydrocarbon phase components, the Gibbs free energy function is formulated

using corresponding expressions for each component. Recognizing that not all components are present in all phases, it is possible to divide total N_c components into two groups - category A with N_{c1} components and category B with N_{c2} components.

The components in the first category (A) participate in only phase equilibrium within the hydrocarbon phases. The heavy hydrocarbon components that have negligible solubility in water are examples of components in this category. The category B components are present in both hydrocarbon phases as well as the aqueous phase. Hydrocarbon components like CH_4, C_2H_6 as well as CO_2 are some examples of components in category B that participate in geochemical reactions occuring between aqueous components and solid rock.

While an elemental balance constraint with just elements C, O, H etc., is used for minimization for all other cases discussed above, for cases involving hydrocarbon and aqueous phase equilibrium computations, category A components are included as base components in the constraint set that are additionally conserved. This ensures that class A components associated with just phase equilibrium remain separate from category B components, associated with phase as well as chemical equilibrium. This is further explained for specific cases discussed in chapter 6.

The total number of phases N_p is the sum of N_{hc} hydrocarbon phases and an aqueous phase. The total Gibbs free energy function for this entire

system is,

$$
\begin{aligned}
G^T(T,P) &= \sum_{i=1}^{N_c}\sum_{j=1}^{N_p} n_{ij}\bar{G}_{ij}(T,P) \\
&= \underbrace{\sum_{i=1}^{N_{c1}}\sum_{j=1}^{N_{hc}} n_{ij}[\underline{G}_i^{IG}(T,P) + RTln(x_{ij}\hat{\phi}_i)]}_{\text{category A}} \\
&+ \underbrace{\sum_{i=1}^{N_{c2}}\sum_{j=1}^{N_{hc}} n_{ij}[\underline{G}_i^{IG}(T,P) + RTln(x_{ij}\hat{\phi}_i)]}_{\text{category B}} \\
&+ \underbrace{\sum_{i=1}^{N_{c2}} n_{iw}[\bar{G}^0_{iw}(T,P) + RTlnx_i\gamma_i] + n_w[\bar{G}^0_w(T,P) + RTlnx_w\gamma_w]}_{\text{category B}}
\end{aligned}
\tag{4.38}
$$

It can be shown, using the argument previously presented for system with only hydrocarbon components in eqns 4.36 and 4.37, that the reference state values for components in category A are not required for the estimation of equilibrium composition for this system. However, the reference state values for components in category B are required. The equivalent H function that has the same minimum as G^T in eq 4.38 for this system is,

$$
\begin{aligned}
H(T,P) &= \sum_{i=1}^{N_{c1}}\sum_{j=1}^{N_{hc}} n_{ij}[RTln(x_{ij}\hat{\phi}_i)] + \sum_{i=1}^{N_{c2}}\sum_{j=1}^{N_{hc}} n_{ij}[\underline{G}_i^{IG}(T,P) + RTln(x_{ij}\hat{\phi}_i)] \\
&+ \sum_{i=1}^{N_{c2}} n_{iw}[\bar{G}^0_{iw}(T,P) + RTlnx_i\gamma_i] + n_w[\bar{G}^0_w(T,P) + RTlnx_w\gamma_w]
\end{aligned}
\tag{4.39}
$$

The examples of equilibrium computations for hydrocarbon and aqueous components with geochemical reactions use the above function and are further

discussed in chapter 6.

The Gibbs free energy minimization approach to find equilibrium composition has been extensively used for process engineering applications as well as for geochemical analysis to predict mineral solubilities in water (Harvie and Weare, 1980; Harvie et al., 1984). Luckas et al. (1994) have used a similar approach to predict phase and chemical equilibrium for flue gas systems and water at low pressures. The Gibbs free energy minimization approach has been extended for higher pressures and temperatures in this dissertation.

Numerous algorithms using this approach, have been developed to compute equilibrium compositions not just for phase equilibrium (Trangenstein, 1987) but also for coupled phase and chemical equilbrium (Gautam and Seider, 1979b; McDonald and Floudas, 1996; Harvie et al., 1987b; Peng Lee et al., 1999; Smith et al., 1993b). The RAND algorithm (White et al., 1958) discussed in the previous chapter is used to find the equilibrium composition for this system.

4.4 Stability Analysis

In the present section, stability analysis for systems having components distributed in different phases, each phase described by different thermodynamic models (EOS and activity coefficients) are presented. The stability analysis for components distributed in the hydrocarbon phase and described using EOS was presented in section 3.1.6. Also, the analysis in section 3.1.6 was particular to cases where all components are present in all phases.

The presence of aqueous phase ions as well as hydrocarbon components results in cases where not all components are present in all phases. This is particularly true of ions that are exclusively present in the aqueous phase for pressure and temperature conditions discussed in this dissertation. The stability analysis, for such cases where all components are not present in all phases and there are no reactions in the system, is presented to identify the global minimum and hence, the equilibrium composition for the system.

Consider a system consisting of hydrocabon phase components as well as aqueous phase components. Let n_{ij} be the number of moles of component i that are present in hydrocarbon phases. The hydrocarbon phases includes both types of components A and B (as defined in section 4.3.2.3). Let n_{iw} be the number of moles of component i in the aqueous phase. The aqueous phase includes the ions as well as component type B that participate in geochemical reactions. For stability analysis, the total system Gibbs free energy G^T for this system (eq 4.38), is equivalently given as,

$$G^T = \sum_{i=1}^{N_1} \sum_{j=1}^{N_{hc}} n_{ij} \bar{G}_{ij} + \sum_{i=1}^{N_{aq}} n_{iw} \bar{G}_{iw}. \tag{4.40}$$

Here, N_{hc} is the total number of hydrocarbon phases, N_1 is the total number of components distributed in all the hydrocarbon phases, whereas, N_{aq} is the total number of components present in the aqueous phase and also includes water as a component.

Let G_{aq} and G_j $(j = 1, 2, \ldots, N_{hc})$ represent the Gibbs free energy of all components in aqueous phase and corresponding components in hydrocarbon

phases respectively. The total Gibbs free energy of the complete system having a composition $\mathbf{n}$ is,

$$G^T(\mathbf{n}) = \sum_{j=1}^{N_{hc}} G_j(\mathbf{n}_j) + G_w(\mathbf{n}_w) \tag{4.41}$$

where,

$$G_w = \sum_{i=1}^{N_{aq}} n_{iw}\bar{G}_{iw}(\mathbf{n}_w); \qquad G_j = \sum_{i=1}^{N_1} n_{ij}\bar{G}_{ij}(\mathbf{n}_j) \quad \forall\, j = 1, 2, \ldots, N_{hc}. \tag{4.42}$$

The equation of tangent plane $L_j(\mathbf{x})$ at any point $\mathbf{n}$, on the Gibbs free energy surface is different for different phases. The tangent plane for hydrocarbon phases is similar to eq 3.28 and given as,

$$L_j(\mathbf{x}) = \sum_{i=1}^{N_1} x_i\bar{G}_{ij}(\mathbf{n}_j) \quad j = 1, 2, \ldots, N_{hc}. \tag{4.43}$$

Here, $\mathbf{n}_j = [n_{1j}, n_{2j}, \ldots, n_{N_1 j}]$ represents the mole number of components in the hydrocarbon phase. The tangent plane for the aqueous phase differs in the number of components and is given as,

$$L_w(\mathbf{x}) = \sum_{i=1}^{N_{aq}} x_i\bar{G}_{iw}(\mathbf{n}_w). \tag{4.44}$$

Here, $\mathbf{n}_w = [n_{1w}, n_{2w}, \ldots, n_{N_{aq}w}]$. L_w is also different in the partial molar expressions for aqueous phase components ($\bar{G}_{iw}$) than for components present in the hydrocarbon phase ($\bar{G}_{ij}$ in eq 4.43).

The corresponding tangent plane distance functions (D) at any point

$\mathbf{z}$ can be given as,

$$D(\mathbf{z}_j) = G_j(\mathbf{z}_j) - L_j(\mathbf{z}_j) = G_j(\mathbf{z}_j) - \sum_{i=1}^{N_1} z_i \bar{G}_{ij}(\mathbf{n}_j) \quad \forall\, j = 1, \ldots, N_{hc}. \tag{4.45}$$

$$D(\mathbf{z}_w) = G_w(\mathbf{z}_w) - L_w(\mathbf{z}_w) = G_w(\mathbf{z}_w) - \sum_{i=1}^{N_{aq}} z_w \bar{G}_{iw}(\mathbf{n}_w). \tag{4.46}$$

Let $\mathbf{m}$ and $\mathbf{n}$ be two compositions, with same components distributed in both in the aqueous phase and in the hydrocarbon phases but different number of hydrocarbon phases - $N_{hc'}$ and N_{hc} respectively. The Gibbs free energy of the system with composition $\mathbf{n}$ can be given as,

$$\sum_{j=1}^{N_{hc}} G_j(\mathbf{n}_j) = \sum_{i=1}^{N_1} \sum_{j=1}^{N_{hc}} n_{ij} \bar{G}_{ij}(\mathbf{n}_j) = \sum_{i=1}^{N_1} \bar{G}_{ij}(\mathbf{n}_j) \sum_{j=1}^{N_{hc}} n_{ij} \tag{4.47}$$

The equality of chemical potential of all components in all phases was used to simplify above equation. Using the component balance for component i,

$$\sum_{j=1}^{N_{hc}} n_{ij} + n_{iw} = \sum_{j=1}^{N_{hc'}} m_{ij} + m_{iw} \tag{4.48}$$

Eq 4.48 holds for class A as well as class B components and when no reactions occur in the system. Using eqns 4.47 and 4.48,

$$\begin{aligned} \sum_{j=1}^{N_{hc}} G_j(\mathbf{n}_j) &= \sum_{i=1}^{N_1} \bar{G}_{ij}(\mathbf{n}_j)(m_{iw} - n_{iw} + \sum_{j=1}^{N_{hc'}} m_{ij}) \\ &= \sum_{i=1}^{N_1} (m_{iw} - n_{iw}) \bar{G}_{ij}(\mathbf{n}_j) + \sum_{j=1}^{N_{hc'}} \sum_{i=1}^{N_1} m_{ij} \bar{G}_{ij}(\mathbf{n}_j) \\ &= \sum_{i=1}^{N_1} (m_{iw} - n_{iw}) \bar{G}_{ij}(\mathbf{n}_j) + \sum_{j=1}^{N_{hc'}} L_j(\mathbf{m}_j) \end{aligned} \tag{4.49}$$

The difference in Gibbs free energy of the system can be given as,

$$\begin{aligned}\Delta G &= G^T(\mathbf{m}) - G^T(\mathbf{n}) \\ &= \left[\sum_{j=1}^{N_{hc'}} G_j(\mathbf{m}_j) + G_w(\mathbf{m}_w)\right] - \left[\sum_{j=1}^{N_{hc}} G_j(\mathbf{n}_j) + G_w(\mathbf{n}_w)\right] \quad (4.50)\end{aligned}$$

Using eq 4.49,

$$\begin{aligned}\Delta G &= \sum_{j=1}^{N_{hc'}}[G_j(\mathbf{m}_j) - L_j(\mathbf{m}_j)] + [G_w(\mathbf{m}_w) - G_w(\mathbf{n}_w)] - \sum_{i=1}^{N_1}(m_{iw} - n_{iw})\bar{G}_{ij}(\mathbf{n}_j) \\ &= \sum_{j=1}^{N_{hc'}} D(\mathbf{m}_j) + [G_w(\mathbf{m}_w) - G_w(\mathbf{n}_w)] - \sum_{i=1}^{N_1}(m_{iw} - n_{iw})\bar{G}_{ij}(\mathbf{n}_j). \quad (4.51)\end{aligned}$$

This equation is different from the difference in total system Gibbs free energy obtained in eq 3.34 for system with all components distributed in all phases. Thus, in addition to $D(\mathbf{m}_j) \geq 0$ for hydrocarbon phases $j = 1, 2, \ldots, N_{hc'}$, the additional function in eq 4.51 should also be greater than zero for $\mathbf{n}$ to be the global minimum of the Gibbs free energy function and hence, the equilibrium composition.

In special cases of two phase equilibrium, between components in gas and aqueous phase, multiple minima are unlikely. This has been shown by the existence of only two phase - gas and aqueous phase, in experimental studies of gas solubility in aqueous phase. These cases are further discussed in chapter 5, where the equilibrium composition are obtained by equating the chemical potential of components directly without any stability analysis.

4.5 Conclusions

A Gibbs free energy model that integrates different phase descriptions (EOS and activity coefficient model) using the Gibbs free energy function of the entire system was presented in this chapter. The Gibbs free energy function of the entire system was simplified, depending on the system and applications, to obtain equivalent functions. These equivalent functions are used in the subsequent chapters to obtain equilibrium composition.

A tangent plane criteria, for stability analysis to identify the global from the local minima, was developed for a case with different phase descriptions and where all components are non-reacting and not present in all phases.

Chapter 5

Applications: Acid Gas Solubility

In this chapter, the application of the Gibbs free energy model to predict acid gas solubility in water (phase equilibrium calculations) as well as brine with ions (phase and chemical equilibrium) is presented. This chapter begins with an introduction to acid gas injection and the need for accurate solubility models for continuous hydrocarbon production from contaminated gas fields as well as for CO_2 sequestration. The details of the solubility model, previously developed is also presented in the literature section.

5.1 Introduction

About 40% of world gas reserves have been estimated to be contaminated with the acid gases - CO_2 and/or H_2S (IHS, May 2009). There are vast reserves of such fields, also called sour gas fields, having more than 10% of such contaminants in Canada, North Africa, SE Asia/NW Australia and the Middle East. New separation technologies (Li et al., 2006b; van Kemenade and Brouwers, 2012; Klaver and Geers, 2007; Northrop and Valencia, 2009) have enabled production of hydrocarbons from these sour gas fields. This, however, brings with it the challenge to safely dispose the acid gas resulting from the

separation process. An effective acid gas disposal strategy is imperative for continuous hydrocarbon production from these sour gas fields. Aquifers are commonly used for the disposal of the acid gas in sour gas operating fields (Bachu and Gunter, 2004a,b).

The International Energy Agency (IEA), as part of the global efforts to reduce CO_2 in the atmosphere, estimates the Carbon Capture and Storage (CCS) technologies to contribute one-fifth of the total target of halving current levels of emission by 2050 (IEA, 2008). The capture and storage of flue gasses from fossil power plants is part of this plan to reduce emissions. Flue gas is a mixture containing CO_2, H_2S and trace amounts of CH_4. The research efforts pertaining to CO_2 capture and storage have also identified aquifers as efficient storage sites for storing CO_2 by the solubility trapping mechanism (Bachu and Adams, 2003).

In the above applications, it is important to accurately estimate the acid gas solubility in both water as well as brine containing ions at equilibrium. Geochemical reactions occur in the presence of ions. Hence, the solubility of gas in brine is likely to be different than that in pure water. The Gibbs free energy minimization approach is a unified approach that can be used to predict acid gas solubility in water, where only phase equilibrium occurs, as well as in brine, where the presence of ions and solid results in reactions and hence, phase and chemical equilibrium. In the next section, details of acid gas solubility model in water is presented followed by solubility model in brine.

5.2 Acid Gas Solubility in Water

In this application, a model for acid gas solubility prediction in water at high temperatures (298-393 K) and pressures (0.1-80 MPa) has been developed. The advantage of the Gibbs free energy model is its flexibility to use different thermodynamic models. This model uses the Peng Robinson (PR) Equation of State (EOS) description for gas components while the liquid components are described using the ideal assumption for the temperature range 298-323 K and the Non Random Two Liquid (NRTL) activity coefficient model at temperatures greater than 323 K.

Unlike conventional approaches, which rely on experimental data to parameterize Henry's law constant, the proposed model for acid gas solubility in water is predictive for the temperature range of 298-323 K and uses only the Gibbs free energy values at the standard state conditions. The Gibbs free energy values at the standard state conditions for different components have been tabulated in the NIST database (Rossini et al., 1952). The predictions from the model compare well with the experimental values for binary mixtures at varying pressures (0.1-55 MPa) in this temperature range.

At temperatures greater than 323K, the ideal liquid assumption is no longer valid and an activity coefficient model is required to describe the solubility of gas in water. The Non Random Two Liquid (NRTL) activity coefficient model for the aqueous phase has been proposed for predicting solubility. The interaction parameters, used in the proposed activity coefficient model, have been developed as a function of temperature for the binary systems - H_2S-

H_2O and CO_2-H_2O to predict solubility at temperatures greater than 50°C. The linear correlation for interaction parameters, obtained using experimental data for binary systems between 323-383 K, is used to predict mixture solubility for the ternary system of CO_2-H_2S-H_2O. The ternary mixture solubility predictions also compare well with the experimental data at 393 K.

5.2.1 Literature Review

The acid gas solubility models, previously developed, can be classified into two broad types depending on the thermodynamic description of phases. In models of the first type (Type I), aqueous phase components are assumed to be ideal while the gas phase components are described by an EOS model. In models of the other type (Type II), both the aqueous phase and the gas phase are described using a modified EOS. Developments in both these types of solubility models are discussed in this section.

The starting equation for most solubility models is equal fugacities of components in different phases. In this system, the solvent is H_2O (*i=1*) while the solute is CO_2 or H_2S (*i=2*).

$$\bar{f}_{ig} = \bar{f}_{il} \qquad \Rightarrow \quad y_i \hat{\phi}_i P = x_i \gamma_i f_i \qquad i = 1, 2. \tag{5.1}$$

Here, x_i and y_i are the mole fractions of the component in the gas and aqueous phases respectively, $\hat{\phi}_i$ is the fugacity coefficient of component i in the gas phase calculated using an EOS at the system pressure P and f_i is the fugacity of the component in the liquid phase at that pressure. The fugacity of the

component in the liquid phase is further simplified in Type I models to be,

$$f_1 = P_1^{sat} exp\left[\frac{\underline{v}_1(P - P_0)}{RT}\right] \qquad f_2 = \mathcal{H} exp\left[\frac{\bar{v}_2{}^{\infty}(P - P_0)}{RT}\right] \tag{5.2}$$

Here, P_1^{sat} is the saturation pressure of water at the temperature of interest, $P_0 = 1$ atm, $\mathcal{H}$ is the Henry's law constant for the binary system. The exponential terms represent corrections to the fugacities at the total system pressure P, $\underline{v}_1$ is the molar volume of water while $\bar{v}_2^{\infty}$ is the partial molar volume of aqueous solute CO_2 or H_2S at infinite dilution. The Henry's law constant $\mathcal{H}$ and the saturation pressure of water P_1^{sat} (eq 5.2) are also related to the reference states[1].

Carroll and Mather (1989) used this relationship (eq 5.2) to predict solubility of acid gas H_2S at low pressures in aqueous phase. The fugacity coefficient was calculated using a modification to the PR EOS suggested by Stryjek and Vera (1986) and a correlation for the Henry's law constant H was developed using experimental values at different temperatures. Enick and Klara (1990) used the PR EOS to develop similar correlations for Henry's

[1]Rearranging eq A.8 and A.10 to get,

$$\frac{y_i \hat{\phi}_i P}{x_i \gamma_i} = f_i exp\left(\frac{\bar{G}_i^0 - G_i^{IG}}{RT}\right) \quad i = 1. \tag{5.3}$$

$$= f_i exp\left(\frac{\underline{G}_i^0 - G_i^{IG}}{RT}\right) \quad i = 2. \tag{5.4}$$

For solutes, the convention is $\gamma_i \to 1$ as $x_i \to 0$ so that the right side reduces to Henry's law constant $\mathcal{H}$. In case of the solvent, the convention is $\gamma_i \to 1$ as $x_i \to 1$ so that the right side reduces to P^{sat} based on Raoult's law.

law constant. Li and Nghiem (1986) have also used the same approach for predicting the solubility of CO_2 and light hydrocarbon gases in pure and saline water.

In Type II models, the equation of state representation by themselves are not capable of describing the aqueous phase. Several modifications to the EOS (Peng and Robinson, 1980; Stryjek and Vera, 1986) have been proposed to incorporate the aqueous phase for better prediction of vapor liquid equilibrium and vapor pressure data. These modifications include either using separate sets of binary interaction parameters for the components in the aqueous and non-aqueous phases or using different mixing rules for polar asymmetric mixtures (Panagiotopoulos and Reid, 1986). More specifically for acid gases, more accurate EOS for the binary system of both H_2S-H_2O and CO_2-H_2O using virial expansions have been proposed to predict the solubilities (Duan et al., 2007, 1995). These EOS models regress on experimental data to find the coefficients in the virial expansion EOS.

The Henry's law approach, used conventionally, works well at low pressures. However, the acid gas disposal for hydrocarbon processing as well as carbon capture and sequestration occurs at high pressures (200-600 bar). Duan et al. (2007) have also shown that Henry's law approach does not predict accurate solubilities for H_2S at high pressures. The number of coefficients in their proposed virial expansion EOS makes it cumbersome for use in simulators that perform phase equilibrium calculations of mixtures.

The other disadvantage of both these models (types I and II) is its

inability to incorporate geochemical reactions as these models are based only on phase equilibrium computations. The Gibbs free energy minimization approach is used in this application to predict solubility. This approach is adapatable to diffferent brine compositions and provides the flexibility to incorporate ion concentrations in the brine for solubility calculations and hence, incorporate geochemical reactions, as discussed in section 5.3.

5.2.2 Method

In this model, the acid gas (CO_2 or H_2S, $i = 1$) and H_2O ($i = 2$) are the only two components in the gas phase ($j = 1$). In addition to these components, the components in the aqueous phase ($j = 2$) include the ions H^+ ($i = 3$) and OH^- ($i = 4$). As discussed chapter 4, the reference state for components in a gas phase described using an EOS is the pure component ideal gas property. The partial molar Gibbs free energy for gas phase components at any T and P is related to the tabulated values for Gibbs free energy $\underline{G_i}^{IG}$ at standard conditions (eq 4.27) by,

$$\bar{G}_{i1}^{IG}(T,P) = \underline{G_i}^{IG}(T_o,P_o) + RTln(\frac{P}{P_o}) + [\underline{H_i}]_{P_o,T_o}\left(1-\frac{T}{T_o}\right) \quad i = 1,2. \quad (5.5)$$

The solvent, H_2O (i=2) in the aqueous phase, on the other hand, is described using a reference state, $\underline{G_2}^0$ which is the pure component water property at P_0 and T_0 and the Gibbs free energy expressions for the solvent (eq 4.30) in the aqueous phase ($j = 2$) is,

$$\bar{G}_{22}^{0}(T,P) = \underline{G_2}^0(T_o,P_o) + (\underline{v_2})_{T_o}(P-P_o) + [\underline{H_2}]_{P_o,T_o}\left(1-\frac{T}{T_o}\right) \quad (5.6)$$

In the aqueous phase, the solutes are described using a reference state $\bar{G}^{*}_{i2}$ of unit molality m of the solutes - CO_2 or H_2S ($i = 1$), H^+ ($i = 3$), OH^- ($i = 4$) at P_0 and T_0 and converted to unit molarity ($\bar{G}^{0}_{i2}$) to obtain the following expression for partial molar Gibbs free energy of solute component (eq 4.28),

$$\bar{G}^{0}_{i2}(T,P) = \bar{G}^{0}_{i2}(T_o,P_o) + \left(\bar{v}^{\infty}_{i}\right)_{T_o}(P - P_o) + \left[\bar{H}_{i2}\right]_{P_o,T_o}\left(1 - \frac{T}{T_o}\right) \quad i = 1,3,4. \tag{5.7}$$

The total Gibbs free energy function of the entire system (G^T) that includes all components in all phases is,

$$G^T(T,P) = \sum_{i=1}^{N_p}\sum_{i=1}^{N_c} n_{ij}\bar{G}_{ij} \tag{5.8}$$

$$= \underbrace{\sum_{i=1}^{2} n_{i1}[\bar{G}^{IG}_{i1}(T,P) + RTlny_i\hat{\phi}_i]}_{\text{gas phase components}} + \underbrace{n_{22}[{G_2}^{0}(T,P) + RTlnx_2\gamma_2]}_{\text{solvent water}}$$

$$+ \underbrace{\sum_{i=1,i\neq 2}^{4} n_{i2}[\bar{G}^{0}_{i2}(T,P) + RTlnx_i\gamma_i]}_{\text{aqueous phase solutes}}. \tag{5.9}$$

G^T is minimized and the solution corresponds to the equilibrium composition. The balance among elements (C or S , O and H) forms the equality constraint for this minimization. For this system with two phases (N_p=2) and two components ($N_{c1} = 2$) in the gas phase and four components in the aqueous phase ($N_{c2} = 4$), the equilibrium composition is the solution to the constrained nonlinear optimization problem below,

$$\begin{aligned} &\text{Minimize} && G^T(T,P) \\ &\text{Subject to} && \mathbf{AN} = \mathbf{E} \quad \text{and} \quad \mathbf{n_{ij}} \geq \mathbf{0}. \end{aligned} \tag{5.10}$$

Here, **A** is the elemental matrix representing the number of specific elements in each component, **N** is the matrix comprising of moles of each component n_{ij} in each phase (unknowns) while **E** is formed by the total number of moles of each element. As an example, the matrices for the binary system comprising of H_2S ($i = 1$) and H_2O ($i = 2$) when both components are present in the gas phase (j=1) and the aqueous phase (j=2) are,

$$\mathbf{A} = \begin{bmatrix} 1 & 0 & 1 & 0 \\ 0 & 1 & 0 & 1 \\ 2 & 2 & 2 & 2 \end{bmatrix} \qquad \mathbf{N} = \begin{bmatrix} n_{11} \\ n_{12} \\ n_{21} \\ n_{22} \end{bmatrix} \qquad \mathbf{E} = \begin{bmatrix} e_S \\ e_O \\ e_H \end{bmatrix} \tag{5.11}$$

The total moles of each element e (S, O and H) is obtained from the initial number of moles. Depending on the pressure and temperature conditions, H_2O may or may not be present in the gas phase. We perform equilibrium computations for both cases and choose the equilibrium composition that gives the lowest total Gibbs free energy (G^T).

If the objective function, G^T, is convex, the global minimum can be obtained irrespective of initial guesses. While G^T for ideal gas mixture and ideal liquid assumption is a convex function (White et al., 1958), the use of Wilson activity coefficient model for aqueous phase components also results in a convex objective function (McDonald and Floudas, 1995) so that the global minimum may be obtained. In this manuscript, the experimental data presented for comparison have been drawn from different sources where only two phases were observed during experiments. The initial guess values to the optimization problem were varied to check for the presence of multiple

solutions. Multiple solutions did not occur at the temperature and pressure conditions of the solubility models presented in this manuscript.

The RAND algorithm (White et al., 1958) has been used to obtain the solution to the optimization problem. The RAND formulation uses Lagrangian multipliers and the steepest descent method (Smith and Missen, 1982a). We use this approach to find the equilibrium composition and hence solubility, for the binary systems of CO_2-H_2O and H_2S-H_2O as well as for the ternary system of CO_2-H_2S-H_2O.

The conventional approach to calculate phase equilibrium composition is by using the Rachford-Rice algorithm (Rachford Jr and Rice, 1952) using successive substitution where components in both phases are described using EOS (Type II models as defined in the Literature Review section) with initial guess provided by Wilson's correlation. A test system was designed to compute equilibrium composition for the CO_2-H_2O system with two phases using the conventional approach and the Gibbs free energy minimization method. As the phases were pre-defined, no phase stability analysis was performed in either approaches. For the test case, the Gibbs free energy minimization approach using the RAND algorithm was found to be 30 % faster than the conventional approach.

In addition to computational speed, the Gibbs free energy minimization algorithm also provides the advantage of combining different phase description of components (EOS and activity coefficient model). This approach can be extended to include ions present in brine as additional components in the aque-

ous phase and hence, incoporate any geochemical reactions that is discussed in section 5.3. The specific parameter values for such ions (molar volumes and partial molar enthalpies at T_0 and P_0) are available in the literature (Johnson et al., 1992).

5.2.3 Results and Observations

The total Gibbs free energy function of the system G^T is minimized to find the equilibrium composition and hence the gas solubility, for the binary systems of CO_2-H_2O and H_2S-H_2O as well as for the ternary system of CO_2-H_2S-H_2O. The reference state values for the Gibbs free energy at any T and P ($\bar{G}_{i1}^{IG}$, $\bar{G}_{i2}^{0}$ and $\bar{G_2}^0$) are evaluated using the standard state properties of components tabulated in Table 5.1 (Garrels and Christ, 1990) and the expressions in eqns 4.27, 4.28 and 4.30. The fugacity coefficient for components at different pressures has been calculated using the standard expressions available for the PR EOS. The critical properties and the binary interaction coefficients K_{ij} for PR EOS are assumed to be constants for all computation. These values are listed in Table 5.2.

A Henry's law model with fugacity correction for CO_2 in the gas phase (Chang, 1990) is typically used in compositional simulators like UTCOMP and CMG. Figure 4.13 shows a comparision of experimental values of solubility with the Gibbs free energy model and a Henry's law model with fugacity correction in UTCOMP at 25°C. While the predictions from either model are close to experimental values at low pressures, the Henry's law model can

Table 5.1: Thermodynamic properties used for equilibrium computation (Garrels and Christ, 1990). Values are in kJ/moles except partial volume in cm^3.

Component	Thermodynamic property at $T_0 = 25°C$ and $P_0 = 1atm$	Value
H_2S	Gibbs free energy of an ideal gas, $\underline{G_{11}}^{IG}$	-33.02
	Molar enthalpy in gas phase, $\underline{H_1}$	-20.15
	Partial volume of at infinite dilution, $\bar{v_1}^{\infty}$	34.92
	Partial molar Gibbs free energy of aqueous solute, $\bar{G}_1^0$	-27.36
	Partial molar enthalpy of solute in aqueous phase, $\bar{H}_{12}$	-39.33
CO_2	Gibbs free energy of an ideal gas, $\underline{G_{11}}^{IG}$	-394.38
	Molar enthalpy in gas phase, $\underline{H_1}$	-393.51
	Partial volume of at infinite dilution, $\bar{v_1}^{\infty}$	32.80
	Partial molar Gibbs free energy of aqueous solute, $\bar{G}_1^0$	-386.23
	Partial molar enthalpy of solute in aqueous phase, $\bar{H}_{12}$	-412.92
H_2O	Gibbs free energy of an ideal gas, $\underline{G_{21}}^{IG}$	-228.57
	Molar enthalpy of in gas phase, $\underline{H_2}$	-241.81
	Molar volume of H_2O, $\underline{v_2}$	19
	Molar Gibbs free energy, $\underline{G_2}^0$	-237.19
	Molar enthalpy of H_2O in aqueous phase, $\underline{H_{22}}$	-285.84
H^+	Molar volume of H^+, $\underline{v_3}$	
	Partial molar Gibbs free energy in the aqueous phase, $\bar{G}_3^0$	
	Partial molar enthalpy of H^+ in the aqueous phase, $\underline{H_{32}}$	

OH^-	Molar volume of OH^-, $\underset{\_}{v_4}$
	Partial molar Gibbs free energy in the aqueous phase, $\bar{G}_4^0$
	Partial molar enthalpy of OH^- in aqueous phase, $\underset{\_}{H_{42}}$

lead to inaccurate predictions of solubility at high pressures, especially at 25 °C. Mohebbinia (2013) has shown that the predictions using Henry's law correlation, available in UTCOMP, compares well with experimental values at high temperatures (>100°C).

A comparison of the binary model predictions for CO_2-H_2O and H_2S-H_2O, assuming ideal liquid solution ($\gamma_i = 1 \quad \forall i = 1, \ldots 4$), with experimental data for varying pressures at different temperatures is presented in Figures 5.2, 5.3 and 5.4. It can be inferred that the ideal liquid assumption is only valid in the temperature range of 298-323 K for both the binary systems and not at higher temperatures. The proposed solubility model has been classfied into two temperature ranges - the moderate temperature range (between 298-323 K) where the liquid phase is ideal and the high temperature range (temperatures greater than) where the liquid phase is described using an activity coefficient model.

5.2.3.1 Ideal aqueous model for binary system

The Gibbs free energy minimization model predictions assuming ideal aqueous solution have been compared with experimental values at the moderate tempeature range of 298-323 K for both binary systems. The model

Table 5.2: Properties used for evaluation of fugacity coefficient using PR EOS for gas mixture (BIP is binary interaction parameter)

Component (i)	Critical Pressure, P_c (MPa)	Critical Temperature, T_c (K)	Accentric factor, ω	BIP K_{i,H_2O}	BIP K_{i,CO_2}
H_2S	8.942	373.2	0.1	0.087	0.097
CO_2	7.373	304.2	0.225	-0.0576	0
H_2O	22.063	647.1	0.345	0	-0.0576

predictions match well with the experimental values (Figure 5.2). This is reflected in the low average deviation values between the model prediction and the experimental values as well as large R^2 at these temperatures[2] (Table 5.3). The only exception is H_2S-H_2O at 323 K where predictions are still reasonable compared to the experimental values. Also, the H_2S-H_2O system pressure range is low because at high pressures, H_2S forms a separate liquid phase.

In this temperature range, there is no regression with the experimental data. This makes the model predictive in this temperature range as only the thermodynamic properties at standard conditions (Table 5.1) are used to obtain the solubility values from the minimization algorithm.

[2]Coefficient of determination R^2 measures the variability of a data set consisting of model predicted values (y_i) and experimental values (f_i) in terms of mean$\bar{y}$ and sums of squares.

$$R^2 = 1 - \frac{\sum_i (y_i - f_i)^2}{\sum_i (y_i - \bar{y})^2}.$$

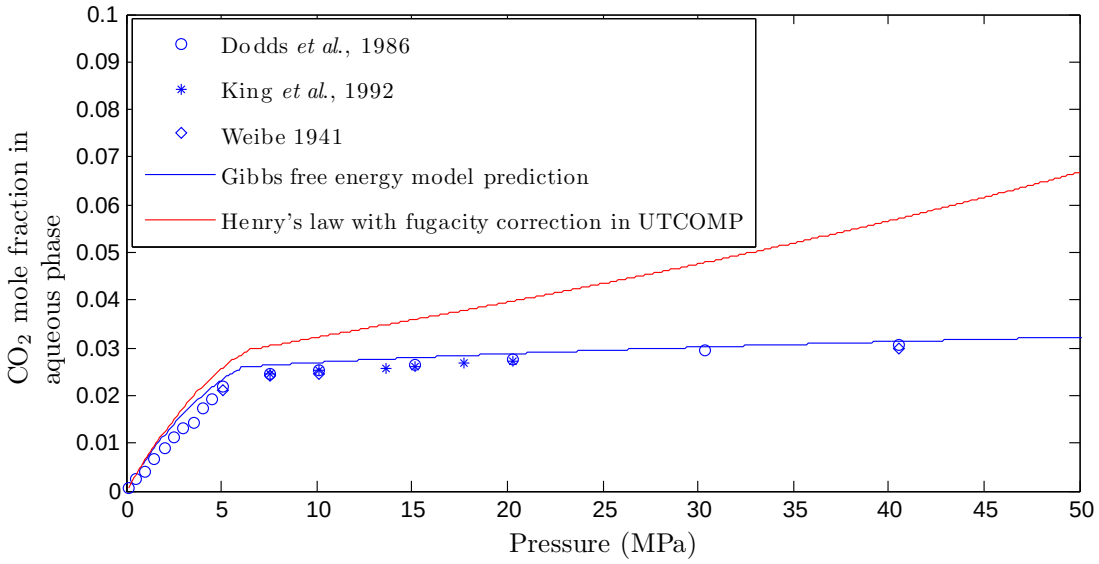

Figure 5.1: Comparison between experimental data with Gibbs free energy model and Henry's law prediction model with fugacity correction prediction at 25° C for CO_2-H_2O system

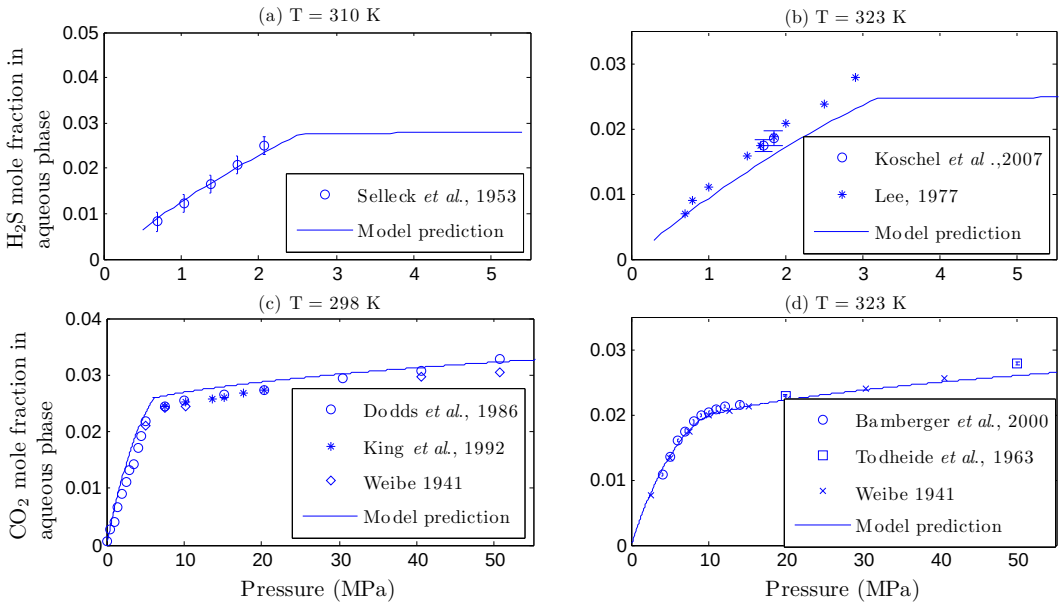

Figure 5.2: Comparison between experimental data and model prediction at moderate temperatures for H_2S-H_2O (a) and (b) and CO_2-H_2O (c) and (d).

Table 5.3: Experimental data source for binary systems and comparison with model prediction

Binary system	Temperature (K)	Experimental data source	R^2	Average deviation (percent)
H_2S-H_2O	310	Selleck et al. (1952)	0.98	4.45 %
H_2S-H_2O	323	Koschel et al. (2007) Lee and Mather (1977)	0.78	14.3 %
CO_2-H_2O	298	Dodds et al. (1956) King et al. (1992) Wiebe (1941)	0.93	13.52%
CO_2-H_2O	323	Bamberger et al. (2000) Tödheide and Franck (1963) Wiebe (1941)	0.98	2.78%

5.2.3.2 NRTL aqueous model for binary system

At higher temperatures, the predictions using the ideal liquid assumption do not match the experimental data at those temperatures for both binary systems (Figures 5.3 and 5.4). To accurately represent the aqueous phase at high temperatures, the NRTL activity coefficient model (Renon and Prausnitz, 1968) is used for components in the aqueous phase. The activity coefficients using the NRTL model along with the thermodynamic properties at standard conditions can be used to estimate the solubility at temperatures greater than 50°C.

The NRTL activity coefficient model has been used extensively to model acid gas solubility in amine solutions (Austgen et al., 1991). In the NRTL model, the activity coefficient is a function of the randomness parameter α_{ij} and the interaction parameter τ_{ij}. The expressions for a binary system (mole

fractions x_1 and x_2) are,

$$
\begin{aligned}
ln\ \gamma_1 &= x_2^2 \left[\tau_{21} \left(\frac{G_{21}}{x_1 + x_2 G_{21}} \right)^2 + \frac{\tau_{12} G_{12}}{(x_2 + x_1 G_{12})^2} \right] \\
ln\ \gamma_2 &= x_1^2 \left[\tau_{12} \left(\frac{G_{12}}{x_2 + x_1 G_{12}} \right)^2 + \frac{\tau_{21} G_{21}}{(x_1 + x_2 G_{21})^2} \right]
\end{aligned}
$$

$$
ln\, G_{12} = -\alpha_{12}\tau_{12} \qquad ln\, G_{21} = -\alpha_{21}\tau_{21} \tag{5.12}
$$

The activity coefficient expression (eq 5.12) reduces to just one variable - the interaction parameter τ, by assuming $\tau_{12} = \tau_{21}$ and $\alpha_{12} = \alpha_{21} = 0.2$ (value for most systems (Renon and Prausnitz, 1968)). The expressions for activity coefficient using this assumption is,

$$
\begin{aligned}
ln\ \gamma_1 &= x_2^2 \left[\tau \left(\frac{G}{x_1 + x_2 G} \right)^2 + \frac{\tau G}{(x_2 + x_1 G)^2} \right] \\
ln\ \gamma_2 &= x_1^2 \left[\tau \left(\frac{G}{x_2 + x_1 G} \right)^2 + \frac{\tau G}{(x_1 + x_2 G)^2} \right]
\end{aligned}
$$

$$
ln\, G = -0.2\tau \qquad \tau = A + \frac{B}{T} \tag{5.13}
$$

A linear correlation for τ is proposed as a function of temperature specific to each binary system (eq 5.13). This correlation is developed using available experimental values in the temperature range 323-383 K. For each binary system, we vary τ to find the particular value τ_0, so that model predictions using the Gibbs free energy minimization method agree well with the available experimental data between 333 and 383 K. We use the coefficient of determination (R^2) as a measure of agreement between the model prediction and the

experimental values. Thus, τ_0 maximizes the coefficient of determination for a dataset containing experimental values of solubility for varying pressures at a particular temperature.

The source of experimental data, the value of τ_0 at that temperature and the largest coefficient of determination at τ_0 are given in Tables 5.4 and 5.5 for both binary systems. In order to ensure continuity, the value of τ_0 at 323 K (zero because ideal solution) has been included in the analysis. Figures 5.3 and 5.4 compares the experimental values and calculated water solubility using the ideal model prediction and the solubility predictions obtained using the τ_0 values in the NRTL activity coefficient model (Tuned NRTL). These τ_0 values have been used to find a linear correlation with (1/T) for both the binary systems (Figure 5.5). Similar linear correlation models have been obtained to describe acid gas solubility in amine solutions (Austgen et al., 1991). The values of the constants A and B in the linear correlation (Table 5.6) are obtained using the linear least-squares minimum approach.

Figures 5.3 and 5.4 compares the experimental values and calculated water solubility using the ideal model prediction and the solubility predictions obtained using the τ_0 values in the NRTL activity coefficient model (Tuned NRTL). These τ_0 values have been used to find a linear correlation with (1/T) for both the binary systems (Figure 5.5). Similar functional relations have been obtained to describe acid gas solubility in amine solutions (Austgen et al., 1991). The values of the constants A and B in the linear correlation obtained using this procedure have been listed in Table 5.6.

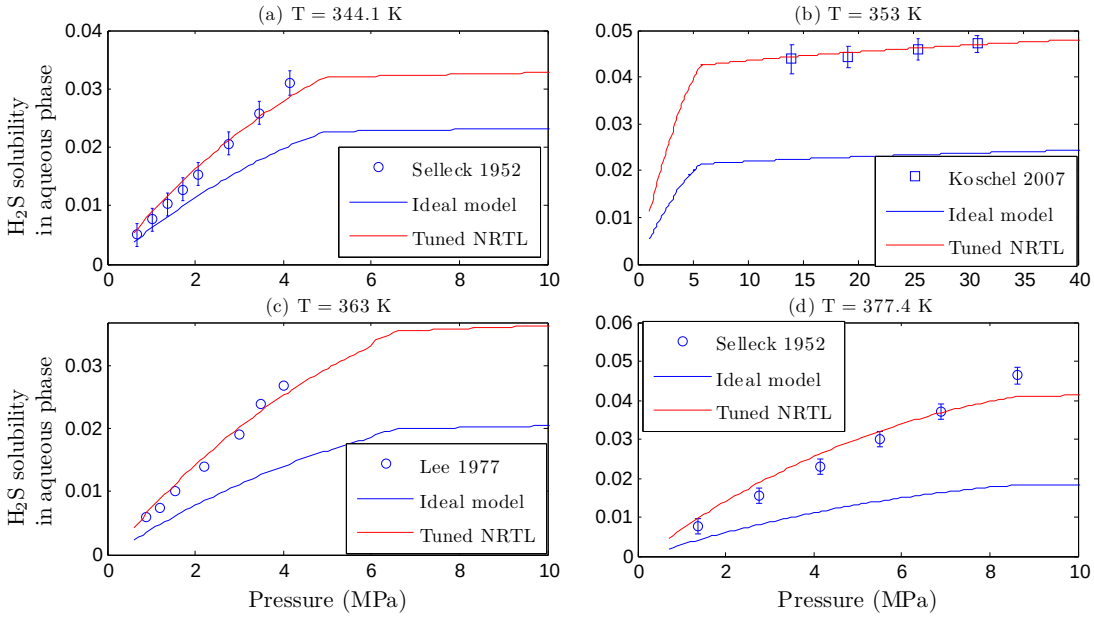

Figure 5.3: Comparison of experimental data with ideal solution prediction and NRTL model with tuned interaction parameter τ_0 to fit experimental data for H_2S-H_2O binary system.

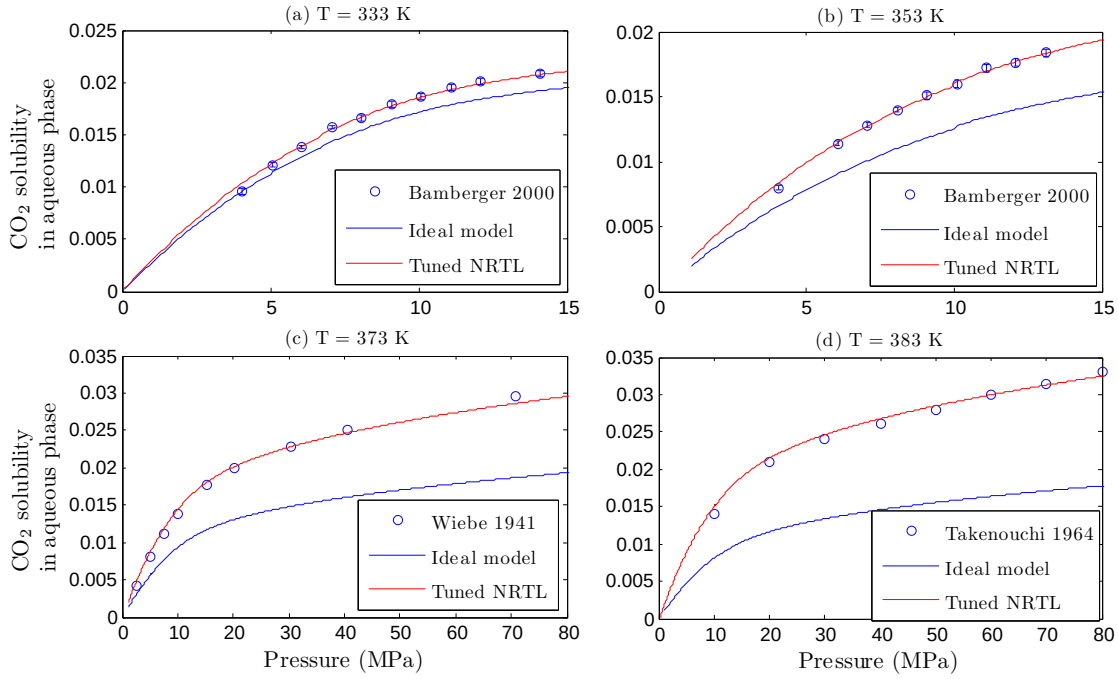

Figure 5.4: Comparison of experimental data with ideal solution prediction and with NRTL tuned interaction parameter τ_0 to fit experimental data for CO_2-H_2O binary system

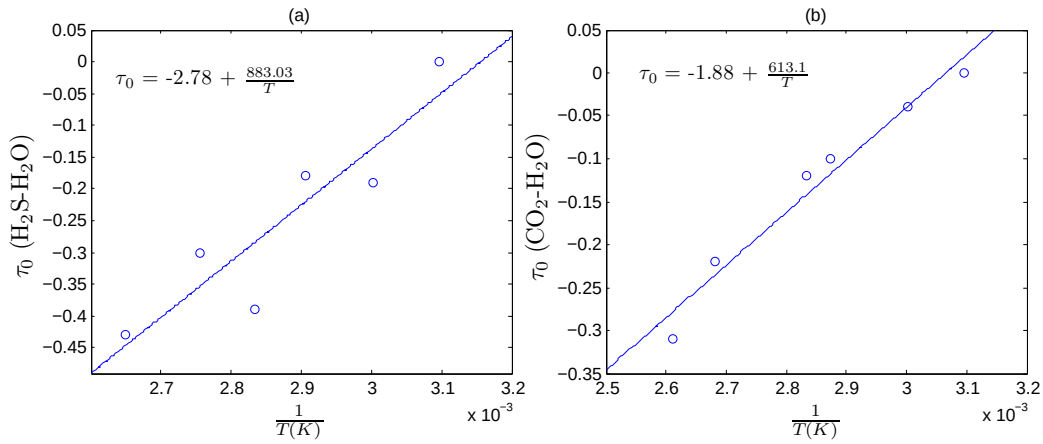

Figure 5.5: (a) Regression over τ_0 to get linear correlation for H_2S-H_2O binary system. (b) Regression over τ_0 to get linear correlation for CO_2-H_2O binary system.

Table 5.4: τ_0 values for H_2S-H_2O system using regression over experimental values

Temperature (K)	Experimental data source	τ_0	Coefficient of determination (R^2)
323	Koschel et al. (2007) Lee and Mather (1977)	0	0.78
333	Lee and Mather (1977)	-0.19	0.98
344.1	Selleck et al. (1952)	-0.18	0.97
353	Koschel et al. (2007)	-0.36	0.83
363	Lee and Mather (1977)	-0.3	0.97
377.4	Selleck et al. (1952)	-0.42	0.94

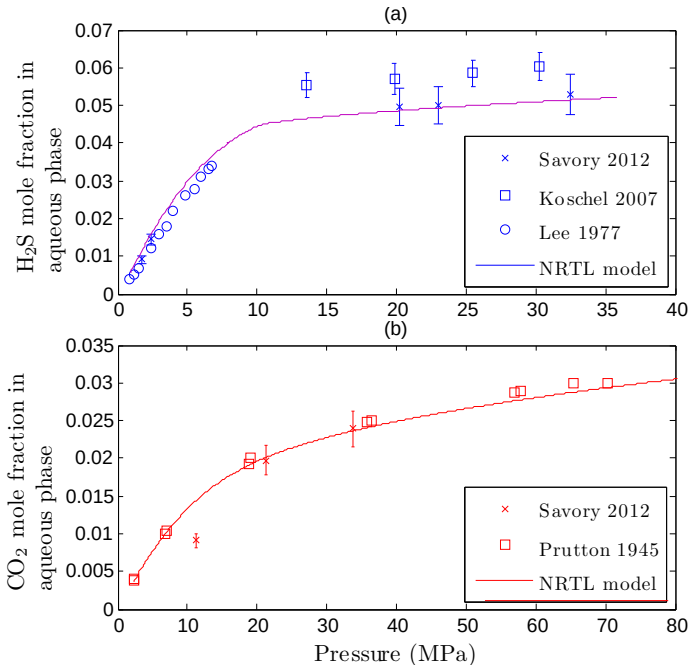

Figure 5.6: (a) Comparision of experimental and model prediction for H_2S solubility in the aqueous phase for the binary system H_2S-H_2O at 393 K. (b) Comparision of experimental and model prediction for CO_2 solubility in the aqueous phase for the binary system CO_2-H_2O at 393 K.

Table 5.5: τ_0 values for CO_2-H_2O system using regression over experimental values

Temperature (K)	Experimental data source	τ_0	Coefficient of determination (R^2)
323	Bamberger et al. (2000) Tödheide and Franck (1963) Wiebe (1941)	0	0.98
333	Bamberger et al. (2000)	-0.04	0.99
348	Wiebe (1941)	-0.1	0.99
353	Bamberger et al. (2000)	-0.12	0.99
373	Wiebe (1941)	-0.22	0.99
383	Takenouchi and Kennedy (1965)	-0.31	0.99

Table 5.6: Constants A and B in the interaction parameter correlation ($\tau = A + \frac{B}{T}$) for binary systems obtained by linear regression over experimental data using least squares method.

Binary system	A	B (K)
H_2S-H_2O	-2.78	883
CO_2-H_2O	-1.88	613.1

Table 5.7: Experimental data source for binary systems at 393 K and comparison with model prediction (Figure 5.6). τ is calculated from the correlation in Table 5.6 for the corresponding binary system.

Binary system	Experimental data source	τ	Coefficient of determination (R^2)	Average deviation
H_2S-H_2O	Lee and Mather (1977) Savary et al. (2012) Koschel et al. (2007)	-0.53	0.94	19 %
CO_2-H_2O	Prutton and Savage (1945) Savary et al. (2012)	-0.32	0.97	6.7 %

The proposed NRTL model, applicable at high temperatures, is validated by comparing with the experimental values at 393 K for the binary systems. This temperature is higher than the range originally used to obtain the interaction parameter correlation and helps validate the correlation. The interaction coefficient τ at 393 K, along with the thermodynamic properties listed in Table 5.1 are used to find the solubility values using the Gibbs free energy minimization method. Figure 5.6 shows a good match between the model prediction and the experimental values and hence validates the correlation for τ. The results are summarized in Table 5.7.

5.2.3.3 Gas phase mole fractions

The critical properties of components used to calculate fugacities of gas phase components are presented in Table 5.2. The binary constant parameters for CO_2-H_2O (Ozah et al., 2005), H_2S-H_2O and CO_2-H_2S (Sandler, 2006) were assumed constants for all equilibrium computations at different pressures and temperatures. A BIP value of 0.087 was assumed for the H_2S-H_2O system.

This assumption was tested by choosing a different value for BIP and finding equilibrium compositions. While similar results were obtained, values lower than 0.03 had convergence problems at high pressures using this approach.

Figure 5.7 shows the impact of varying BIPs on model prediction for the CO_2-H_2O system. The choice of BIP has an influence on equilibrium computations of gas phase compositions but not on the aqueous phase composition. As the value of BIP's are increased, the match with gas phase mole fractions is better. The same procedure can be employed to obtain NRTL parameters with a different choice of BIP for either binary systems.

5.2.3.4 Mixture solubility

The interaction parameters in the NRTL activity coefficient model developed for the binary system are further used to investigate whether it can predict solubility for the ternary mixture of CO_2-H_2S-H_2O. Savary et al. (2012) reported several batch experiments to measure solubility for this ternary system at 393 K. These batch experiments were performed with different initial overall compositions of the mixture. The predictions from the Gibbs free energy minimization model are compared with the experimental results available at 393 K (Figures 5.8(a) and 5.8(c)). The percentage deviation between the model prediction and the experimental value at every data point has been shown in Figures 5.8(b) and 5.8(d). The error in the experimental measurements are about 10-20 % for the mixture solubilities (Savary et al., 2012). It can be seen that the percentage deviation of the majority of points for both

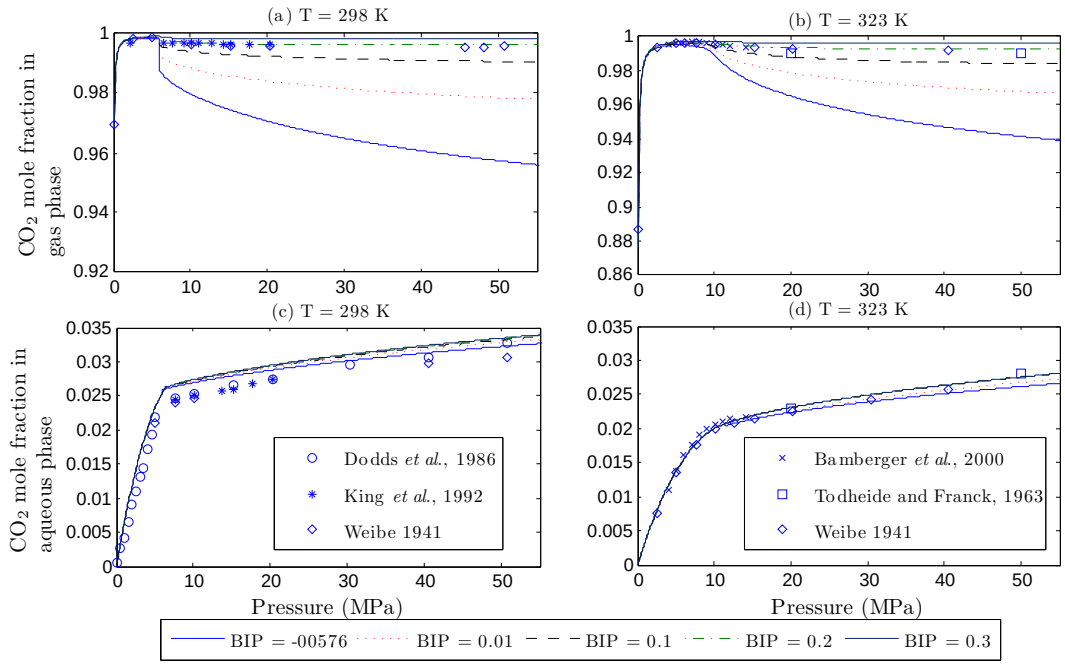

Figure 5.7: Varying BIP's and the comparison between experimental data and model prediction of gas phase mole fractions (a) and (b) and aqueous phase mole fractions (c) and (d) for CO_2-H_2O system at 298 K and 323 K.

H_2S as well as CO_2 lie in this experimental error range.

Experimental data for the ternary mixture is not available at other temperatures, currently. As more data becomes available, a comparison between the experimental data and model prediction, using the interaction coefficients from the binary mixture data, can further help establish temperature ranges where this model is applicable.

In summary, the PR EOS description for gas phase components together with the ideal aqueous solution (between 298-323 K) and the NRTL activity coefficient model with a temperature dependent interaction parameter τ (for temperatures greater than 323 K) can be used to predict the solubility of acid gases in water for the binary systems of H_2S-H_2O and CO_2-H_2O. This approach can also be used to obtain estimates for solubility in the complete mixture (H_2S-CO_2-H_2O) at high temperatures and in the absence of any experimental data.

5.3 Acid Gas Solubility in Brine

In this application, the Gibbs free energy minimization algorithm is extended to a case of phase and chemical equilibrium in the presence of geochemical reactions as result of ions present in brine. Local equilibrium is assumed so that all reactions occuring in the system are at equilibrium. The aqueous phase components are described using the Pitzers activity coefficient model while the gas phase components are described using the PR Equation of State (EOS).

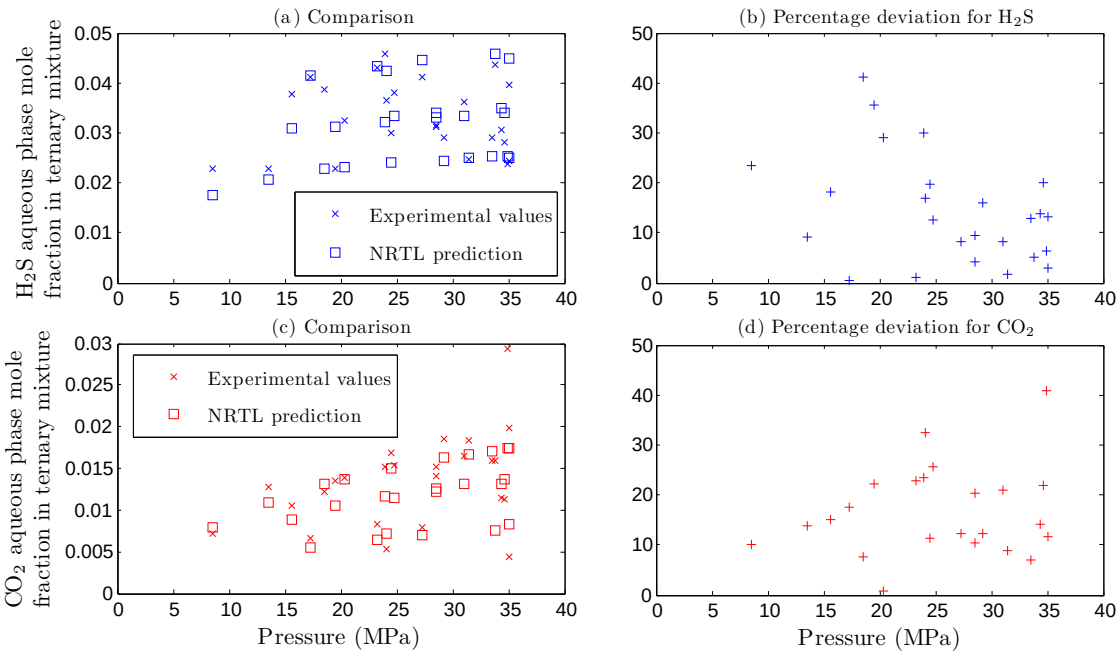

Figure 5.8: (a) Comparision of experimental and model prediction for H_2S solubility in the aqueous phase for the mixture H_2S-CO_2-H_2O at 120°C. (b) Comparision of experimental and model prediction for CO_2 solubility in the aqueous phase for the ternary mixture H_2S-CO_2-H_2O at 120°C.

The Pitzers activity coefficient model extends the ability to make computations for high salinity brine. This activity model accounts for interaction between different ions as well as between molecules (neutral components) and ions (Pitzer, 1973) present in the aqueous phase. Pitzer proposed equations for the activity coefficients for 1-1 (Pitzer and Mayorga, 1973), 2-2 (Pitzer and Mayorga, 1974) as well as mixed electrolytes (Pitzer and Kim, 1974). This activity coefficient model has been used extensively in several geochemical applications including prediction of mineral equilbiria in sea water system (Harvie et al., 1982). The equations corresponding to the Pitzer's activity coefficient model as well as the interaction coefficients between ions are presented in Appendix B.

The interaction parameters listed in Appendix B have been obtained from mineral solubility experiments (Harvie et al., 1982). An example of using experimental data from simple systems to find interaction coefficients (benchmarking) and using the coefficients to make predictions for a more complex system is presented in the following section.

5.3.1 CO_2-$CaCl_2$-H_2O System

The Gibbs free energy minimization algorithm is used to predict CO_2 solubility as a function of pressure in three different $CaCl_2$ solutions of varying mole percents (10.1 mole %, 20.2 mole % and 30.2 mole %) at 120°C in water. This CO_2-$CaCl_2$-H_2O system is chosen for solubility prediction in brine as experimental data is available for this system. Here, CO_2 and H_2O are

gas phase components and CO_2, H^+, OH^-, Ca^{2+}, Cl^- and $CaCl_2$ are aqueous phase solute components in solvent H_2O. The values for the binary interaction coefficients at 25°C for CO_2 and Ca^{2+} ($\lambda_{CO_2-Ca^{2+}}$) and CO_2 and Cl^- ($\lambda_{CO_2-Cl^-}$) as well as the ternary interaction coefficient for CO_2, Ca^{2+} and Cl^- ($\xi_{CO_2-Ca^{2+}-Cl^-}$), as listed in Appendix B, are used in the activity coefficient model. The total Gibbs free energy for the entire system is as given in eq 5.9 and this function is minimized to obtain equilibrium composition values. Figure 5.9 shows the comparison between the model and experiments.

The model qualitatively predicts the experimental behavior of decreasing solubility as $CaCl_2$ concentration in water is increased. The model predictions are reasonably close to experimental values at the high concentration of 30.2 mole % $CaCl_2$ solution but do not match at lower concentrations. One possible reason is that the interaction coefficients in the Pitzer activity coefficient model vary with temperature and pressure and we have considered them as constants (values at 25°C and 1 atm pressure).

The interaction parameters ($\lambda_{CO_2-Ca^{2+}}$, $\lambda_{CO_2-Cl^-}$and $\xi_{CO_2-Ca^{2+}-Cl^-}$) in the Pitzer activity coefficient model are obtained by matching experimental data. As in the previous section, the coefficient of determination (R^2) is used as a measure to these parameter values. The closer the value of R^2 to 1, the better the match between model and experimental data. The tuned parameter values for different $CaCl_2$ concentrations in H_2O are given in Table 5.8. Figure 5.10 a shows comparison of tuned model for CO_2 solubility with experimental data for 10.1 % $CaCl_2$ solution.

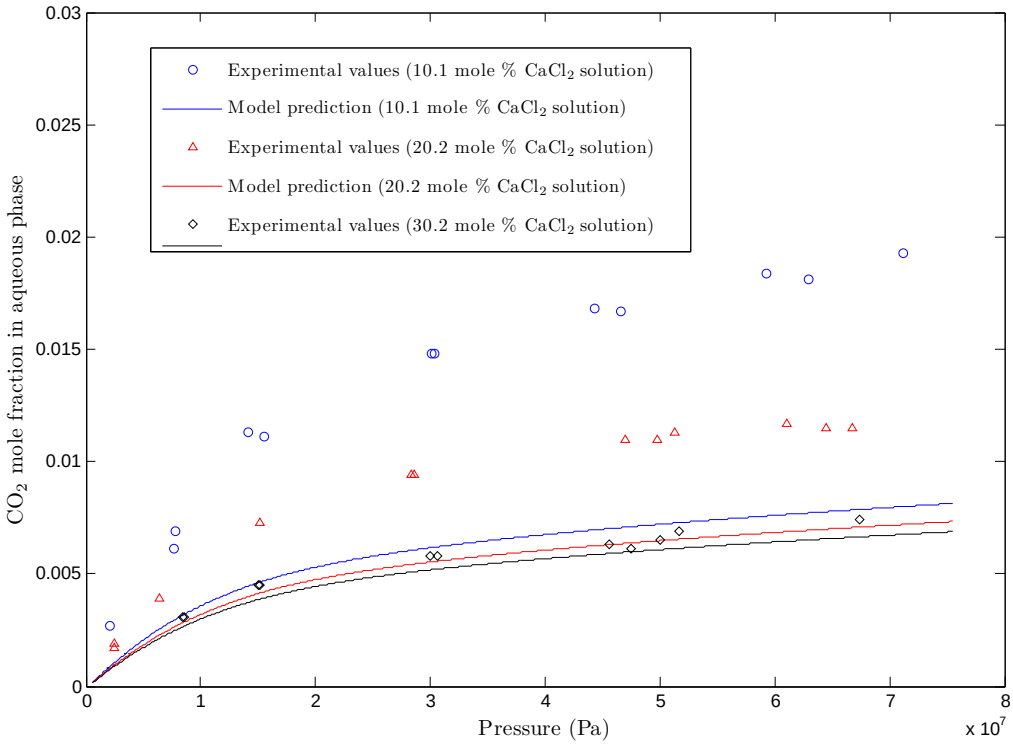

Figure 5.9: Comparision of experimental values (Prutton and Savage, 1945) and model prediction for CO_2 solubility in different concentrations of $CaCl_2$ solution at 120°C.

Table 5.8: Tuned Pitzer activity coefficient parameter values for CO_2-$CaCl_2$-H_2O system

$CaCl_2$ mole in H_2O	Tuned binary parameter ($\lambda_{CO_2-Ca^{2+}}$, $\lambda_{CO_2-Cl^-}$)	Tuned ternary parameter ($\xi_{CO_2-Ca^{2+}-Cl^-}$)	R^2
10.1 %	-0.02, -0.02	-0.0002	0.99
20.2 %	0.025, 0.025	-0.0002	0.99
30.2 %	0.061, 0.061	-0.0002	0.97

5.3.2 Model Prediction for CO_2-$CaCl_2$-H_2O and $CaCO_3$ (Solid)

The Pitzer activity coefficient along with the tuned interaction parameter values obtained from the above section are used to predict the solubility for a complex system that contains calcite ($CaCO_3$ solid) in addition to the $CaCl_2$ solution. The model predictions have been compared with the corresponding experimental predictions and help validate the parameter values obtained in the previous section.

The presence of solid phase (calcite) introduces additional components in the aqueous phase. The complete system then consists of three phases - gas phase ($j = 1$) with components CO_2 ($i = 1$), H_2O ($i = 2$), solvent H_2O, aqueous phase ($j = 2$) components CO_2, Ca^{2+} ($i = 3$), HCO_3^- ($i = 4$), Cl^- ($i = 5$), H_2CO_3 ($i = 6$), $CaCO_3$($i = 7$) and and solid phase ($j = 3$) component

$CaCO_3$. The total Gibbs free energy of the system (G^T) is given as,

$$\begin{aligned} G^T(T,P) &= \underbrace{\sum_{i=1}^{2} n_{i1}[\bar{G}_{i1}^{IG}(T,P) + RTlny_i\hat{\phi}_i]}_{\text{gas phase components}} + \underbrace{n_{22}[\underline{G}_2{}^0(T,P) + RTlnx_2\gamma_2]}_{\text{solvent water}} \\ &+ \underbrace{\sum_{i=1,i\neq 2}^{7} n_{i2}[\bar{G}_{i2}^{0}(T,P) + RTlnx_i\gamma_i]}_{\text{aqueous phase solutes}} + \underbrace{n_7[\underline{G}_7(T,P)]}_{\text{solid } CaCO_3}. \end{aligned} \tag{5.14}$$

The optimization formulation to find equilibrium composition for this system can be given as,

$$\begin{aligned} &Minimize \qquad G^T(T,P) \\ &\text{Subject to} \qquad \mathbf{AN} = \mathbf{E} \quad \text{and} \quad \mathbf{n_{ij}} \geq \mathbf{0}. \end{aligned} \tag{5.15}$$

$$\mathbf{A} = \begin{bmatrix} 1 & 0 & 1 & 0 & 0 & 1 & 0 & 1 & 1 & 1 \\ 2 & 1 & 2 & 1 & 0 & 3 & 0 & 3 & 3 & 3 \\ 0 & 2 & 0 & 2 & 0 & 1 & 0 & 2 & 0 & 0 \\ 0 & 0 & 0 & 0 & 1 & 0 & 0 & 0 & 1 & 1 \\ 0 & 0 & 0 & 0 & 0 & 0 & 1 & 0 & 0 & 0 \end{bmatrix} \qquad \mathbf{E} = \begin{bmatrix} e_C \\ e_O \\ e_H \\ e_{Ca} \\ e_{Cl} \end{bmatrix}$$

$$\mathbf{N} = \begin{bmatrix} n_{11} & n_{21} & n_{12} & n_{22} & n_{32} & n_{42} & n_{52} & n_{62} & n_{72} & n_{73} \end{bmatrix}^T \tag{5.16}$$

The thermodynamic properties for the different components in the complete system at 25°C used for equilibrium calculation using the Gibbs free minimization approach are listed in Tables 5.1 and 5.9. The model predictions compare well with the experimental observations ($R^2 = 0.77$ in Figure 5.10).

In summary, unlike the acid gas solubility model in pure water at low temperatures (section 5.2.3.1), regression is used to obtain the activity coefficient model interaction parameters that match the experimental solubility

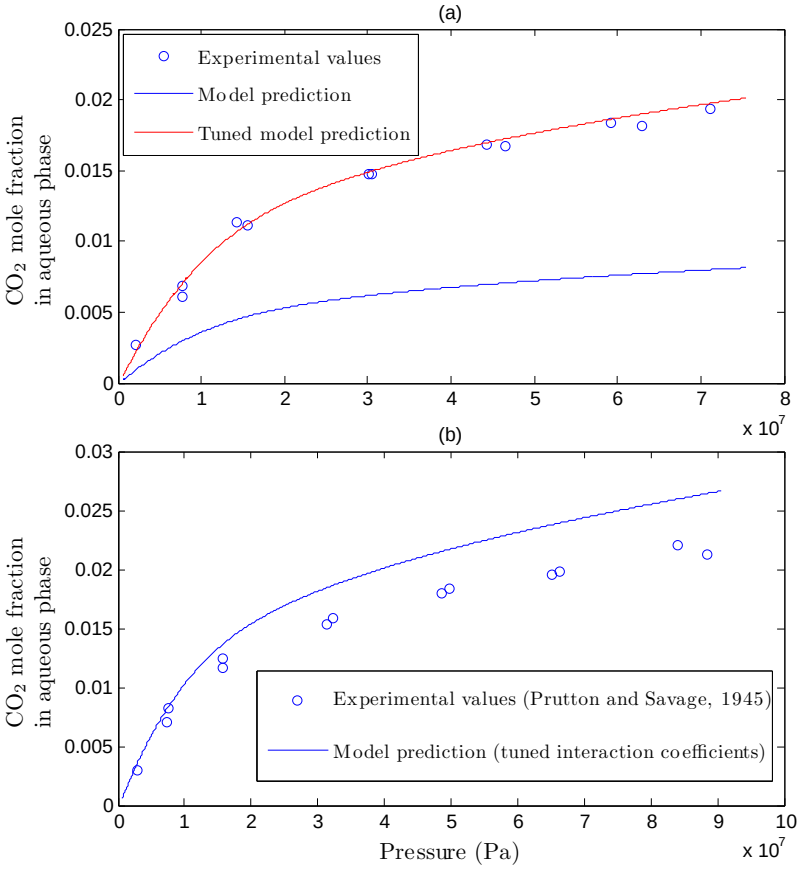

Figure 5.10: (a) Model prediction and tuning interaction parameters for match with experiments (Prutton and Savage, 1945) for benchmarking case of 10.1 mole % CO_2-$CaCl_2$ system at 120°C. (b) Comparision of model prediction and experiments (Prutton and Savage, 1945) for complex system of CO_2-$CaCl_2$ and solid $CaCO_3$ at 120°C.

Table 5.9: Thermodynamic properties of components (Garrels and Christ, 1990). Values are in kJ/moles except partial volume in cm^3.

Component	Thermodynamic property at $T_0 = 25°C$ and $P_0 = 1atm$	Value
Ca^{2+}	Molar volume, $\bar{v}_1$	
	Partial molar Gibbs free energy of in the aqueous phase, $\bar{G}_1^0$	-553.04
	Partial molar enthalpy in the aqueous phase, $\bar{H}_{12}$	-542.96
Cl^-	Molar volume, $\bar{v}_2$	
	Partial molar Gibbs free energy of in the aqueous phase, $\bar{G}_2^0$	-131.17
	Partial molar enthalpy in the aqueous phase, $\bar{H}_{22}$	-167.46
CO_3^-	Molar volume, $\bar{v}_3$	
	Partial molar Gibbs free energy of in the aqueous phase, $\bar{G}_3^0$	-528.10
	Partial molar enthalpy in the aqueous phase, $\bar{H}_{32}$	-676.26
HCO_3^-	Molar volume, $\bar{v}_4$	
	Partial molar Gibbs free energy of in the aqueous phase, $\bar{G}_4^0$	-587.06
	Partial molar enthalpy in the aqueous phase, $\bar{H}_{42}$	-691.11
$CaCl_2$	Molar volume, $\bar{v}_5$	
	Partial molar Gibbs free energy of in the aqueous phase, $\bar{G}_5^0$	-816.05
	Partial molar enthalpy in the aqueous phase, $\bar{H}_{52}$	-877.3
H_2CO_3	Molar volume, $\bar{v}_6$	
	Partial molar Gibbs free energy of in the aqueous phase, $\bar{G}_6^0$	-623.42
	Partial molar enthalpy in the aqueous phase, $\bar{H}_{62}$	-698.73

	Molar volume , $\underline{v}_7$	
	Partial molar Gibbs free energy of in the aqueous phase, $\bar{G}_7^0$	-1099.39
	Partial molar enthalpy	-1196.62
$CaCO_3$	in the aqueous phase, $\bar{H}_{72}$	
	Molar Gibbs free energy of	-1128.76
	in the solid phase, $\underline{G}_7$	
	Molar enthalpy	-1206.87
	in the aqueous phase, $\bar{H}_{72}$	

predictions for the simpler case of CO_2 in $CaCl_2$ aqueous solution. These parameters are further used to predict the solubility for a complex system containing solid $CaCO_3$ in addition to the aqueous and the gas phase. A comprehensive list of of binary and ternary interaction coefficients for commonly occuring ions have been presented in the Appendix B. These coefficients can be used to predict solubility of brine having any composition.

The Gibbs free energy minimization approach can thus be used to predict solubility of gases in high salinity brine containing different ions by utilizing the experimental data available for a simplified system.

5.4 Conclusions

In the first application of phase equilibrium (no reactions), an acid gas solubility model was developed using the Gibbs free energy minimization method for binary systems of H_2S-H_2O and CO_2-H_2O at high temperatures (298-393 K) and varying pressures (1-80 MPa). This model uses the tabulated thermodynamic properties (Rossini et al., 1952) at standard conditions.

The Henry's law approach with fugacity corrections commonly used in simulators like UTCOMP result in inaccurate solubility estimates at high pressures (pressures >10 MPa). The Gibbs free energy model predictions in the temperature range of 298-323 K, assuming ideal liquid phase and PR EOS for gas phase components, compare well with experimental values. The NRTL activity coefficient model with temperature dependent interaction parameters (τ) have been proposed to predict solubility at temperatures greater than 323 K.

The interaction parameters for the binary systems can be further used as an estimate for CO_2 and H_2S solubility in the ternary system of H_2S-CO_2-H_2O. The average deviation for the ternary model prediction with the experimental values at 393 K is 14.4% for H_2S and 21.1% for CO_2 in the pressure range 1-40 MPa. However, ternary mixture experimental data at different temperatures are required to establish when interaction parameters, obtained from binary mixture data, can be used for predicting the ternary mixture solubility.

The Gibbs free energy minimization approach has also been used for a system with geochemical reactions in addition to phase equilibrium. In this case, the aqueous phase components were described using the Pitzer activity coefficient model. Models using the interaction coefficients in the Pitzer activity coefficient from mineral solubility data do not match experimental values. The interaction parameters were tuned to match available experimental data of simple systems and further make predictions for more complex systems.

This approach was illustrated using a particular case of CO_2-$CaCl_2$ system, where available experimental data was used to obtain the interaction coefficients. The new interaction coefficients were further used to predict solubility of CO_2 in more complex system with $CaCO_3$ solid. The model predictions compare well with experimental values.

Thus, the solubility estimates of gas in water as well as brine obtained using this model can aid in designing acid gas injection schemes that are critical to producing hydrocarbons from these sour gas fields. These estimates can also be used to evaluate the storage capacity of potential aquifers for flue gases. The solubility models developed in this chapter helps demonstrate the applications of the Gibbs free energy minimization as a unified approach in not just phase equilibrium calculations but also phase and chemical equilibrium calculations of solubility in the presence of brine and solid.

Chapter 6

Applications: Hydrocarbon Phase Behavior

The application of Gibbs free energy model to predict phase behavior of three different hydrocarbon mixtures - CO_2-CH_4-H_2O, CO_2-$nC_{14}H_{30}$-H_2O and CH_4-CO_2-$nC_{16}H_{34}$-H_2O are presented in this chapter. The impact of geochemical reactions on the phase behavior of hydrocarbon mixture is also presented using the Gibbs free energy model. This further demonstrates the applicability of the Gibbs free energy approach to predict not just phase equilibrium (no reactions) but also phase and chemical equilibrium (with reactions).

6.1 Introduction

CO_2 is injected in hydrocarbon reservoirs under specific conditions of temperature and pressure to attain miscibility with the hydrocarbon phases and thereby, increase oil recovery. The Gibbs free energy model can be used to predict hydrocarbon phase changes associated with this injection.

The CO_2 injection may also result in geochemical reactions because of ions in the brine as well as the solid phase components of a carbonate reservoir. The equilibrium composition arising out of geochemical reactions can be obtained using the stochiometric as well as the Gibbs free energy minimization

approach. As illustrated in the case study presented in section 3.22, the Gibbs free energy model is faster than the stochiometric approach when solving the same number of nonlinear equations.

The current methods (Nghiem et al., 2010; Chang, 1990) to model hydrocarbon phase behavior with geochemical reactions solve the phase and the reaction equilibrium problems separately. In these methods, Henry's law is used to estimate CO_2 concentration in aqueous phase that is further used as the initial CO_2 aqueous concentration to obtain equilibrium composition arising out of geochemical reactions.

As shown in section 5.2.3, estimates of CO_2 concentration in the aqueous phase using the Henry's law are not accurate at higher pressures. Because equilibrium concentration of a reactive system depend on initial concentrations, this method of decoupling phase and chemical equilibrium problems could result in inaccurate predictions of equilibrium concentration of components. Further, as the concentration of components change after the reactions, the fugacities of CO_2 in aqueous phase and the hydrocarbon phases are not equal. This further impacts the hydrocarbon phase behavior computations and is not accounted in these methods.

The Gibbs free energy model can be used to accurately model such cases. The Gibbs free energy approach integrates phase behavior computations corresponding to the hydrocarbons as well as geochemical reaction equilibrium computations corresponding to the ions in the brine and the solid phase. The global minimum of the Gibbs free energy function of the entire system, in-

cluding all components in oleic, aqueous and solid phases, correponds to the equilibrium composition arising out of both phase equilibrium and chemical reactions between the components in the system. At the global minimum of the Gibbs free energy function, the partial molar Gibbs free energy of the components distributed in different phases are equal and hence, are their fugacities. Additionally, at the global minimum, geochemical reactions occuring between components result in relationships like eq 3.45 at equilibrium.

The Gibbs free energy model is used to compute the equilibrium composition corresponding to phase and chemical equilibrium for different mixtures in this chapter. The reservoir rock constitutes the solid phase in the Gibbs free energy model in addition to hydrocarbon and aqueous phases. While a carbonate reservoir rock may consist of a mixture of components, the solid phase is represented by a single component - calcite ($CaCO_3$), for all cases of geochemical reactions discussed in this chapter.

6.2 Hydrocarbon Phase Equilibrium

In this section, the Gibbs free energy minimization approach is used to predict equilibrium composition for cases of phase equilibrium of hydrocarbon mixtures. There are no reactions considered in this section and the equilibrium compositions are only because of phase equilibrium. The two specific mixtures discussed in the following sections were chosen as experimental values are available for these systems.

6.2.1 CO_2-$nC_{14}H_{30}$ and CO_2-$nC_{14}H_{30}$-H_2O Mixture

Mangone (1985) performed experiments on the CO_2-$nC_{14}H_{30}$ system to obtain the two-phase envelope for this system. These experiments were performed at 343 K for different compositions. For a particular composition, the pressure is varied and the bubble and the dew points are inferred from the volumetric measurement of phases. An additional set of experiments were performed in the presence of water to obtain the phase envelope for the CO_2-$nC_{14}H_{30}$-H_2O system.

The Gibbs free energy model was used to obtain the equilibrium composition of the CO_2-$nC_{14}H_{30}$ system for a fixed overall composition at 343 K and various pressures. As all components are described using the PR EOS, the reference state of components is the ideal gas state so that the equivalent function H can be minimized to find equilibrium compositions (section 4.3.2.2). The equilibrium compositions are the solution to the following optimization problem,

$$\begin{aligned} &Minimize \quad H = \sum_{i=1}^{N_c} \sum_{j=1}^{N_p} n_{ij}[RTln(x_{ij}\hat{\phi}_i)] \\ &\text{Subject to} \qquad \mathbf{AN} = \mathbf{E} \quad \text{and} \quad \mathbf{n_{ij}} \geq \mathbf{0}. \end{aligned} \tag{6.1}$$

If there are two phases at equilibrium, $N_p = 2$. The constraint equation can be given as,

$$\begin{aligned} \mathbf{A} &= \begin{bmatrix} 1 & 14 & 1 & 14 \\ 2 & 0 & 2 & 0 \\ 0 & 30 & 0 & 30 \end{bmatrix}; \qquad \mathbf{E} = \begin{bmatrix} e_C \\ e_O \\ e_H \end{bmatrix}; \\ \mathbf{N} &= \begin{bmatrix} n_{11} & n_{21} & n_{21} & n_{22} \end{bmatrix}^T. \end{aligned} \tag{6.2}$$

In the above equation, C, O and H are the elements that are conserved. As this is a phase equilibrium problem, an equivalent constraint set can be given using the components (CO_2 and n-$C_{14}H_{30}$) as base components that are conserved. While **N** remains the same, the matrices **A** and **E** in this equivalent constraint set is,

$$\mathbf{A} = \begin{bmatrix} 1 & 0 \\ 0 & 1 \end{bmatrix}; \qquad \mathbf{E} = \begin{bmatrix} e_{CH_4} \\ e_{C_{14}H_{30}} \end{bmatrix}. \tag{6.3}$$

Equilibrium computations were performed for a fixed overall composition assuming two phases and the total Gibbs free energy of the system, G^T (or, equivalently H) is compared with that of a single phase system. The combination corresponding to lowest G^T is the equilibrium composition at that temperature and pressure. This information is used to plot the phase envelope for the CO_2-n$C_{14}H_{30}$ binary system in Figure 6.1. All components are described using the PR EOS for this binary system.

For the CO_2-n$C_{14}H_{30}$-H_2O mixture, the hydrocarbon phase components are described using the PR EOS while the aqueous phase is described using the Pitzer activity coefficient model (Appendix B). The equilibrium composition for this system is the minimum of the Gibbs free energy function for this system (similar to eq 4.32) given as,

$$\begin{aligned} G^T(T,P) &= \sum_{i=1}^{3} n_{i1}[\underline{G_i}^{IG}(T,P) + RTlny_i\hat{\phi}_i] + \sum_{i=1}^{2} n_{i2}[\bar{G}^0_{i2}(T,P) + RTlnx_i\gamma_i] \\ &+ n_{32}[\bar{G}^0_3(T,P) + RTlnx_3\gamma_3]. \end{aligned} \tag{6.4}$$

The matrices in the elemental balance contraint for this system are,

$$\begin{aligned}
\mathbf{A} &= \begin{bmatrix} 1 & 14 & 0 & 1 & 14 & 0 \\ 2 & 0 & 1 & 2 & 0 & 1 \\ 0 & 30 & 2 & 0 & 30 & 2 \end{bmatrix}; \qquad \mathbf{E} = \begin{bmatrix} e_C \\ e_O \\ e_H \end{bmatrix}; \\
\mathbf{N} &= \begin{bmatrix} n_{11} & n_{21} & n_{31} & n_{12} & n_{22} & n_{32} \end{bmatrix}^T. \qquad (6.5)
\end{aligned}$$

The experimental measurements for the CO_2-$nC_{14}H_{30}$-H_2O mixture (Mangone, 1985) were made for equal initial volumes of water and $nC_{14}H_{30}$. This corresponds to a constant mole ratio of 14.45 between total moles of H_2O and total moles of $nC_{14}H_{30}$, calculated using the molecular weights and densities of H_2O and $nC_{14}H_{30}$. A comparison of model prediction for the CO_2-$nC_{14}H_{30}$-H_2O with experimental measurements, converted to a water-free basis, are also shown in Figure 6.1. As an example, consider a case of $nC_{14}H_{30}$ = 0.0157, CO_2 = 0.7582 and H_2O = 0.2261 (equal volume of $nC_{14}H_{30}$). The equivalent mole fraction excluding water, also refered to as the water free basis in this representation, corresponds to $nC_{14}H_{30}$ = 0.02 and CO_2 = 0.88.

The binary interaction parameters (Table 6.1) were obtained by tuning the experimental data in Figure 6.1. The thermodynamic properties are listed in Table 6.2. These parameters are further used for computations involving geochemical reactions (phase and chemical equilibrium). The presence of H_2O shifts the two-phase envelope of the hydrocarbon system towards lower moles of $nC_{14}H_{30}$. This shift occurs because some CO_2 enters the aqueous phase and the overall mole faction of CO_2 in phase equilibrium with $nC_{14}H_{30}$ decreases.

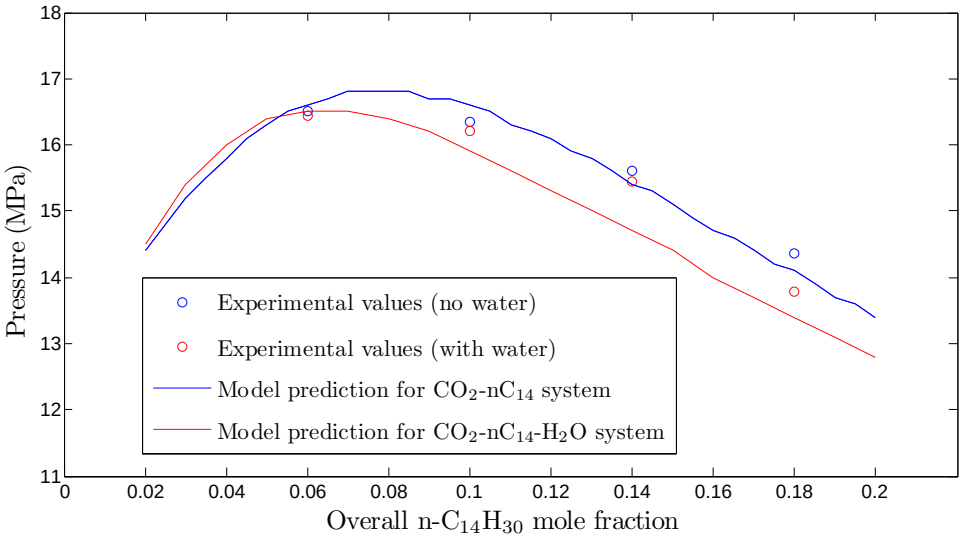

Figure 6.1: Two-phase envelope for CO_2-$C_{14}H_{30}$ and CO_2-$C_{14}H_{30}$-H_2O mixtures at 343 K.

Table 6.1: Properties of components used in PR EOS for CO_2-$C_{14}H_{30}$ and CO_2-$C_{14}H_{30}$-H_2O mixtures

Component (i)	Critical Pressure (MPa)	Critical Temperature (K)	Accentric Factor (w)	BIP K_{i,H_2O} (tuned)	BIP K_{i,CO_2} (tuned)
$C_{14}H_{30}$	1.62	693	0.644	0.95	0.0889
CO_2	7.376	304.2	0.225	0.4	0
H_2O	22.06	647	0.344	0	0.4

6.2.2 CH_4-CO_2-H_2O Mixture

Song and Kobayashi (1994) have performed experiments of water solubility in a CH_4 (5.31 mole %) - CO_2 (94.69 mole %) mixture. The Gibbs free energy minimization is used to predict the solubility values for this system. All three components - CH_4 ($i = 1$) , CO_2 ($i = 2$) and H_2O ($i = 3$) are present in the gas phase ($j = 1$) and the aqueous phase ($j = 2$). The Gibbs free energy function for this system with PR EOS and activity coefficient is also given by eq 6.4. The matrices in the elemental balance constraint are,

$$\begin{aligned} \mathbf{A} &= \begin{bmatrix} 1 & 1 & 0 & 1 & 1 & 0 \\ 0 & 2 & 1 & 0 & 2 & 1 \\ 4 & 0 & 2 & 4 & 0 & 2 \end{bmatrix}; \qquad \mathbf{E} = \begin{bmatrix} e_C \\ e_O \\ e_H \end{bmatrix}; \\ \mathbf{N} &= \begin{bmatrix} n_{11} & n_{21} & n_{31} & n_{12} & n_{22} & n_{32} \end{bmatrix}^T. \end{aligned} \tag{6.6}$$

As no ions are present in the aqueous phase, this is an example of only phase equilibrium. The PR EOS is used to describe the gas phase while the aqueous phase is described using the Pitzer activity coefficient model. The Gibbs free energy model predictions compare well with experimental results (Figure 6.2). The thermodynamic values used for this model are listed in Table 6.2 while the PR EOS parameters used are given in Table 6.3.

6.2.3 CH_4-CO_2-n-$C_{16}H_{34}$ Mixture

In this section, the Gibbs free energy minimization approach is used to predict equilibrium composition of the hydrocarbon mixture consisting of 5 mole % CH_4 ($i = 1$), 90 mole % CO_2 ($i = 2$) and 5 mole % n-$C_{16}H_{34}$ ($i = 3$). Pan et al. (1998) have shown that an additional CO_2 rich phase is formed

Table 6.2: Thermodynamic properties used for equilibrium computation (Garrels and Christ, 1990). Values are in kJ/moles. Partial volume is in cm^3.

Component (i)	Thermodynamic property at $T_0 = 25°C$ and $P_0 = 1atm$	Value
	Gibbs free energy of an ideal gas, $\underline{G_i}^{IG}$	-394.38
	Molar enthalpy in gas phase, $\underline{H_i}$	-393.51
CO_2	Partial volume of at infinite dilution, $\bar{v}_1{}^{\infty}$	32.80
	Partial molar Gibbs free energy of aqueous solute, $\bar{G}_1^0$	-386.23
	Partial molar enthalpy of solute in aqueous phase, $\bar{H}_{12}$	-412.92
	Gibbs free energy of an ideal gas, $\underline{G_i}^{IG}$	-228.57
	Molar enthalpy of in gas phase, $\underline{H_i}$	-241.81
H_2O	Molar volume of H_2O, $\underline{v_2}$	19
	Molar Gibbs free energy, $\underline{G_2}^0$	-237.19
	Molar enthalpy of H_2O in aqueous phase, $\underline{H_{22}}$	-285.84
	Gibbs free energy of an ideal gas, $\underline{G_i}^{IG}$	-50.79
	Molar enthalpy of in gas phase, $\underline{H_i}$	-74.85
CH_4	Partial volume of at infinite dilution, $\bar{v}_1{}^{\infty}$	37.14
	Partial molar Gibbs free energy of aqueous solute, $\bar{G}_1^0$	16.26
	Partial molar enthalpy of solute in aqueous phase, $\bar{H}_{12}$	-13.16
	Gibbs free energy of an ideal gas, $\underline{G_i}^{IG}$	65.64
$C_{14}H_{30}$	Molar enthalpy of in gas phase, $\underline{H_i}$	-329.8133

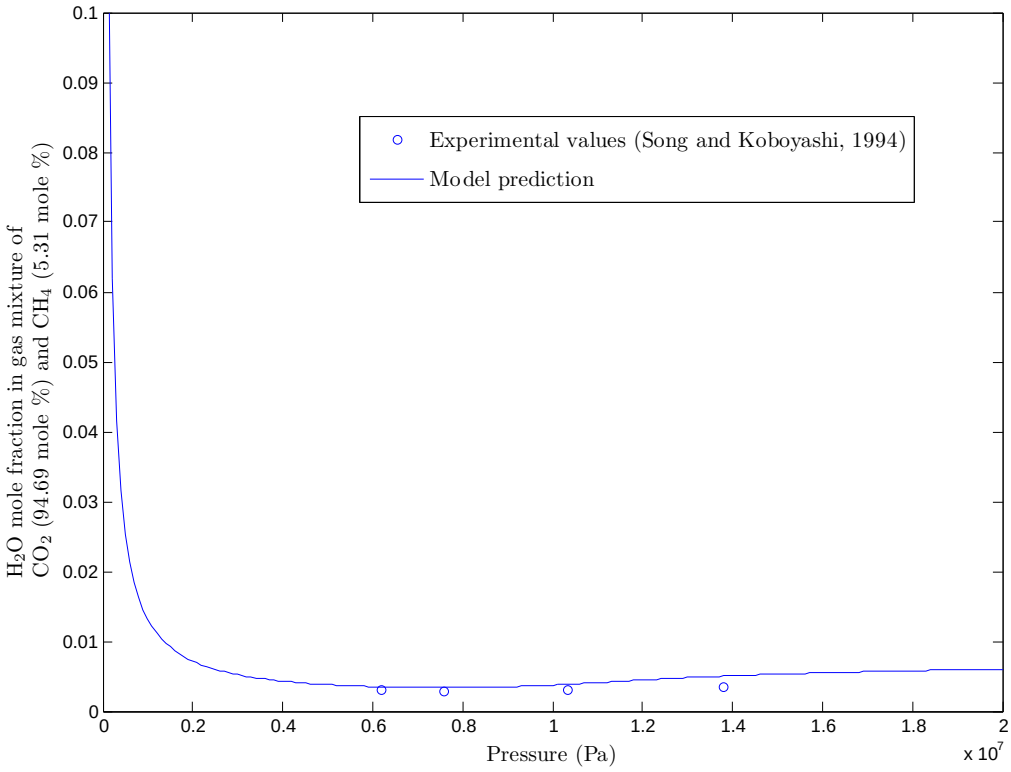

Figure 6.2: Solubility of H_2O in gas mixture of CH_4 (5.31 mole %) and CO_2 (94.69 mole %) at 50°C.

Table 6.3: Properties of components used in PR EOS for CH_4-CO_2-H_2O mixture

Component (i)	Critical Pressure (MPa)	Critical Temperature (K)	Accentric Factor (w)	BIP K_{i,H_2O} (tuned)	BIP K_{i,CO_2} (tuned)
CH_4	4.596	190.6	0.008	0.485	0.1
CO_2	7.376	304.2	0.225	0.1896	0
H_2O	22.06	647	0.344	0	0.1896

between 64 bar and 70 bar at 294.3 K in addition to the two hydrocarbon phases formed by this mixture.

All components are described using the PR EOS, so that the components use ideal gas state at standard conditions as reference state and hence, the equivalent function H to be minimized is eq 6.1 and the matrices in the elemental constraint equation can be given as,

$$\begin{aligned} \mathbf{A} &= \begin{bmatrix} 1 & 1 & 16 & 1 & 1 & 16 & 1 & 1 & 16 \\ 0 & 2 & 0 & 0 & 2 & 0 & 0 & 2 & 0 \\ 4 & 0 & 34 & 4 & 0 & 34 & 4 & 0 & 34 \end{bmatrix}; \qquad \mathbf{E} = \begin{bmatrix} e_C \\ e_O \\ e_H \end{bmatrix}; \\ \mathbf{N} &= \begin{bmatrix} n_{11} & n_{21} & n_{31} & n_{12} & n_{22} & n_{32} & n_{13} & n_{23} & n_{33} \end{bmatrix}^T. \end{aligned} \tag{6.7}$$

The constraint equation has been written for the conserved elements C, O and H. The matrices in the equivalent constraint set using the components (CO_2, CH_4 and n-$C_{16}H_{34}$) as base components that are conserved can be given as,

$$\mathbf{A} = \begin{bmatrix} 1 & 0 & 0 & 1 & 0 & 0 & 1 & 0 & 0 \\ 0 & 1 & 0 & 0 & 1 & 0 & 0 & 1 & 0 \\ 0 & 0 & 1 & 0 & 0 & 1 & 0 & 0 & 1 \end{bmatrix}; \qquad \mathbf{E} = \begin{bmatrix} e_{CH_4} \\ e_{CO_2} \\ e_{C_{16}H_{34}} \end{bmatrix}. \tag{6.8}$$

The phase mole fractions at equilibrium, obtained from the results of the minimization problem, as a function of varying pressure and constant

Table 6.4: Properties of components used in PR EOS for CH_4-CO_2-$nC_{16}H_{34}$ mixture (Pan et al., 1998)

Component (i)	Critical Pressure (MPa)	Critical Temperature (K)	Accentric factor (w)	BIP $K_{i,nC_{16}}$ (tuned)	BIP K_{i,CO_2} (tuned)
CH_4	4.596	190.6	0.008	0.078	0.1
CO_2	7.376	304.2	0.225	0.125	0
n-$C_{16}H_{34}$	1.4189	717	0.742	0	0.125

temperature of 294.3 K are in Figure 6.3. The Gibbs free energy model predicts the presence of an additional CO_2 phase between 6.4 and 7.1 MPa. The PR EOS parameters used in the equilibrium computations are given in Table 6.4.

6.3 Phase and Chemical Equilibrium

The impact of geochemical reactions on hydrocarbon mixtures of CO_2-$nC_{14}H_{30}$ and CO_2-CH_4 is presented in this section. The complete system includes

- Hydrocarbon phases with corresponding components - CO_2, H_2O, $nC_{14}H_{30}$ and CH_4 that are described using PR EOS.
- Aqueous phase with components that include ions along with undissociated components are present. The aqueous phase components are described using the Pitzer activity coefficient model (Appendix B).
- A single solid phase component ($CaCO_3$) that is assumed ideal.

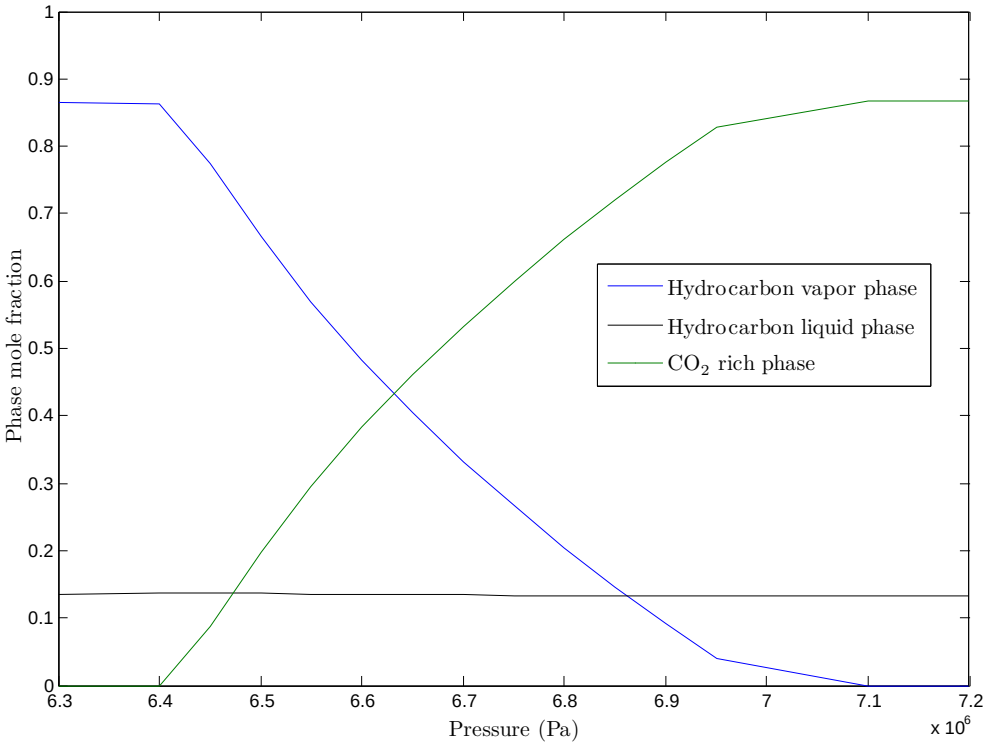

Figure 6.3: Equilibrium phase mole fractions of CH_4 (5 mole %) -CO_2 (90 mole %) and n-$C_{16}H_{34}$ (5 mole %) mixture at 294.3K.

It is assumed that the heavy hydrocarbon component ($nC_{14}H_{30}$) is not present in the aqueous phase owing to its negligible solubility. This is included as a separate constraint and is explained for each specific case in the following sections. Hence, the changes in the hydrocarbon phase behavior occur as CO_2 (and CH_4) enters the aqueous phase and participates in the geochemical reactions.

In the absence of experimental data for the complete system, the parameters obtained for systems where experimental data is available are used for all cases discussed in the following sections. The binary interaction parameters listed in Tables 6.1, 6.3 and 6.4 and obtained by tuning hydrocarbon phase behavior experiments are used for analysis of geochemical reactions. Similarly, the Pitzer activity parameters for 10.1 % $CaCl_2$ solution, listed in Table 5.8 and obtained by comparing experimental data for CO_2-$CaCl_2$-H_2O-$CaCO_3$ (solid) system in section 5.3.2 are also used for the aqueous phase components. These parameter values are assumed constants for the sensitivity study discussed in the following sections.

6.3.1 CO_2-$nC_{14}H_{30}$-H_2O System With Geochemical Reactions

The phase envelope of CO_2-$nC_{14}H_{30}$ hydrocarbon mixture was obtained both in the absence and the presence of H_2O in section 6.2.1. A carbonate system with ions in the aqueous phase can induce geochemical reactions. In this section, the impact of geochemical reactions on the phase envelope of this hydrocarbon mixture as well as the phase mole fractions are obtained for

different initial mole ratios.

The components in the hydrocarbon phases are $nC_{14}H_{30}$ ($i = 1$), CO_2 ($i = 2$) and H_2O ($i = 3$). The aqueous phase components are ions typically present in a carbonate system are - Ca^{2+} ($i = 4$), HCO_3^- ($i = 5$), CO_3^{2-} ($i = 6$), H^+ ($i = 7$), OH^- ($i = 8$), Cl^- ($i = 9$) as well as undissociated components - H_2CO_3 ($i = 10$), $CaCO_3$ ($i = 11$), $CaCl_2$ ($i = 12$), CO_2 ($i = 13$) and H_2O. The solid component $CaCO_3$ ($i = 14$) is assumed ideal. As discussed in section 4.3, $nC_{14}H_{30}$ is identified as a class A component that participates only in phase equilibrium while CO_2 is a class B component that participates in both phase and chemical equilibrium. We can write the equivalent function H (eq 4.39) specific to this mixture as,

$$\begin{aligned} H(T,P) &= n_{11}[RTln(x_{11}\hat{\phi}_1)] + n_{21}[\underline{G}_2^{IG}(T,P) + RTln(x_{21}\hat{\phi}_2)] \\ &+ \sum_{i=4}^{13} n_{iw}[\bar{G}^0_{iw}(T,P) + RTlnx_i\gamma_i] + n_{14}[\bar{G}^0_{14}] \\ &+ n_3[\bar{G}^0_3(T,P) + RTlnx_3\gamma_3]. \end{aligned} \tag{6.9}$$

The elemental balance contraint for this system corresponding to a single hydrocarbon phase at equilibrium and including

$$\mathbf{A} = \begin{bmatrix} 0 & 1 & 0 & 0 & 1 & 1 & 0 & 0 & 0 & 1 & 1 & 0 & 1 & 0 & 1 \\ 0 & 2 & 1 & 0 & 3 & 3 & 0 & 1 & 0 & 3 & 3 & 0 & 2 & 1 & 3 \\ 0 & 0 & 2 & 0 & 1 & 0 & 1 & 1 & 0 & 2 & 0 & 0 & 0 & 2 & 0 \\ 0 & 0 & 0 & 1 & 0 & 0 & 0 & 0 & 0 & 0 & 1 & 1 & 0 & 0 & 1 \\ 0 & 0 & 0 & 0 & 0 & 0 & 0 & 0 & 1 & 0 & 0 & 2 & 0 & 0 & 0 \\ 1 & 0 & 0 & 0 & 0 & 0 & 0 & 0 & 0 & 0 & 0 & 0 & 0 & 0 & 0 \end{bmatrix}; \quad \mathbf{E} = \begin{bmatrix} e_C \\ e_O \\ e_H \\ e_{Ca} \\ e_{Cl} \\ e_{C_{14}H_{30}} \end{bmatrix}. \tag{6.10}$$

The component n-$C_{14}H_{30}$ identified as class A is included as a separate base component that is conserved in addition to the elements in **E**. This iadditional constraint helps define that n-$C_{14}H_{30}$ does not participate in reactions and the C and H elements in this component are not available for reactions. An additional hydrocarbon phase with components CO_2 and n-$C_{14}H_{30}$ may be present depending on the pressure and temperature conditions. The total system Gibbs free energy (G^T) for both cases are compared and the combination with lowest G^T corresponds to the equilibrium concentration of the system.

As equilibrium concentration of components for a reactive system depends on the initial concentration of components, the impact of geochemical reactions on phase behavior of the hydrocarbon mixture can vary based on the initial mole number of components. The equilibrium composition corresponding to this case of both phase and chemical equilibrium can depend on

- Moles of the solid relative to the aqueous phase moles.
- Volume ratio of H_2O and nC_{14} and hence, molar ratio. A volume ratio is preferable owing to analogous measurements of initial saturations of water and oil that is possible in an oil field.
- $CaCl_2$ concentration in aqueous phase, which is representative of ionic concentration of species and is analogous to the salinity of the reservoir brine.

A sensitivity study is done to determine how a change in initial mole

numbers of the above identified parameters can change the phase envelope of the CO_2-n-$C_{14}H_{30}$ hydrocarbon mixture.

6.3.1.1 Base case

A base case is defined as the case where volume of water is equal to the volume of n-$C_{14}H_{30}$ similar to the experiments for the CO_2-$C_{14}H_{30}$-H_2O system (Mangone, 1985). This corresponds to a constant molar ratio of 14.45, obtained using densities and molecular weights of H_2O and n-$C_{14}H_{30}$. Also, the number of moles of solid and water are equal in the base case. The concentration of $CaCl_2$ in the base case is taken as 10.1 mole % of water.

The Pitzer parameters obtained in section 5.3.1 (Table 5.8) as well as the binary interaction parameters in Table 6.1 are used for phase and chemical equilibrium computations. Figure 6.4 shows the impact of geochemical reactions on the phase envelope for two different concentrations of $CaCl_2$. It can be seen that the phase envelope of the hydrocarbon mixture shifts further towards decreasing concentration of C_{14} in the presence of geochemical reactions than just water. At an overall mole fraction of 0.2 mole % of C_{14}, the bubble point pressure of the CO_2-C_{14} mixture in the presence of water changes by about 5 % while in the presence of geochemical reactions, the bubble point pressure decreases by about 10 %.

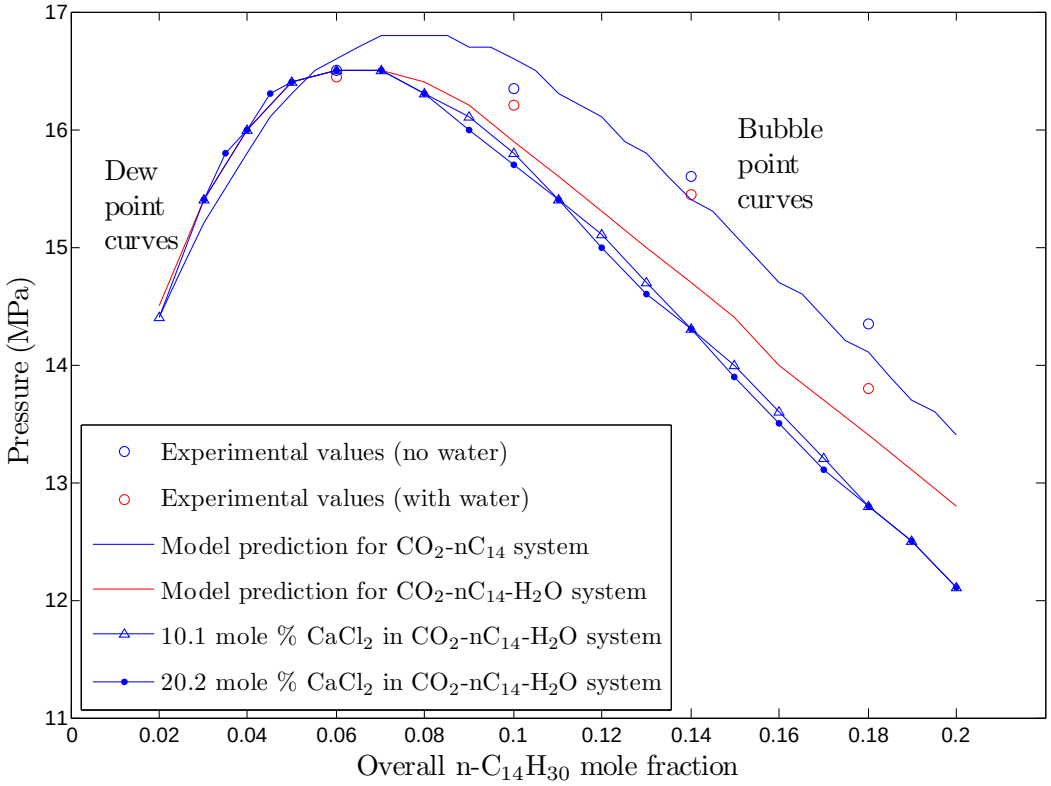

Figure 6.4: Two-phase envelopes for CO_2-$C_{14}H_{30}$ system in presence of water (no reactions) as well as with 10.1 and 20.2 mole % of $CaCl_2$ solution at 343 K. The mole fraction of n-$C_{14}H_{30}$ is water-free basis.

6.3.1.2 Moles of solid relative to the aqueous phase moles

The moles of solid relative to the aqueous phase moles have no effect on the phase behavior of the hydrocarbon mixture. As solid is a pure component phase that is assumed ideal in the model, its fugacity is fixed by the pressure. At equilibrium, since the fugacity of $CaCO_3$ in the aqueous phase is equal to that of $CaCO_3$ solid the concentration of $CaCO_3$ in the aqueous phase is fixed. Hence, increasing solid moles do not have an effect on the hydrocarbon phase behavior.

6.3.1.3 Volume ratio of H_2O and nC_{14}

This is an important parameter that may be determined in the field based on the saturation data. Figure 6.5 shows that the difference in phase envelope between cases of only phase equilibrium with no reactions and phase equilibrium with geochemical reactions when other parameters are held constant as in the base case. The moles of solid are equal to the moles of water and the $CaCl_2$ is 10 % of H_2O in all cases considered.

Figure 6.5 shows that the difference between the phase envelopes for cases with and without reactions increases as the initial ratio of H_2O to nC_{14} (Y) increases. The difference in phase envelopes for the case where $Y = 5$ is greater than that for $Y = 0.5$. If Y is higher, the geochemical reactions have a greater impact on the phase envelope of CO_2-$C_{14}H_{30}$-H_2O system. At a C_{14} overall mole fraction of 0.2 %, the bubble point pressure decrease for $Y = 0.5$ and in the presence of reactions fis insignificant. However, at the same C_{14}

overall mole fraction of 0.2 %, the decrease in bubble point pressure for $Y = 5$ is about 27 % in the presence of reactions. In summary, the initial volume ratio of H_2O and nC_{14} is an important parameter that influences the shift in phase envelope.

6.3.1.4 $CaCl_2$ concentration in aqueous phase

An intial mole ratio of 5 between H_2O and nC_{14} was chosen to magnify the impact of geochemical reactions and study the effect of varying $CaCl_2$ concentration. Also the amount of solid was taken equal to the amount of H_2O (as in the base case). Figure 6.6 shows the phase envelope for different $CaCl_2$ concentration.

The geochemical reactions, occuring because of $CaCl_2$ solution in the aqueous phase along with solid $CaCO_3$ and all the aqueous phase ions associated with the carbonate system, shift the phase envelope even further towards lower nC_{14}. This has implications for oil recovery predictions using compositional simulations. The equilibrium concentrations obtained as solution to the Gibbs free energy minimization indicate that the aqueous concentration of CO_2 increases as the concentration of $CaCl_2$ in the aqueous phase increases. The amount of CO_2 available for phase equilibrium with nC_{14} decreases and hence, a shift is observed. The decrease in bubble point pressure at 0.2 % overall mole fraction of C_{14} is about 35% at 30% $CaCl_2$ concentration (Figure 6.6).

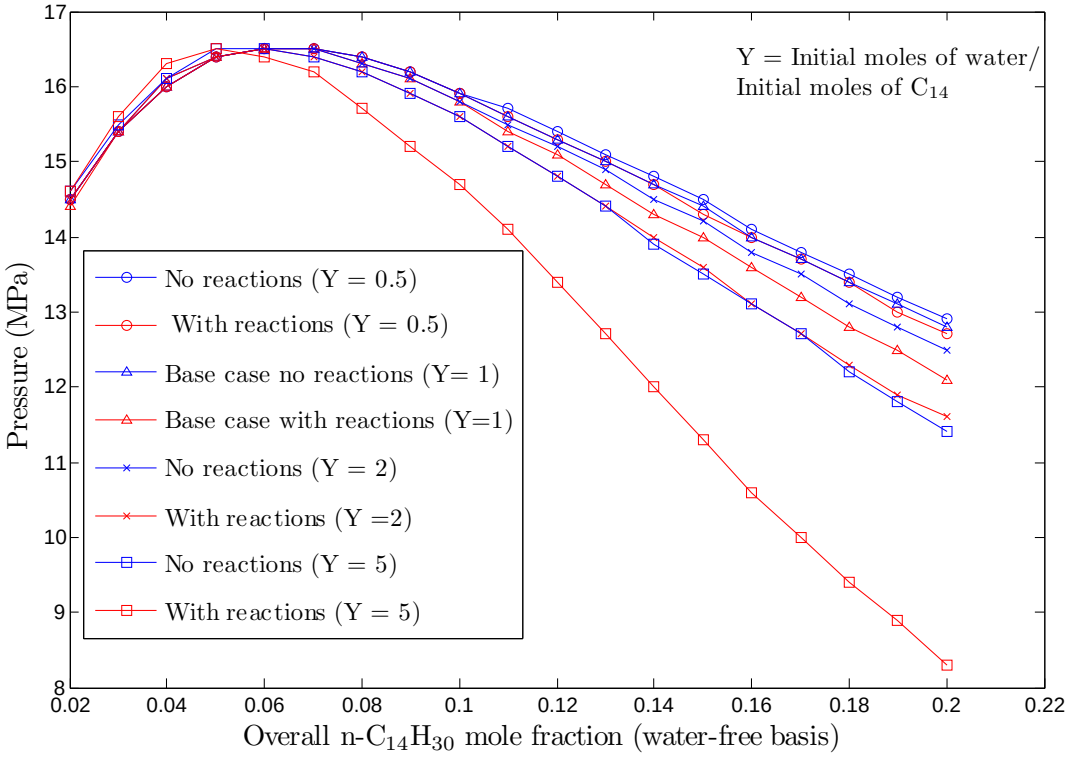

Figure 6.5: Two-phase envelopes for CO_2-$C_{14}H_{30}$-H_2O system for varying initial ratios of H_2O and nC_{14} at 343 K.

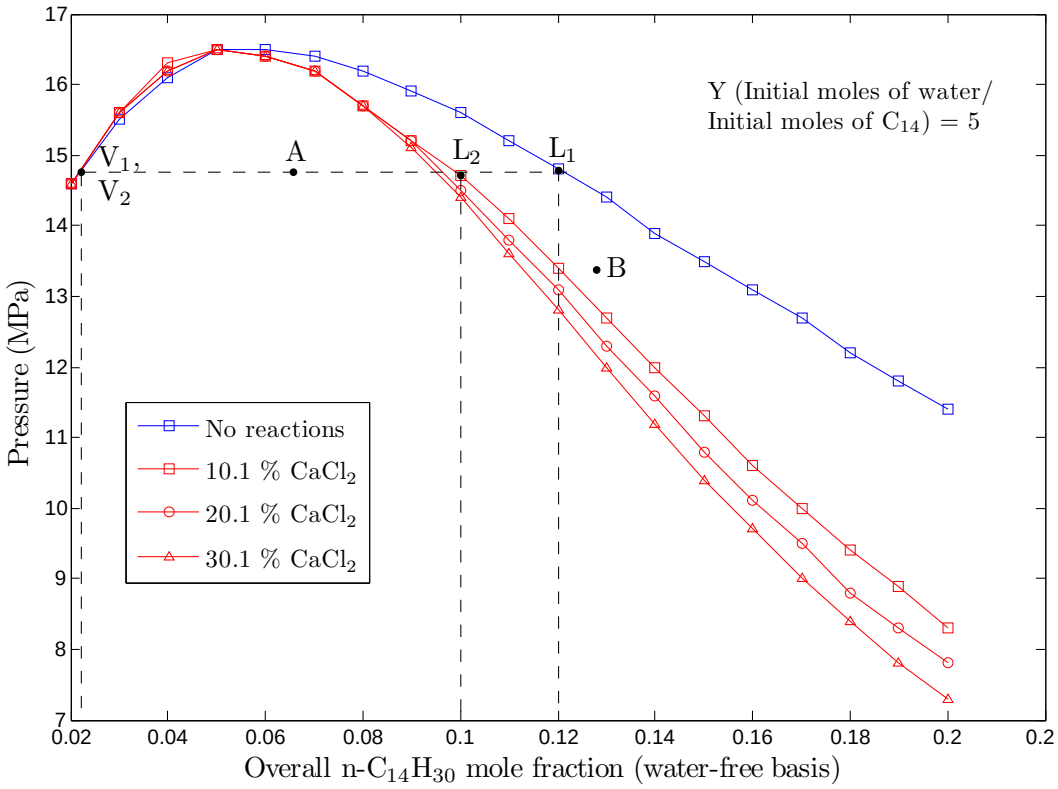

Figure 6.6: Two-phase envelopes for CO_2-$C_{14}H_{30}$-H_2O system for varying $CaCl_2$ mole % in H_2O at 343 K. Initial mole ratio of H_2O to nC_{16} (Y) is 5 for these cases.

6.3.1.5 Discussion

The changes in two-phase envelope of the CO_2-nC_{14} mixture has implications in oil recovery predictions. As an example, let point A in Figure 6.6 represent an overall mole fraction and pressure occuring during reservoir simulation. As point A lies within the two phase envelope, two phases are present at equilibrium and this is also obtained by flash calculations and stability analysis performed in compositional simulations. If no reactions are considered, the vapor and liquid compositions at equilibrium are represented by points L_1 and V_1, respectively. However, if the new two-phase envelope due to reactions (say 10.1 % $CaCl_2$) are considered, the equilibrium composition are represented by points L_2 and V_2. While there is little difference between compositions represented by points V_1 and V_2, the difference in composition represented by points L_1 and L_2, impacts liquid mole fractions at equilibrium and hence, oil recovery predictions.

Let point B in Figure 6.6 represent an overall mole fraction and pressure occuring during reservoir simulation. If no geochemical reactions are occuring in the system, a flash computation in compositional simulation will predict a two phase system (as it lies within the two phase envelope for CO_2-nC_{14} system without any reactions). If geochemical reactions are considered, point B lies outside the two-phase envelope so that only a single phase is present at equilibrium at that overall mole fraction and pressure. Thus, the changes in two-phase envelope impacts the equilibrium compositions at different mole fractions and pressures and hence, the oil recovery predictions.

6.3.1.6 Summary

The initial mole ratio of H_2O and nC_{14} and the concentration of $CaCl_2$ in H_2O are important parameters that influences the impact of geochemical reactions on the phase envelope of the CO_2-$C_{14}H_{30}$ system. The changes in phase envelope may further impact oil recovery predictions.

6.3.2 CO_2-CH_4-H_2O System With Geochemical Reactions

The CO_2-CH_4-H_2O mixture is used to analyze the impact of overall mole fractions due to geochemical reactions. This is an important representative mixture as the gas typically injected for miscibility contains varying amounts of these components and geochemical reactions may occur in the presence of aqueous phase ions and the solid phase ($CaCO_3$). The components in the gas phase are CO_2 ($i = 1$), CH_4 ($i = 2$) and H_2O ($i = 3$) while the components in the aqueous phase are Ca^{2+} ($i = 4$), HCO_3^- ($i = 5$), CO_3^{2-} ($i = 6$), H^+ ($i = 7$), OH^- ($i = 8$), as well as undissociated components - H_2CO_3 ($i = 9$), $CaCO_3$ ($i = 10$), CO_2 ($i = 11$), CH_4 ($i = 12$) and H_2O.The solid component $CaCO_3$ ($i = 13$) is assumed ideal.

There are no class A components present in this system and both CO_2 and CH_4 are class B components that participate in phase and chemical equilibrium. The equilibrium composition is the minimum of the total system

Gibbs free energy given as,

$$\begin{aligned} G(T,P) &= \sum_{i=1}^{3} n_{i1}[\underline{G_i}^{IG}(T,P) + RTln(x_{i1}\hat{\phi}_i)] \\ &+ \sum_{i=4}^{12} n_{iw}[\bar{G}^0_{iw}(T,P) + RTlnx_i\gamma_i] + n_{13}[\bar{G}^0_{13}] \\ &+ n_3[\bar{G}^0_3(T,P) + RTlnx_3\gamma_3]. \end{aligned} \tag{6.11}$$

The matrices that constitute the elemental balance constraint for this system are,

$$\mathbf{A} = \begin{bmatrix} 1 & 1 & 0 & 0 & 1 & 1 & 0 & 0 & 1 & 1 & 1 & 1 & 0 & 1 \\ 2 & 0 & 1 & 0 & 3 & 3 & 0 & 1 & 3 & 3 & 2 & 0 & 1 & 3 \\ 0 & 4 & 2 & 0 & 1 & 0 & 1 & 1 & 2 & 0 & 0 & 4 & 2 & 0 \\ 0 & 0 & 0 & 1 & 0 & 0 & 0 & 0 & 0 & 1 & 0 & 0 & 0 & 1 \end{bmatrix}; \qquad \mathbf{E} = \begin{bmatrix} e_C \\ e_O \\ e_H \\ e_{Ca} \end{bmatrix}. \tag{6.12}$$

Three cases of varying CH_4 mole % in the CO_2-CH_4 mixture are considered (5.41 %, 15.41 % and 25.41 %). In the absence of experimental data for 15.41 mole% and 25.41 mole% CH_4 in CO_2-CH_4 mixture, it is assumed that each system with different compositions of CH_4, CO_2, $CaCO_3$ and H_2O can be each described using the PR EOS for gas phase components and the Pitzers activity coefficient model for the aqueous phase components similar to the system in section 6.2.2 with 5.31 mole % CO_2. As the inlet gas composition changes, it can potentially influence the overall aqueous and gas phase moles and hence, the distribution of components in those phases.

The Gibbs free energy minimization approach is used to find the equilibrium composition for each case of varying inlet composition (5%, 15% and

25% CH_4 in CO_2-CH_4 mixture). In each case, minimization was performed using different combination of phases to find the combination with lowest Gibbs free energy (global minimum). This global minimum in the Gibbs free energy function of the system corresponds to the equilibrium composition. The equilibrium composition predicted for each case of varying CH_4 mole fractions has components distributed in all phases.

As the initial gas composition changes, the changes in the mole fraction of the phases (solid, aqueous and the gas phase) are not significant (Figure 6.7). Also, as the molality of $CaCO_3$ in the aqueous solution increases to 10, the aqueous and gas phase mole fraction do not vary significantly with pressure (Figure 6.8). The initial mole fraction of $CaCO_3$ also does not have an impact on the aqueous and gas phase mole fraction varation with pressure (Figure 6.9).

In summary, for the hydrocarbon mixture considered in this study and for the pressure range of 0.1-20 MPa and T = 50°C, the ions present in the brine in a typical carbonate system that participate in geochemical reactions, do not change the number of phases or influence the overall mole fractions of the different phases. The equilibrium mole fraction of phases for this sytem is thus independent of pressure. However, the moles of the component in each of the phases may change owing to these reactions.

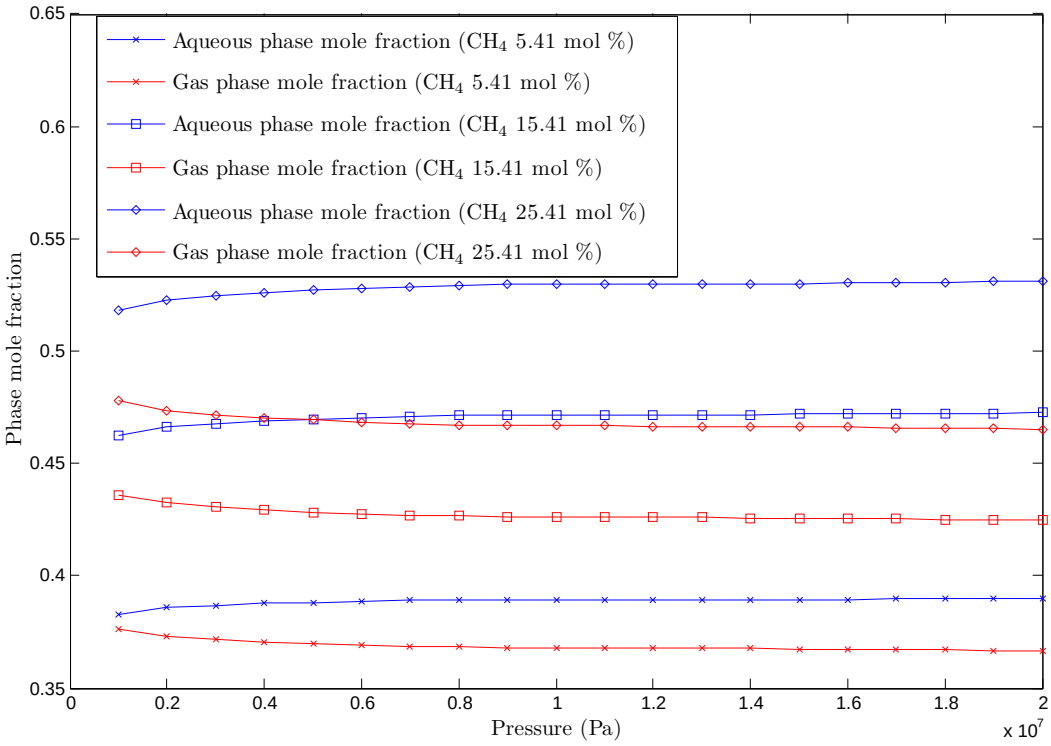

Figure 6.7: The impact of geochemical reactions on the mole fractions of aqueous and gas phase for one molal $CaCO_3$ (aq) solution with varying initial gas mixture composition of CH_4-CO_2 at 50°C.

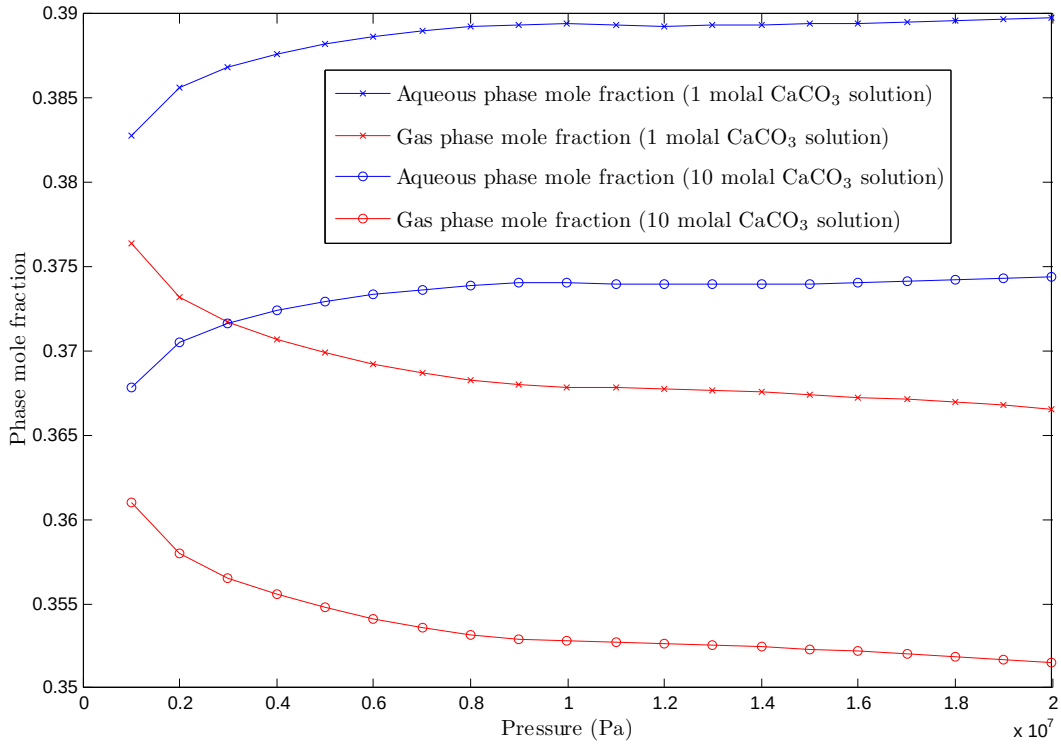

Figure 6.8: The impact of geochemical reactions on the the mole fractions of aqueous and gas phase with varying molality of $CaCO_3$ (aq) solution for an initial gas composition of 5.41 mole % CH_4-CO_2 gas mixture at 50°C.

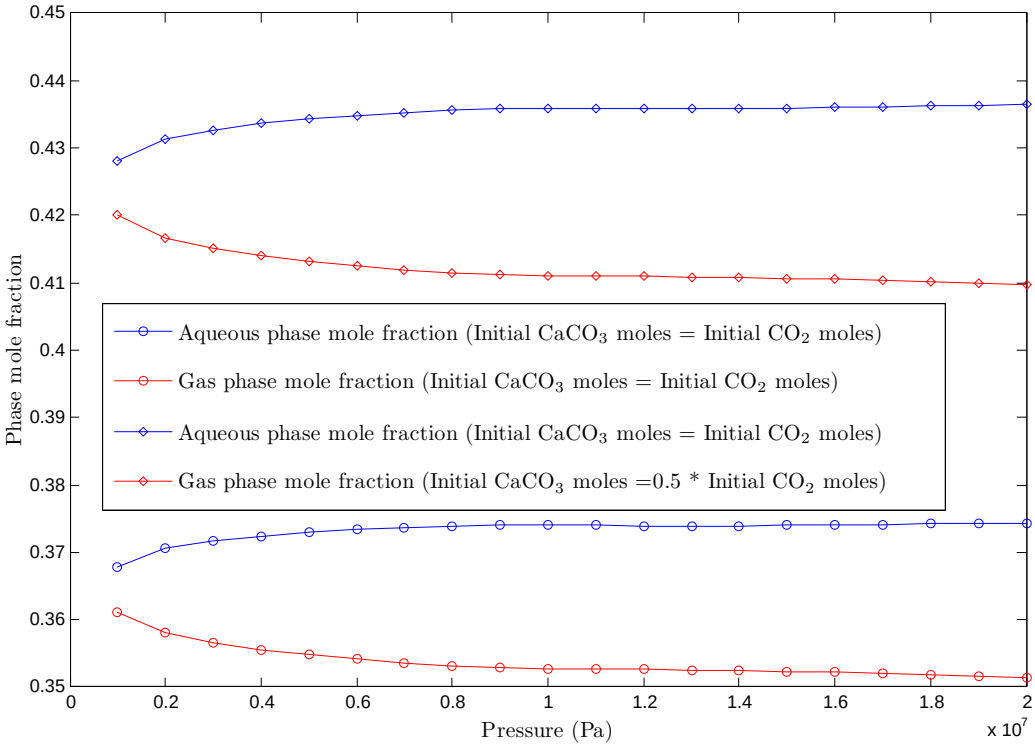

Figure 6.9: Equilibrium composition for different ratio of initial moles of $CaCO_3$ (solid) and CO_2 (gas) on gas and aqueous phase mole fractions for 10 molal $CaCO_3$ (aq) solution and 5.41 mole % CH_4-CO_2 gas mixture at 50°C.

6.4 Conclusions

The Gibbs free energy model can predict the phase behavior of three different hydrocarbon mixtures - CO_2-$nC_{14}H_{30}$, CO_2-CH_4-H_2O and CH_4-CO_2-$nC_{16}H_{34}$. In these models, the PR EOS was used for components in the hydrocarbon phase while the aqueous phase components, if present, were described using the Pitzer activity coefficient model. Some predictions from the model have been compared with experimental values.

The binary interaction parameters obtained from the phase equilibrium calculations were used to analyze the impact of geochemical reactions on the phase envelope of the CO_2-$nC_{14}H_{30}$ system. While the presence of water shifts the saturation pressures in the direction of lower C_{16} mole fraction, the geochemical reactions shift this envelope further. Also, the changes in the phase envelope of CO_2-nC_{14} mixture, due to geochemical reactions is specific to the initial mole ratio of components. The important parameters that influence the phase envelope are the mole ratios of water to n-C_{16} present initially in the system and the $CaCl_2$ concentration in H_2O.

The impact of geochemical reactions on the CO_2-CH_4-H_2O system because of the presence of typical ions of a carbonate system was also investigated. In this case too, the PR EOS was used for gas phase components while the Pitzer activity coefficient model was used for aqueous phase components. The geochemical reactions have little impact on the equilibrium mole fraction of phases at 50°C in the pressure range 0.1-20 MPa.

The Gibbs free energy model is a comprehensive approach since it integrates phase equilibrium computations with geochemical reactions to model CO_2 injection for enhancing oil recovery. The initial mole ratios of aqueous and solid phase along with brine samples can help identify the major components present in the system. These components can be used to construct a specific Gibbs free energy model for the reservoir. In addition to the phase behavior changes induced by CO_2 injection, the Gibbs free energy model can also help predict the impact of geochemical reactions.

Chapter 7

Integration of Equilibrium Model with Flow

In this chapter, the algorithms used to find equilibrium composition arising out of reactions are coupled with flow. The coupling is illustrated by developing a 1-D flow model with cation exchange reactions using the stochiometric algorithm and the Gibbs free energy minimization algorithm. A comparison between the two methods is presented for a particular system.

7.1 Phase and Chemical Equilibrium with Flow

As discussed in chapter 3, the Gibbs free energy minimization approach and the stochiometric approach are the two methods to estimate equilibrium composition for a reactive system. These computations, performed at a particular temperature, pressure and for a fixed value of initial composition, are also commonly referred to as batch calculations. The applications presented in chapters 5 and 6 are all examples of batch calculations using the Gibbs free energy minimization approach.

The batch calculations using both the methods can be coupled with flow to describe processes when reactions occur during transport of fluids. The Local Equilibrium Assumption (LEA) is invoked and the system is assumed

to be in phase and chemical equilibrium at every time step. This implies that reactions between components occur at a higher rate than the rate of transport of components. Thus, LEA provides for easy integration of batch calculations with flow.

The stochiometric approach was described in chapter 3 for a single phase system where the law of mass actions are used for all reactions to obtain nonlinear equations along with the associated reaction constants. In case of a multiphase system, in addition to the law of mass action equations, phase equilibrium relationships that equate fugacities of components in different phases are required to find equilibrium compositions for cases of phase and chemical equilibrium.

The solution to the Gibbs free energy minimization gives equilibrium composition of a system with phase and chemical equilibrium directly. Hence, no additional equations are required in the Gibbs free energy approach.

7.2 Numerical Model for Cation Exchange Reactions

Cation exchange reactions commonly occur with flow of groundwater in reservoirs and aquifers. The cations in the aqueous phase (flowing phase) can exchange with those adsorbed in the solid phase (stationary phase). One important application of these reactions is the remediation of aquifers to potable standards. Another complimentary application is the safe disposal of nuclear waste to prevent radionuclides intrusion in groundwater. The exchange reactions determine the mobility of ions or radionuclide (Lichtner et al., 2004) and

therefore, the appropriate remediation strategy (Bethke and Brady, 2000).

Cation exchange reactions also occur during the intrusion of seawater into fresh water zones or vice-versa owing to the difference in cation concentrations. The resulting displacement patterns are used to determine whether the seawater or the fresh water is advancing and make predictions on aquifer water quality where such intrusion occurs (Appelo, 1994).

In this section, a numerical model is developed to describe the process of cation exchange reactions occuring during flow. In particular, a 1-D numerical flow model is presented for a case of cation exchange reactions occuring between flowing aqueous phase and a stationary solid phase to illustrate coupling of flow and reactions. Separate numerical models using two methods of coupling using stochiometric approach as well as the Gibbs free energy minimization approach is presented.

The system consists of three cations - Na^+, Ca^{2+} and Mg^{2+} in the aqueous phase that is capable of adsorbing on the solid surface and an anion, Cl^-, that does not adsorb. This system was chosen as experimental results are available for this system at the field scale (Valocchi et al., 1981b). The numerical models developed in this chapter are further modified in the next chapter to verify analytical solution predictions presented in the next chapter.

7.2.1 Assumptions And General Equations

The assumptions associated with this numerical model are -

1. The cation exchange capacity for the solid surface (Z_v), where all the adsorption reactions occur, is a constant.

2. The phases are ideal and hence, the activities of components are equivalent to dimensionless concentrations (ς_i/ς_0, ς_i is the concentration of component i in the aqueous phase and ς_0 is unit concentration of the component).

3. The medium has a constant porosity, ϕ, and the heterogeneities of the solid phase are neglected. The fluid velocity in the medium, v, is also constant in this model.

4. The process is assumed to be isothermal.

The general conservation equation for 1-D flow for a cation component i in the flowing aqueous phase and capable of adsorbing on stationary solid phase can be written as (Lake et al., 2003),

$$\phi\frac{\partial(\varsigma_i+\hat{\varsigma}_i)}{\partial t}+\frac{\partial(\varsigma_i v)}{\partial x}=\mathcal{D}\frac{\partial^2\varsigma_i}{\partial x^2}\quad\forall\, i=1,2,3.\,\text{and}\,x\in[0,L]. \tag{7.1}$$

Here, v is the velocity of the aqueous phase, $\mathcal{D}$ is the dispersion coefficient while ς_i and $\hat{\varsigma}_i$ are the aqueous and solid phase concentration of cation component i, repectively. All concentrations are in moles/pore volume. Eq 7.1 is valid for all the three cations - Na^+ ($i=1$), Ca^{2+} ($i=2$) and Mg^{2+} ($i=3$). Eq 7.1 is modified by introducing dimensionless variables $\xi=x/L$, $\tau=vt/(\phi L)$ and Peclet number, $Pe=(vL)/\mathcal{D}$ to obtain,

$$\frac{\partial(\varsigma_i+\hat{\varsigma}_i)}{\partial\tau}+\frac{\partial\varsigma_i}{\partial\xi}=\frac{1}{Pe}\left(\frac{\partial^2\varsigma_i}{\partial\xi^2}\right)\quad\forall\, i=1,2,3.\,\text{and}\,\xi\in[0,1]. \tag{7.2}$$

This conservation equation is adapted and discretized to develop a numerical solution. The advection term is discretized explicitly while the dispersion term is integrated implicitly (LeVeque, 1994). The domain ξ is divided into N_x+2 cells each of width $\Delta\xi = 1/(N_x+1)$ and the two boundary cells are of width $\Delta\xi/2$. The domain τ is also divided into N_t+1 cells each of width $\Delta\tau = 1/(N_t+1)$. The discretized equation describing cation flow is given as,

$$\frac{(\varsigma_{i,m}^{n+1} + \hat{\varsigma}_{i,m}^{n+1}) - (\varsigma_{i,m}^{n} + \hat{\varsigma}_{i,m}^{n})}{\Delta\tau} + \frac{(\varsigma_{i,m}^{n} - \varsigma_{i,m-1}^{n})}{\Delta\xi} - \frac{1}{Pe}\left(\frac{\varsigma_{i,m+1}^{n+1} - 2\varsigma_{i,m}^{n+1} + \varsigma_{i,m-1}^{n+1}}{\Delta\xi^2}\right) = 0.$$
$$\forall\, m = 2, \ldots, N_x+1 \quad \& \quad n = 1, 2, N_t+1. \tag{7.3}$$

As the anion does not adsorb on the solid surface, the discretized equation for anion with concentration ς_a is,

$$\frac{(\varsigma_{a,m}^{n+1} - \varsigma_{a,m}^{n})}{\Delta\tau} + \frac{(\varsigma_{a,m}^{n} - \varsigma_{a,m-1}^{n})}{\Delta\xi} - \frac{1}{Pe}\left(\frac{\varsigma_{a,m+1}^{n+1} - 2\varsigma_{a,m}^{n+1} + \varsigma_{a,m-1}^{n+1}}{\Delta\xi^2}\right) = 0.$$
$$\forall\, m = 2, \ldots, N_x+1 \quad \& \quad n = 1, 2, N_t+1. \tag{7.4}$$

Eq 7.4 for all points in space ($\forall\, m = 2, \ldots, N_x+1$) can be rearranged as a matrix equation to obtain,

$$L_1 \begin{bmatrix} \varsigma_{a,2}^{n+1} \\ \varsigma_{a,3}^{n+1} \\ \\ \vdots \\ \varsigma_{a,N_x+1}^{n+1} \end{bmatrix} + L_2 \begin{bmatrix} \varsigma_{a,2}^{n} \\ \varsigma_{a,3}^{n} \\ \\ \vdots \\ \varsigma_{a,N_x+1}^{n} \end{bmatrix} = \begin{bmatrix} \frac{\varsigma_{a,1}^{n}}{Pe\Delta\xi^2} + \frac{\varsigma_{a,1}^{n-1}}{\Delta\xi} \\ 0 \\ \vdots \\ \\ 0 \end{bmatrix} \quad \forall\, n = 2, 3, \ldots, N_t+1. \tag{7.5}$$

Here, L_1 and L_2 are N_x X N_x matrices that are constants and given as,

$$L_1 = \begin{bmatrix} \left(\frac{2}{Pe\Delta\xi^2}+\frac{1}{\Delta\tau}\right) & \left(\frac{-1}{Pe\Delta\xi^2}\right) & 0 & \dots & 0 \\ \left(\frac{-1}{Pe\Delta\xi^2}\right) & \left(\frac{2}{Pe\Delta\xi^2}+\frac{1}{\Delta\tau}\right) & \left(\frac{-1}{Pe\Delta\xi^2}\right) & \dots & \vdots \\ 0 & \left(\frac{-1}{Pe\Delta\xi^2}\right) & \left(\frac{2}{Pe\Delta\xi^2}+\frac{1}{\Delta\tau}\right) & \ddots & \vdots \\ \vdots & \ddots & \ddots & \ddots & \vdots \\ 0 & \dots & 0 & \left(\frac{-1}{Pe\Delta\xi^2}\right) & \left(\frac{1}{Pe\Delta\xi^2}+\frac{1}{\Delta\tau}\right) \end{bmatrix};$$

$$L_2 = \begin{bmatrix} \left(\frac{1}{\Delta\xi}-\frac{1}{\Delta\tau}\right) & 0 & \dots & 0 \\ \left(\frac{-1}{\Delta\xi}\right) & \left(\frac{1}{\Delta\xi}-\frac{1}{\Delta\tau}\right) & \dots & \vdots \\ 0 & \left(\frac{-1}{\Delta\xi}\right) & \left(\frac{1}{\Delta\xi}-\frac{1}{\Delta\tau}\right) & \vdots \\ \vdots & \ddots & \ddots & \vdots \\ 0 & \dots & \left(\frac{-1}{\Delta\xi}\right) & \left(\frac{1}{\Delta\xi}-\frac{1}{\Delta\tau}\right) \end{bmatrix}.$$

The experimental data used for comparison are a series of experiments that were performed using a constant initial concentration and a constant injection concentration of components, also referred to as Riemann problems. A constant initial (ς_{aI}) and a constant injection (ς_{aJ}) concentration for the anion component in the discretized system can be written as,

$$\begin{aligned} \varsigma_{a,1}^{n} &= \varsigma_{aI} \quad n = 1; \\ &= \varsigma_{aJ} \quad \forall\, n = 2, 3, \dots, N_t + 1. \end{aligned} \tag{7.6}$$

Hence, the RHS of eq 7.5 is the forcing function, which is also a constant (eq 7.6). Hence, eq 7.4 can be solved independently to obtain values at all points

in space and time. This approach of obtaining values of anion concentration is the same for both the methods. The anion concentration values are used for the solution of the cation concentrations obtained from both the methods.

According to the assumptions listed, the charge balance holds in the aqueous phase while in the solid phase, the cation exchange capacity is a constant. The balance equations for the two phases are,

$$\varsigma_1 + 2\varsigma_2 + 2\varsigma_3 = \varsigma_a \qquad \text{and} \qquad \hat{\varsigma}_1 + 2\hat{\varsigma}_2 + 2\hat{\varsigma}_3 = Z_v. \tag{7.7}$$

Having obtained the anion concentration at every cell, the charge and the cation exchange capacity conservation equations can be used to eliminate aqueous and solid concentration (ς_1 and $\hat{\varsigma}_1$) of Na^+. There are then $4N_x$ variables ($\varsigma_{2,m}^{n+1}$, $\hat{\varsigma}_{2,m}^{n+1}$, $\varsigma_{3,m}^{n+1}$ and $\hat{\varsigma}_{3,m}^{n+1}$ $\forall\, m = 2, 3, ..., N_x + 1$) at every time step. There are two approaches to obtain values of these $4N_x$ variables.

7.2.2 Stochiometric Approach

The law of mass action equations are directly used in the stochiometric approach. The two independent reactions for this system with three cations and the corresponding law of mass action equations are,

$$Mg^{2+} + 2\hat{N}a \rightleftharpoons 2Na^+ + \hat{M}g \qquad K_{10} = \frac{\hat{\varsigma}_2\varsigma_1^2}{\hat{\varsigma}_1^2\varsigma_2}; \tag{7.8}$$

$$Ca^{2+} + 2\hat{N}a \rightleftharpoons 2Na^+ + \hat{C}a \qquad K_{20} = \frac{\hat{\varsigma}_3\varsigma_1^2}{\hat{\varsigma}_1^2\varsigma_3}. \tag{7.9}$$

The charge balance and cation exchange capacity equations are valid at every discretized cell. They are used to simplify the law of mass action equations.

This results in,

$$\left[K_{10}(\varsigma_{2,m}^{n+1})(Z_v - \hat{\varsigma}_{2,m}^{n+1} - \hat{\varsigma}_{3,m}^{n+1})^2\right] - \left[(\hat{\varsigma}_{2,m}^{n+1})(\varsigma_{a,m}^{n+1} - \varsigma_{2,m}^{n+1} - \varsigma_{3,m}^{n+1})^2\right] = 0; \quad (7.10)$$

$$\left[K_{20}(\varsigma_{3,m}^{n+1})(Z_v - \hat{\varsigma}_{2,m}^{n+1} - \hat{\varsigma}_{3,m}^{n+1})^2\right] - \left[(\hat{\varsigma}_{3,m}^{n+1})(\varsigma_{a,m}^{n+1} - \varsigma_{2,m}^{n+1} - \varsigma_{3,m}^{n+1})^2\right] = 0; \quad (7.11)$$

$$\forall\, m = 2, 3, \ldots, N_x + 1.$$

The conservation equations for Ca and Mg are,

$$\frac{(\varsigma_{2,m}^{n+1} + \hat{\varsigma}_{2,m}^{n+1}) - (\varsigma_{2,m}^{n} + \hat{\varsigma}_{2,m}^{n})}{\Delta\tau} + \frac{(\varsigma_{2,m}^{n} - \varsigma_{2,m-1}^{n})}{\Delta\xi} - \frac{1}{Pe}\left(\frac{\varsigma_{2,m+1}^{n+1} - 2\varsigma_{2,m}^{n+1} + \varsigma_{2,m-1}^{n+1}}{\Delta\xi^2}\right) = 0; \quad (7.12)$$

$$\frac{(\varsigma_{3,m}^{n+1} + \hat{\varsigma}_{3,m}^{n+1}) - (\varsigma_{3,m}^{n} + \hat{\varsigma}_{3,m}^{n})}{\Delta\tau} + \frac{(\varsigma_{3,m}^{n} - \varsigma_{3,m-1}^{n})}{\Delta\xi} - \frac{1}{Pe}\left(\frac{\varsigma_{3,m+1}^{n+1} - 2\varsigma_{3,m}^{n+1} + \varsigma_{3,m-1}^{n+1}}{\Delta\xi^2}\right) = 0;$$

$$\forall\, m = 2, 3, \ldots, N_x + 1. \quad (7.13)$$

The two law of mass action expressions at every cell (7.10 and 7.11) along with the discretized conservation equation for the two cations (7.12 and 7.13) form a set of $4N_x$ nonlinear equations at every time step. We solve this nonlinear system of equations at every time step using the Newton-Raphson method to obtain cation concentration values at all cells.

The advantage of this numerical formulation is the direct coupling of reactions using law of mass actions. Hence, the complexity of the reactions can be increased to account for nonidealities. This formulation can also be extended to include more number of cations.

7.2.3 Gibbs Free Energy Minimization Approach

In the Gibbs Free Energy Minimization approach, the cation concentrations are obtained by minimizing the Gibbs free energy function for cation components in both aqueous and solid phase in every cell. The solution to the minimization problem is the cation concentration while the anion concentrations are obtained independently, as described in the previous section. The operator splitting approach is employed in the Gibbs free energy minimization approach of integrating flow and reactions.

In the operator splitting approach, the transport step and the reaction step occur discretely. In the first step, called the transport step, the concentration of components arising out of only transport (advection and diffusion but no reactions) are obtained. The concentrations resulting from transport are referred to as transported concentrations, $\varsigma_{i,m}^{t_n}$ and are obtained from the conservation equation for cations. The discretized equation to obtain transported concentrations is,

$$\frac{(\varsigma_{i,m}^{t_n} - \varsigma_{i,m}^{n})}{\Delta\tau} + \frac{(\varsigma_{i,m}^{n} - \varsigma_{i,m-1}^{n})}{\Delta\xi} - \frac{1}{Pe}\left(\frac{\varsigma_{i,m+1}^{t_n} - 2\varsigma_{i,m}^{t_n} + \varsigma_{i,m-1}^{t_n}}{\Delta\xi^2}\right) = 0;$$
$$\forall\, i = 1, 2, 3; \quad m = 2, \ldots, N_x + 1 \quad \& \quad n = 1, 2, N_t + 1. \quad (7.14)$$

Eq 7.14 is similar to the anion concentration equation (eq 7.4) that was used to obtain anion concentration independently at every cell. The same approach, described in the previous section, is used to find the transported cation concentrations, $\varsigma_{i,m}^{t_n}$, at all points in space.

In the next reaction step, concentrations arising out of cation exchange reactions are obtained. The only unknowns are the cation concentrations in the aqueous phase and the solid phase. Because either phase concentrations (ς_i and $\hat{\varsigma}_i$) are expressed as moles/pore volume, the number of moles of the component in either phases can be obtained by multiplying the concentration of that component with pore volume of the cell. As the components are assumed to be ideal, the Gibbs free energy function for cation components in both aqueous and solid phase at every cell m is G_m^N and is given as,

$$\begin{aligned} G_m^C = \frac{G_m^N}{PV_c} &= \sum_{i=1}^{3} \varsigma_{i,m}(\bar{G}_{iw})_m + \sum_{p=1}^{3} \varsigma_{p,m}(\bar{G}_{ps})_m \\ &= \underbrace{\sum_{i=1}^{3} \varsigma_{i,m}\left(\bar{G}_i^0 + RTln\frac{\varsigma_{i,m}}{\sum_i \varsigma_{i,m}}\right)}_{\text{aqueous phase components}} + \underbrace{\sum_{p=1}^{3} \hat{\varsigma}_{p,m}\left(\bar{G}_p^0 + RTln\frac{\hat{\varsigma}_{p,m}}{\sum_p \hat{\varsigma}_{p,m}}\right)}_{\text{solid phase components}}. \end{aligned} \tag{7.15}$$

Here, $PV_c = A\phi\Delta\xi$ is the pore volume for every cell with cross sectional area A and width $\Delta\xi$. As PV_c is a constant, G_m^C (in units kJ/pore volume) can be minimized directly to obtain the cation concentration in every cell. Also, $\bar{G}_i^0$ and $\bar{G}_p^0$ are the standard state Gibbs free energy values of components in aqueous phase and solid phase respectively.

While tabulated standard state values (Rossini et al., 1952) were used in earlier applications, the standard state values for a system of reacting components can also be obtained from equilibrium constant data measured experimentally. Inorder to provide better comparison between the two numerical

models and the experimental values, the standard state Gibbs free energy values were obtained from the equilibrium constants. Appendix C describes the method of obtaining reference state values from the equilibrium constant data. The reference state values, listed in Table C.1, are used to obtain equilibrium compositions using the Gibbs free energy method presented in this section.

The equilibrium composition is obtained by minimizing G_m^C. The minimization is performed for all points in space ($m = 2, 3, \ldots, N_x + 1$). The minimization problem can be written as,

$$\begin{aligned} \text{Minimize} \quad G_m^C &= \sum_{i=1}^{3} \varsigma_{i,m} \left(\bar{G}_i^0 + RTln\frac{\varsigma_{i,m}}{\varsigma_{a,m}} \right) + \sum_{p=1}^{3} \hat{\varsigma}_{p,m} \left(\bar{G}_p^0 + RTln\frac{\hat{\varsigma}_{p,m}}{Z_v} \right). \\ \text{Subject to} \quad \mathbf{AC} &= \mathbf{E} \qquad \text{and} \qquad \varsigma_{i,m} \geq 0, \hat{\varsigma}_{i,m} \geq 0. \end{aligned} \tag{7.16}$$

Here, $\mathbf{A}$ is the elemental matrix, $\mathbf{C}$ is the matrix of component concentration while $\mathbf{E}$ is the matrix of total element concentration, as described in chapter 4. The elements are ordered as Na ($k = 1$), Ca ($k = 2$) and Mg ($k = 3$). The cation exchange capacity equation is added as additional equality constraint for this minimization problem. The matrices for this minimization are,

$$\mathbf{A} = \begin{bmatrix} 1 & 0 & 0 & 1 & 0 & 0 \\ 0 & 1 & 0 & 0 & 1 & 0 \\ 0 & 0 & 1 & 0 & 0 & 1 \\ 0 & 0 & 0 & 1 & 2 & 2 \end{bmatrix}; \qquad \mathbf{C} = \begin{bmatrix} \varsigma_{1,m} \\ \varsigma_{2,m} \\ \varsigma_{3,m} \\ \hat{\varsigma}_{1,m} \\ \hat{\varsigma}_{2,m} \\ \hat{\varsigma}_{3,m} \end{bmatrix}; \qquad \mathbf{E} = \begin{bmatrix} \epsilon_{1,m} \\ \epsilon_{2,m} \\ \epsilon_{3,m} \\ Z_v \end{bmatrix}.$$

The transported concentrations are used as inputs to the elemental balance equation for the Gibbs free energy minimization approach. The total amount

of any element k at any cell m is $\epsilon_{k,m}$ and is obtained using,

$$\epsilon_{k,m} = \sum_{k=1}^{3} a_{i,k} \left[\hat{\varsigma}_{i,m}^{n} + \varsigma_{i,m}^{t_n} \right] \quad \forall\, m = 2, 3, \ldots, N_x + 1 \quad \text{and} \quad n = 2, 3, N_t + 1. \tag{7.17}$$

7.3 Case Study

Valocchi et al. (1981b) has described field scale measurements for ternary cation transport observed in a shallow alluvial aquifer in the Palo Alto Baylands region. They presented a numerical solution to the 1-D problem. The original field description along with the evolution of the groundwater composition at different wells is available in Valocchi et al. (1981a). In an effort to charge groundwater, treated municipal effluent was injected at a constant composition value and water composition was monitored over time at an observation well. The native groundwater composition at the monitoring well and the injected water composition are listed in Table 7.1.

The numerical models using both the stochiometric approach as well as the Gibbs free energy minimization approach are developed for this particular case of constant initial and injection concentration of cations (Table 7.1). The values of the variables used in the numerical solution are listed in Table 7.2. The longitudinal dispersivity, $\alpha_L = 1$, and distance between L, between the producer and injector well is given as 16 m (Valocchi et al., 1981b). The Peclect number is then $Pe = L/\alpha_L = 16$.

The magnitude of $\Delta\xi$ and $\Delta\tau$ impact numerical dispersion and conver-

Table 7.1: Component compositions adapated from Valocchi et al. (1981b). Anion concentration calculated using charge balance for construction of numerical solutions.

Component	Initial composition (mM)	Injected composition (mM)
Na^+	86.52	9.4
Mg^{2+}	17.95	0.5
Ca^{2+}	11.1	2.15
Cl^-	144.62	14.7

gence, respectively. For both the numerical models, the values of $\Delta\xi = 0.005$ and $\Delta\tau = 0.004$ are chosen to minimize numerical dispersion and for convergence. Similar results were obtained using either approach.

The computational times required to solve the nonlinear equations presented in the two approaches were compared. When the same initial guesses were used, the Gibbs free energy approach was about 35% faster than the stochiometric approach for this particular case of three cation system.

The operator splitting method used in the Gibbs free energy approach offers the advantage of decoupling flow and reactions. Hence, the Gibbs free energy approach is likely faster than the stochiometric approach where flow and reactions are coupled in one single system. The computational time advantage of the Gibbs free energy approach make it more favourable over the stochiometric approach to obtain equilibrium compositions for the three cation case discussed in this chapter. Figure 7.1 shows that the prediction from the numerical model constructed using the Gibbs free energy approach compares well with the effluent cation concentration measured in the field.

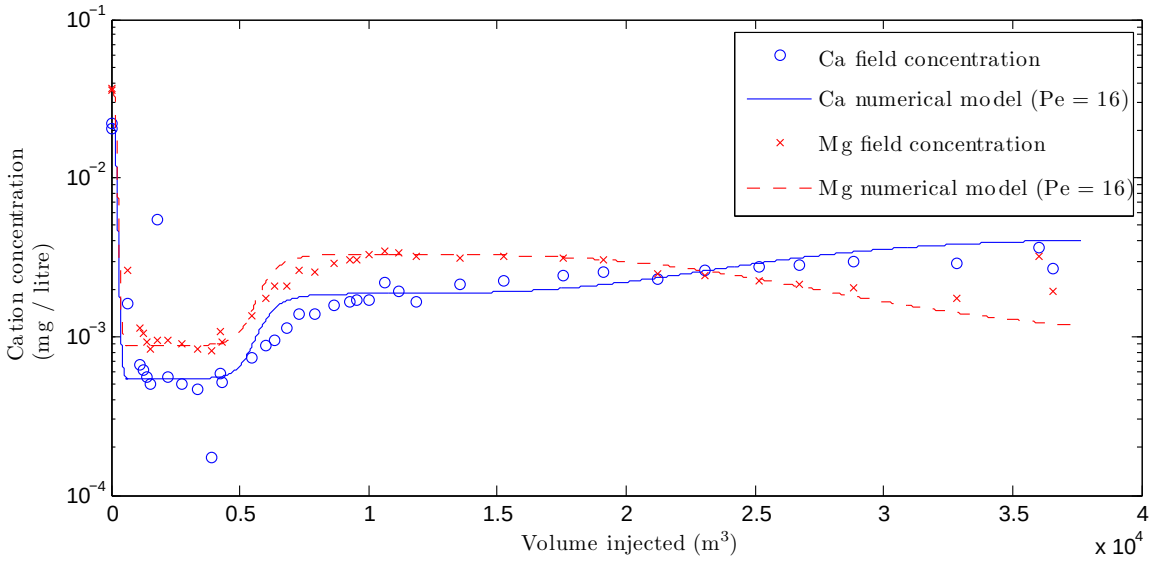

Figure 7.1: Comparison of Gibbs free energy numerical model with field measurements (Valocchi et al., 1981b).

Table 7.2: Constants used in Numerical Model Solution (Valocchi et al., 1981b)

Parameters	Value
K_{10}	2.667
K_{20}	4.0
Z_v	0.75

7.4 Conclusions

Numerical models were presented using both the stochiometric approach and the Gibbs free energy approach. In either approach, the advection term was discretized explicitly while the dispersion term was discretized implicitly. A case study of three-cation exchange and flow with constant initial and injection concentration described in Valocchi et al. (1981b) was used to compare numerical solutions.

A comparison of computation times indicated that the Gibbs free energy approach was 35% faster than the stochiometric approach. The results from the numerical models compare well with the field experimental values.

Chapter 8

Analytical Solutions for Cation Exchange Reactions

In this chapter, analytical solutions have been developed to predict effluent profiles for dispersion-free flow of the three cations introduced in chapter 7. The predictions from the analytical solution as well as from the numerical model (from chapter 7) are compared with experimental data for this system.

8.1 Introduction

Analytical solutions have been developed for 1-D flow equations that describe solute chromatography as well as cation exchange by neglecting dispersion. The underlying mass conservation equation for solute chromatography as well as cation exchange neglecting dispersion is,

$$\frac{\partial \mathbf{a}(\mathbf{c})}{\partial t} + \frac{\partial \mathbf{c}}{\partial x} = 0. \tag{8.1}$$

Here, $\mathbf{a(c)}$ is the accumulation term and is a function of independent variables in $\mathbf{c}$, usually, the concentration of components. Analytical solutions can be developed when the system of equations represented by eq 8.1 is hyperbolic. The solution of hyperbolic systems comprises series of intermediate regions of constant concentration (also referred to as constant state) connected by waves

with changing concentrations. The solution in composition space is subsequently translated onto profile or history plots by connecting the intermediate points by waves. The waves can be self-sharpening (shocks) or spreading (rarefactions).

The solution for hyperbolic systems are constructed and analyzed in a space of dependent variables, here the composition space. The composition space is formed $\mathbf{c}$, for a two component system where $\mathbf{c} = [c_1, c_2]$, the composition space is formed by c_1 and c_2 as the x and y axes, respectively. The intermediate constant states and waves connecting them are obtained by analyzing the solution for hyperbolic systems in the composition space. The composition space helps summarize possible solutions for different combinations of initial and injected concentrations and hence, provides unique insights. The solution in composition space is subsequently translated onto profile or history plots.

Analytical solutions offer the advantage of quick estimation of intermediate compositions observed during displacements resulting from a case of constant injection and initial compositions. The number and nature of waves as well as when they occur can be predicted to a reasonable accuracy using this theory. This is useful for sensitivity analysis of the displacement behavior for different injection concentrations for these applications. These solutions can also guide design of experiments. Additionally, analytical solutions can be used to benchmark results from numerical models.

A review of adsorption and cation exchange isotherms that are central

to the development of analytical solutions is presented in this section along with analytical solution developments specific to the ternary cation case of interest.

8.1.1 Adsorption and Ion Exchange Isotherms

Adsorption isotherms are expressions that relate the concentration of the adsorbed concentration of components to the aqueous phase concentrations. The typical isotherms used are linear, Freundlich and Langmuir, and BET isotherms (Mazzotti and Rajendran, 2013). The coefficients in the isotherm expression are obtained by fitting experimental data to cover a wide range of concentrations.

Glueckauf (1949) presented the general theory for two solute adsorption in a column. He also obtained analytical solutions for the specific case of a Langmuir isotherm by identifying the solution paths along which compositions appear. Rhee et al. (1972) describe analytical solutions for flow with adsorption for a binary system. In this approach, the method of characteristics is used to find the solutions that lie on characteristic curves in the hodographic plane. A hodographic plane is formed by component concentrations and also referred to as the composition space. The functional form of the Langmuir isotherms are used to get the characteristic curves. The slope of these curves, called characteristic parameters (Rhee and Amundson, 1970), are used to predict shocks or rarefaction waves during the displacement.

The theory by Glueckauf (1949) was extended to ion exchange processes

by Klein et al. (1967), Tondeur and Klein (1967) and Helfferich and Klein (1970). They use a different approach, obtaining the isotherm expressions from the charge balance equation, the adsoption site balance equation and the law of mass action. This approach can be used to not only derive most well known isotherms (see Appendix F) but also isotherms for electrostatic surface complexation models to predict pH variations in soil (Buergisser et al., 1994).

Helfferich and Klein (1970) developed analytical solutions using coherence theory, originally for chromatographic separation. This theory stipulates equal concentration velocities for all components at any given point in space and time. The coherence theory is, infact, a consequence of Riemann boundary conditions for the hyperbolic system (See Appendix E).

8.1.2 Ternary System with Cation Exchange Reactions

Pope et al. (1978b) introduced analytical solutions in the context of incorporating cation exchange reactions in chemical (surfactant) flooding design. They used a combination of method of characteristics and the coherence theory to predict the composition path for a two cation case and a three cation case (identical to the system considered in this study). They estimated the intermediate composition using coherence theory.

Valocchi et al. (1981b) used the theory of chromatography to understand the evolution of water quality during aquifer recharge with a municipal effluent. Appelo et al. (1993) introduced the shock front solution by estimating the pleateau concentrations (constant states) to match the field observations

in Valocchi et al. (1981b). The constant states were obtained by solving a set of non-linear equations using the jump conditions (see section 4.2).

Charbeneau (1988) has also presented the solution to the general ternary system with heterovalent ions using the method of characteristics. He identified the presence of constant states and obtained the three eigenvalues associated with the analytical solution. While the general problem is discussed, only a solution with sharp fronts has been reported and compared with field data in Valocchi et al. (1981b). The waves for a general hyperbolic system, however, can be shocks or rarefactions (LeVeque, 1994). The shock solution developed by Appelo et al. (1993) is just one of four types of waves that can be obtained for a ternary system.

8.2 General Solution

Equivalent concentrations, c_i and $\hat{c}_i$, defined as $c_i = \nu_i \varsigma_i$ and $\hat{c}_i = \nu_i \hat{\varsigma}_i$, where ν_i is the valency of the cation component, are used in the construction of analytical solutions. All concentrations are in moles/pore volume. The mass balance and the cation exchange capacity equation for a system of N_c cation components in terms of equivalent concentrations is,

$$\sum_{i=1}^{N_c} c_i = c_a \qquad \text{and} \sum_{i=1}^{N_c} \hat{c}_i = Z_v. \tag{8.2}$$

The law of mass action expression for cation exchange reactions in equivalent concentrations is,

$$K_{ij} = \frac{(c_j)^{\nu_i}(\hat{c}_i)^{\nu_j}}{(\hat{c}_j)^{\nu_i}(c_i)^{\nu_j}} \qquad \forall\, i, j = 0, 1, 2, \cdots, N_c - 1. \tag{8.3}$$

Table 8.1: Unknowns and Equations for n Component System

Unknowns	Cations (c_i, $i = 1, 2, ..., N_c$)	N_c
	Anion (c_a)	1
	Adsorbed cations ($\hat{c}_i$, $i = 1, 2, ..., N_c$)	N_c
	Total unknowns	$2N_c + 1$
Equations	Charge balance	1
	Cation exchange capacity	1
	Reactions (K_{ij})	$N_c - 1$
	Total equations	$N_c + 1$
Independent variables	Unknowns - Equations	N_c

There are N_c independent variables for this system (Table 8.1). The concentrations of N_c cations $(c_1, c_2, \ldots, c_{N_c})$ are the chosen set of independent variables for subsequent development. With this choice of independent variables, the adsorbed concentrations are the dependent variables that can be expressed as a function of the aqueous concentrations. These expressions that relate the adsorbed concentrations and aqueous concentrations are referred to as adsorption isotherms (Lake et al., 2003) or ion exchange isotherms (Charbeneau, 1982). Klein et al. (1967) have also given the implicit expressions for cation exchange isotherm. The explicit expressions for isotherms for an ideal system with two and three cations, using this choice of independent variables, are listed in Table 8.2.

A total concentration, a_i, for component i where $a_i = c_i + \hat{c}_i$ can be defined so that the conservation equation, neglecting dispersion ($\mathcal{D} = 0$ in eq 7.2) is,

$$\frac{\partial \mathbf{a}}{\partial \tau} + \frac{\partial \mathbf{c}}{\partial \xi} = 0, \quad 0 \leq \xi < 1, \quad \tau \geq 0. \tag{8.4}$$

Table 8.2: Adsorption Isotherms for Systems with Monovalent Anion

Cation type and valency	Exchange expression	Isotherm expressions
Mono (c_1) - Mono (c_2)	$K_{21} = \frac{\hat{c}_2 c_1}{\hat{c}_1 c_2}$	$\hat{c}_1 = \frac{Z_v c_1}{c_1 + K_{21} c_1}; \quad \hat{c}_2 = \frac{Z_v K_{21} c_1}{c_1 + K_{21} c_2}.$
Mono (c_1) - Di (c_2)	$K_{21} = \frac{\hat{c}_2 c_1^2}{\hat{c}_1^2 c_2}$	$\hat{c}_1 = \frac{c_1\sqrt{c_1^2 + 4Z_v K_{21} c_2} - c_1^2}{2K_{21} c_2};$ $\hat{c}_2 = Z_v - \left[\frac{c_1\sqrt{c_1^2 + 4Z_v K_{21} c_2} - c_1^2}{2K_{21} c_2}\right].$
Mono (c_1, c_2 and c_3)	$K_{21} = \frac{\hat{c}_2 c_1}{\hat{c}_1 c_2},$ $K_{31} = \frac{\hat{c}_3 c_0}{\hat{c}_0 c_2}.$	$\hat{c}_1 = \frac{Z_v c_1}{c_1 + K_{21} c_2 + K_{31} c_3};$ $\hat{c}_2 = \frac{Z_v c_2 K_{21}}{c_1 + K_{21} c_2 + K_{31} c_3};$ $\hat{c}_3 = \frac{Z_v c_3 K_{31}}{c_1 + K_{21} c_2 + K_{31} c_3}.$
Mono (c_1) - Di (c_2 and c_3)	$K_{21} = \frac{\hat{c}_2 c_1^2}{\hat{c}_1^2 c_2}\ ,$ $K_{31} = \frac{\hat{c}_3 c_1^2}{\hat{c}_1^2 c_3}.$	$\hat{c}_1 = \frac{c_1\sqrt{c_1^2 + 4Z_v(K_{21} c_2 + K_{31} c_3)} - c_1^2}{2(K_{21} c_2 + K_{31} c_3)};$ $\hat{c}_2 = \frac{K_{21} c_2(\sqrt{c_1^2 + 4Z_v(K_{21} c_2 + K_{31} c_3)} - c_1)^2}{4(K_{21} c_2 + K_{31} c_3)^2};$ $\hat{c}_3 = \frac{K_{31} c_3(\sqrt{c_1^2 + 4Z_v(K_{21} c_2 + K_{31} c_3)} - c_1)^2}{4(K_{21} c_2 + K_{31} c_3)^2}.$

Here, $\mathbf{a} = [a_1, a_2, \cdots, a_{N_c}]^T$, $\hat{\mathbf{c}} = [\hat{c}_1, \hat{c}_2, \cdots, \hat{c}_{N_c}]^T$ and $\mathbf{c} = [c_1, c_2, \cdots, c_{N_c}]^T$. Eq (8.4) can be written in the following quasilinear form,

$$\mathbf{A}\frac{\partial \mathbf{c}}{\partial \tau} + \frac{\partial \mathbf{c}}{\partial \xi} = \mathbf{0}, \tag{8.5}$$

where, $\mathbf{A}$ is the Jacobian matrix given as,

$$\mathbf{A} = \nabla_c \, \mathbf{a} = \begin{bmatrix} 1 + \frac{\partial \hat{c}_1}{\partial c_1} & \frac{\partial \hat{c}_1}{\partial c_2} & \cdots & \frac{\partial \hat{c}_1}{\partial c_{N_c}} \\ \frac{\partial \hat{c}_2}{\partial c_1} & 1 + \frac{\partial \hat{c}_2}{\partial c_2} & \cdots & \frac{\partial \hat{c}_2}{\partial c_{N_c}} \\ \vdots & \vdots & \ddots & \vdots \\ \frac{\partial \hat{c}_{N_c}}{\partial c_1} & \frac{\partial \hat{c}_{N_c}}{\partial c_2} & \cdots & 1 + \frac{\partial \hat{c}_{N_c}}{\partial c_{N_c}} \end{bmatrix}. \tag{8.6}$$

This system is strictly hyperbolic if $\mathbf{A}$ is diagonizable with real and distinct eigenvalues for all values of concentrations in the range of the solution (LeVeque, 1994).

If $\mathbf{A}$ is strictly hyperbolic, $\mathbf{A} = \mathbf{R}\mathbf{\Gamma}\mathbf{R^{-1}}$ where $\mathbf{\Gamma} = diag(\sigma_1, \sigma_2, \cdots, \sigma_n)$ is the diagonal matrix of eigenvalues σ_p and $\mathbf{R} = [\mathbf{r}_1|\mathbf{r}_2|\cdots|\mathbf{r}_n]$ is the matrix of right eigenvectors $\mathbf{r}_p$. The constant coefficient linear system assumption for $\mathbf{A}$ implies these eigenvalues are constants. Multiplying (8.5) by $\mathbf{R}^{-1}$ and defining a new variable $\mathbf{v}$=$\mathbf{R}^{-1}\mathbf{c}$ to obtain,

$$\mathbf{\Gamma}\frac{\partial \mathbf{v}}{\partial \tau} + \frac{\partial \mathbf{v}}{\partial \xi} = 0.$$

This is equivalent to the following n linear advection equations,

$$\frac{\partial v_p}{\partial \tau} + \lambda_p \frac{\partial v_p}{\partial \xi} = 0 \quad \forall \; p = 1, 2, \cdots, n. \tag{8.7}$$

Here, $\lambda_p = 1/\sigma_p$. The solution to such a linear advection equation is just the initial condition propogated with velocity λ_p given by,

$$\mathbf{c}(\xi, \tau) = \sum_{p=1}^{n} v_p(\xi, \tau)\mathbf{r}_p = \sum_{p=1}^{n} v_p(\xi - \lambda_p \tau, 0)\mathbf{r}_p \, . \tag{8.8}$$

A distinction in the velocity of propogation should be noted between the conservation equation developed in LeVeque (1994) and our conservation equation (eq 8.5). The velocity of propogation is the reciprocal of the eigenvalues of matrix **A** rather than the eigenvalues themselves in LeVeque (1994).

Analytical solutions have been developed to the Riemann problem for this quasilinear system. A single discontinuity in a piecewise constant data like in the case of a constant initial, $\mathbf{c}_I$, and a constant injected concentration, $\mathbf{c}_J$, are commonly referred to as Riemann problems . This is given as,

$$\mathbf{c}(\xi,\tau) = \begin{cases} \mathbf{c}_I & 0 \leq \xi \leq 1 \quad \text{and} \quad \tau = 0, \\ \mathbf{c}_J & \xi = 0 \quad \text{and} \quad \tau \geq 0. \end{cases} \tag{8.9}$$

The Riemann condition in equation (8.9) can be further decomposed into eigenvectors with constant coefficients α_p and β_p so that,

$$\mathbf{c}_I = \sum_{p=1}^{N_c} \alpha_p \mathbf{r}_p \quad \text{and} \quad \mathbf{c}_J = \sum_{p=1}^{N_c} \beta_p \mathbf{r}_p \,. \tag{8.10}$$

The solution can be written in the coordinates of the eigenvectors as,

$$\mathbf{c}(x,t) = \sum_{p=1}^{P(\xi,\tau)} \alpha_p \mathbf{r}_p + \sum_{p=P(\xi,\tau)+1}^{N_c} \beta_p \mathbf{r}_p \,. \tag{8.11}$$

Here, $P(\xi,\tau)$ is the maximum value of p for which $x - \lambda_p t > 0$. This implies that the solution propagates as a series of discontinuities.

The solution to the Riemann problem for a strictly hyperbolic linear system is often visualized in a composition space. This composition space, more generally called the phase space (LeVeque, 1994), is formed by the linearly independent component concentrations of the system. In a composition

space with N_c linearly independent component concentrations, the injected (J) and initial (I) concentrations are points $\mathbf{c}_J$ and $\mathbf{c}_I$ with coordinates $\mathbf{c}_J = (c_{1J}, c_{2J}, \cdots, c_{N_cJ})$ and $\mathbf{c}_I$=$(c_{1I}, c_{2I}, \cdots, c_{N_cI})$. The solution to the Riemann problem in this space consists of $N_c - 1$ intermediate points (or compositions) between $\mathbf{c}_I$ and $\mathbf{c}_J$ connected by N_c waves along the eigenvectors. These intermediate compositions, represented as intermediate points in the composition space, are also referred to as constant states $\mathbf{c}_{M_i}$. In the strictly hyperbolic linear system, the eigenvalues are distinct and the wave velocities are ordered as,

$$\lambda_1 > \lambda_2 > \cdots > \lambda_{N_c}. \tag{8.12}$$

Each wave $\mathcal{W}_p$ is advected with velocity λ_p. The waves occur sequentially, in the order of decreasing velocities at the observation point $\xi = 1$. Therefore, the general solution can be given as,

$$\mathbf{c}_I \xrightarrow{\mathcal{W}_1} \mathbf{c}_{M_1} \xrightarrow{\mathcal{W}_2} \mathbf{c}_{M_2} \xrightarrow{\mathcal{W}_3} \quad \cdots \quad \xrightarrow{\mathcal{W}_{N_c-1}} \mathbf{c}_{M_{N_c-1}} \xrightarrow{\mathcal{W}_{N_c}} \mathbf{c}_J. \tag{8.13}$$

It can also be shown that each discontinuity, for the constant coefficient linear system, satisfies the Rankine-Hugoniot jump condition (LeVeque, 1994). Each wave connecting these intermediate points are contact discontinuities (Lax, 1957).

The matrix $\mathbf{A}$ in eq 8.6 is nonlinear. However, the structure of solution, shown in eq 8.13, also holds for a genuinely nonlinear hyperbolic system, where the eigenvalues vary monotonically along the associated eigenvectors (LeVeque, 1994). Therefore, the solution consists of N_c waves with $N_c - 1$ intermediate

states arranged in increasing order of their velocities. However, unlike the constant coefficient linear system, where all waves are contact discontinuities, the individual waves for the genuinely nonlinear case can be either rarefactions or shocks. The entropy condition is used to identify the type of wave between any two intermediate states in the composition space (Lax, 1957). The details of the construction of each type of wave, specific to the three cation and one anion problem, in the next section.

8.3 Analytical Solution for Three Cations

In this section, analytical solutions are presented for the specific case of three cations Na^+ (c_1), Ca^{2+} (c_2) and Mg^{2+} (c_3) along with an anion Cl^- (c_a). The conservation equations in equivalent concentrations for this system are,

$$c_1 + c_2 + c_3 = c_a \quad \text{and} \quad \hat{c}_1 + \hat{c}_2 + \hat{c}_3 = Z_v. \tag{8.14}$$

The cation exchange reaction equations for this system are,

$$K_{21} = \frac{\hat{c}_2 c_1^2}{\hat{c}_1^2 c_2} \qquad \text{and} \qquad K_{31} = \frac{\hat{c}_3 c_1^2}{\hat{c}_1^2 c_3}. \tag{8.15}$$

There are seven unknowns (c_1, c_2, c_3, $\hat{c}_1$, $\hat{c}_2$, $\hat{c}_3$ and c_a) and four equations (8.14-8.15) for this system. The divalent cation equivalent concentrations c_2 and c_3 and the anion equivalent concentration c_a are chosen as the three independent variables for this system. The isotherm expressions for adsorbed concentrations, using this set of independent variables, is given in Table 8.2.

Define similarity variable $\sigma = \tau/\xi$, and transforming equation (8.5) to an eigenvalue-eigenvector problem,

$$(\mathbf{A} - \sigma\mathbf{I})\,\frac{d\mathbf{c}}{d\sigma} = 0. \tag{8.16}$$

The boundary conditions for the Riemann problem can also be transformed using this variable. Here, $\mathbf{I}$ is a 3×3 identity matrix and $\mathbf{A}$ is given as,

$$\mathbf{A} = \begin{bmatrix} 1+\hat{c}_{22} & \hat{c}_{23} & \hat{c}_{2a} \\ \hat{c}_{32} & 1+\hat{c}_{33} & \hat{c}_{3a} \\ 0 & 0 & 1 \end{bmatrix}. \tag{8.17}$$

The last row in matrix $\mathbf{A}$ simplifies because the anion c_3 does not adsorb. Also, $\hat{c}_{ij} = \partial\hat{c}_i/\partial c_j$ is used to denote the partial derivatives of the isotherms. The eigenvalues of $\mathbf{A}$ are,

$$\begin{aligned} \sigma_1 &= 1, \\ \sigma_2 &= 1 + \frac{\hat{c}_{22} + \hat{c}_{33} - \sqrt{(\hat{c}_{22} - \hat{c}_{33})^2 + 4\hat{c}_{23}\hat{c}_{32}}}{2}, \\ \sigma_3 &= 1 + \frac{\hat{c}_{22} + \hat{c}_{33} + \sqrt{(\hat{c}_{22} - \hat{c}_{33})^2 + 4\hat{c}_{23}\hat{c}_{32}}}{2}. \end{aligned} \tag{8.18}$$

The eigenvalues obtained for all analytical solutions presented in this chapter (laboratory and field case) were real, distinct and positive and are ordered as follows,

$$\sigma_1 < \sigma_2 < \sigma_3. \tag{8.19}$$

Here, the eigenvalues are reciprocal of wave velocities ($\sigma = 1/\lambda$), also referred to as retardations. The characteristic field represented by σ_1=1 is linearly degenerate . Also, the characteristic fields represented by σ_2 and σ_3 are genuinely

nonlinear (LeVeque, 1994) for all the solutions developed in this chapter. The analytical solution to the Riemann problem can then be constructed in the composition space.

The three unknowns for this system form a three dimensional composition space (Figure 8.1). The initial and the injected concentrations are points $\mathbf{c}_I$ and $\mathbf{c}_J$ with coordinates (c_{1I}, c_{2I}, c_{aI}) and (c_{1J}, c_{2J}, c_{aJ}) respectively. The Riemann solution in this composition space consists of three waves and two intermediate points (or constant states) $\mathbf{c}_{M_1}$ and $\mathbf{c}_{M_2}$ (eq 8.13). These waves arrive in the increasing order of retardations at the observation point $\xi = 1$. Hence, all solutions can be represented as,

$$\mathbf{c}_I \xrightarrow{\mathcal{W}_1} \mathbf{c}_{M_1} \xrightarrow{\mathcal{W}_2} \mathbf{c}_{M_2} \xrightarrow{\mathcal{W}_3} \mathbf{c}_J. \tag{8.20}$$

The fast wave has a constant speed (σ_1=1) so the wave $\mathcal{W}_1$ is a contact discontinuity ($\mathcal{D}$). The other two waves can be rarefactions or shocks. The analytical solution for this system then consists of finding the intermediate points $\mathbf{c}_{M_1}$ and $\mathbf{c}_{M_2}$ and the nature of waves $\mathcal{W}_2$ and $\mathcal{W}_3$ (shock or rarefaction), that connect them.

8.3.1 Anion Wave and Cation Exchange Waves

Lake et al. (2003) have shown that the eigenvector equations offer insights into the nature of the solution in the composition space. The eigenvalue associated with $\mathcal{W}_1$, also called the anion wave, is $\sigma_1 = 1$. The eigenvector

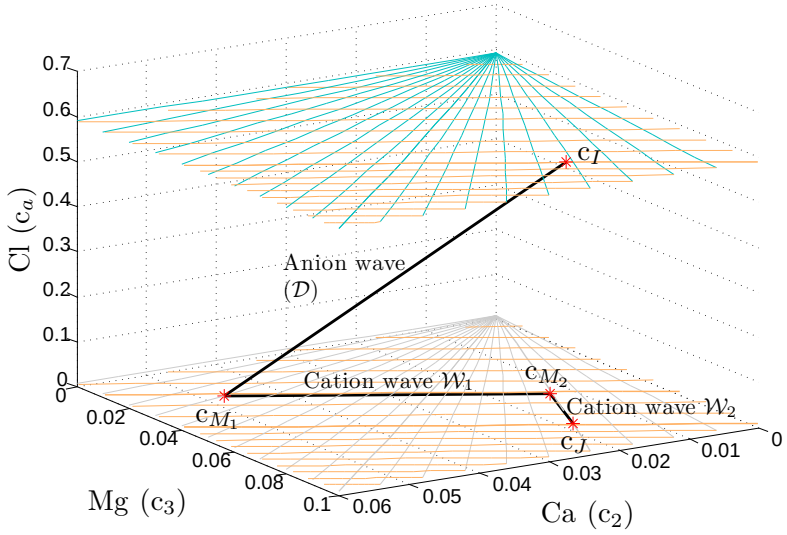

Figure 8.1: Composition space and waves for a system with three cations and one anion. The lines in constant anion plane represent solution paths in the composition space.

equation for σ_1 can be simplied to obtain,

$$\begin{aligned} \hat{c}_{22}\frac{dc_2}{d\sigma} + \hat{c}_{23}\frac{dc_3}{d\sigma} + \hat{c}_{2a}\frac{dc_a}{d\sigma} = 0 \quad &\Rightarrow \quad \frac{d\hat{c}_2}{d\sigma} = 0. \\ \hat{c}_{32}\frac{dc_2}{d\sigma} + \hat{c}_{33}\frac{dc_3}{d\sigma} + \hat{c}_{3a}\frac{dc_a}{d\sigma} = 0 \quad &\Rightarrow \quad \frac{d\hat{c}_3}{d\sigma} = 0. \end{aligned} \tag{8.21}$$

Eq 8.21 implies that the adsorbed concentrations, $\hat{c}_2$ and $\hat{c}_3$, do not change along the anion wave $\mathcal{W}_1$. Hence, $\mathbf{c}_{M_1} = \mathbf{c}_I$.

The eigenvector equations for the other eigenvalues σ_i $(i = 2, 3)$ can also be simplified to obtain,

$$\begin{aligned} (1-\sigma_i)\frac{dc_a}{d\sigma_i} = 0 \quad &\Rightarrow \quad \frac{dc_a}{d\sigma_i} = 0. \\ (1+\hat{c}_{22}-\sigma_i)\frac{dc_2}{d\sigma_i} + \hat{c}_{23}\frac{dc_3}{d\sigma_i} = 0 \quad &\Rightarrow \quad \frac{dc_2}{dc_3} = \frac{\hat{c}_{12}}{\sigma_i - 1 - \hat{c}_{11}}. \end{aligned} \tag{8.22}$$

This implies that the anion concentration does not change along $\mathcal{W}_2$ and $\mathcal{W}_3$. Thus, in the composition space, the points $\mathbf{c}_{M_1}$, $\mathbf{c}_{M_2}$ and $\mathbf{c}_J$ lie on a plane of constant anion concentration (See Figure 8.1). Because only cation concentrations changes along $\mathcal{W}_2$ and $\mathcal{W}_3$, they are referred to as the cation exchange waves.

In summary, the adsorbed concentrations do not change along anion wave $\mathcal{W}_1$, so that $\hat{\mathbf{c}}_{M_1} = \hat{\mathbf{c}}_I$. Hence, at point $\mathbf{c}_{M_1}$, all the adsorbed concentrations are known. Also, the intermediate point $\mathbf{c}_{M_1}$ lies in the plane of injected anion concentration so that $c_{3M_1} = c_{3J}$. The law of mass action equations and charge conservation at anion plane c_{3J} are used to obtain a quadratic equation.

Using the positive root,

$$c_{1M_1} = \frac{-1 + \sqrt{1 + 4c_{aJ}\left(\frac{\hat{c}_{2I}}{\hat{c}_{1I}^2 K_{21}} + \frac{\hat{c}_{3I}}{\hat{c}_{1I}^2 K_{31}}\right)}}{2\left(\frac{\hat{c}_{2I}}{\hat{c}_{1I}^2 K_{21}} + \frac{\hat{c}_{3I}}{\hat{c}_{1I}^2 K_{31}}\right)}. \tag{8.23}$$

The other flowing concentrations are calculated using the law of mass action,

$$c_{2M_1} = \frac{\hat{c}_{2M_1} c_{1M_1}^2}{K_{21}\hat{c}_{1M_1}^2} \qquad \text{and} \qquad c_{3M_1} = \frac{\hat{c}_{3M_1} c_{1M_1}^2}{K_{31}\hat{c}_{1M_1}^2}. \tag{8.24}$$

The eigenvalue-eigenvector analysis (8.21-8.22) is generic and can be extended to a system of N_c cations and one anion. The matrix $\mathbf{A}$ will have N_c eigenvalues including $\sigma_1 = 1$ corresponding to anion wave $\mathcal{W}_1$. The anion concentration changes from the initial to the injected concentration along $\mathcal{W}_1$ and will remain constant along all the other $N_c - 1$ cation waves. The adsorbed concentrations are constant across $\mathcal{W}_1$ and can be used to obtain the first intermediate point $\mathbf{c}_{M_1}$.

In the three cation case, the other intermediate point $\mathbf{c}_{M_2}$ lies at the intersection of wave $\mathcal{W}_2$ from point $\mathbf{c}_{M_1}$ and wave $\mathcal{W}_3$ from point $\mathbf{c}_J$ (Figure 8.1). The waves $\mathcal{W}_2$ and $\mathcal{W}_3$ can be rarefactions or shocks. Hugoniot loci and integral curves are sets of admissible shocks and rarefaction waves, respectively.

8.3.2 Hugoniot Loci and Integral Curves

Hugoniot loci are the set of all points in the composition space that connect two states with a discontinuity and satisfy the Rankine-Hugoniot jump condition. The Rankine-Hugoniot jump condition connecting any two points,

$\mathbf{c}_L$ as the left state and $\mathbf{c}_R$ as the right state can be given as,

$$\tilde{\sigma}_p = \frac{(\hat{\mathbf{c}}_R + \mathbf{c}_R) - (\hat{\mathbf{c}}_L + \mathbf{c}_L)}{\mathbf{c}_R - \mathbf{c}_L}. \tag{8.25}$$

The Hugoniot curve from point $\mathbf{c}_{M_1}$ (left state for wave $\mathcal{W}_2$) is the locus of all points $\mathbf{c}_R$, the right state, that satisfy this jump condition. The vector equation (G.4) results in the following scalar equation,

$$\frac{(\hat{c}_{2R} + c_{2R}) - (\hat{c}_{2M_1} + c_{2M_1})}{c_{2R} - c_{2M_1}} = \frac{(\hat{c}_{3R} + c_{3R}) - (\hat{c}_{3M_1} + c_{3M_1})}{c_{3R} - c_{3M_1}}. \tag{8.26}$$

In this equation, the adsorbed concentrations can be expressed as a function of aqueous concentrations using isotherm expressions available in Table 8.2. The Hugoniot curves from point $\mathbf{c}_{M_1}$ are obtained by solving for the root of this algebraic equation numerically in the plane of constant anion concentration c_{aJ}. A similar algebraic equation for the Hugoniot curve from point $\mathbf{c}_J$, the right state for wave $\mathcal{W}_3$, is used to obtain the unknown compositions $\mathbf{c}_L$, representing the left state, that satisfy the Rankine-Hugoniot condition.

The integral curves from any point in the composition space is the set of points obtained by integrating along the eigenvectors from that point. The two ODEs resulting from the two eigenvalues in (8.22) are,

$$\left(\frac{dc_2}{dc_3}\right)_{\sigma_2} = \left[\frac{2\hat{c}_{23}}{\hat{c}_{33} - \hat{c}_{22} - \sqrt{(\hat{c}_{22} - \hat{c}_{33})^2 + 4\hat{c}_{23}\hat{c}_{32}}}\right]; \tag{8.27}$$

$$\left(\frac{dc_2}{dc_3}\right)_{\sigma_3} = \left[\frac{2\hat{c}_{23}}{\hat{c}_{33} - \hat{c}_{22} + \sqrt{(\hat{c}_{22} - \hat{c}_{33})^2 + 4\hat{c}_{23}\hat{c}_{32}}}\right]. \tag{8.28}$$

The integral curves from $\mathbf{c}_J$ can be obtained by numerically integrating these ODEs and using the initial condition,

$$c_2(c_{3J}) = c_{2J}. \tag{8.29}$$

Table 8.3: Classification of Cation Exchange Waves for Three Cation and One Anion System . Here, $\mathcal{S}_i$ represents wave $\mathcal{W}_i$ is a shock wave while $\mathcal{R}_i$ represents wave $\mathcal{W}_i$ is a rarefaction wave.

Wave combination ($\mathcal{W}_2$-$\mathcal{W}_3$)	Condition on $\mathcal{W}_2$	Condition on $\mathcal{W}_3$
$\mathcal{S}_2 - \mathcal{S}_3$	$(\sigma_2)_{M_1} \geq (\sigma_2)_R \geq (\sigma_2)_{M_2}$	$(\sigma_3)_{M_2} \geq (\sigma_3)_L \geq (\sigma_3)_J$
$\mathcal{R}_2 - \mathcal{R}_3$	$(\sigma_2)_{M_1} \leq (\sigma_2)_R \leq (\sigma_2)_{M_2}$	$(\sigma_3)_{M_2} \leq (\sigma_3)_L \leq (\sigma_3)_J$
$\mathcal{S}_2 - \mathcal{R}_3$	$(\sigma_2)_{M_1} \geq (\sigma_2)_R \geq (\sigma_2)_{M_2}$	$(\sigma_3)_{M_2} \leq (\sigma_3)_L \leq (\sigma_3)_J$
$\mathcal{R}_2 - \mathcal{S}_3$	$(\sigma_2)_{M_1} \leq (\sigma_2)_R \leq (\sigma_2)_{M_2}$	$(\sigma_3)_{M_2} \geq (\sigma_3)_L \geq (\sigma_3)_J$

A similar set of equations are used to obtain the integral curve from $\mathbf{c}_{M_1}$. The derivatives of the adsorbed concentrations in (eqs G.6) and (G.7) are obtained from the adsorption isotherm expressions in Table 8.2.

The entropy condition is used to determine the nature of waves $\mathcal{W}_2$ and $\mathcal{W}_3$ (Lax, 1957). There are four posssibilities, two each (rarefaction and shock) for waves $\mathcal{W}_2$ and $\mathcal{W}_3$, depending on the behavior of eigenvalues along these waves. The appropriate wave can be identified using conditions listed in Table 8.3. The point $\mathbf{c}_{M_2}$ lies at the intersection of the waves from $\mathbf{c}_J$ and $\mathbf{c}_{M_1}$. The intermediate points, $\mathbf{c}_{M_1}$ and $\mathbf{c}_{M_2}$, along with the appropriate waves (shocks or rarefactions) connecting them is the complete analytical solution in the composition space for this system.

The composition space solution can be used to obtain concentration history (concentration versus time) as well as profile (concentration versus distance). The initial, $\mathbf{c}_I$, injected, $\mathbf{c}_J$, and the intermediate concentrations,

$\mathbf{c}_{M_1}$ and $\mathbf{c}_{M_2}$, appear as constant states in these plots and are connected by appropriately identified waves (shocks or rarefactions). If the wave $\mathcal{W}_p$ is a shock, there will be a sharp discontinuity in the concentration between the constant states. This discontinuity travels with velocity given by the Rankine-Hugoniot jump condition ($\tilde{\sigma}_p$ is reciprocal of velocity in eq G.4). However, if the wave $\mathcal{W}_p$ is a rarefaction wave, all concentrations between the constant states occur in the plot. Each concentration travels with velocity given by the reciprocal of eigenvalue, $1/\sigma_p$, at that point. The analytical solution from the composition space can thus be used to construct composition profile/history plots for any combination of initial and injection composition.

8.4 Results and Discussion

The prediction of concentration histories from the analytical solution, developed in the previous section, was compared with experimental data at laboratory and field scale. This is the first direct comparison of analytical solution with experimental values at both scales.

8.4.1 Laboratory Scale

Voegelin et al. (2000) performed laboratory experiments to study the cation exchange and transport between cations Na^+, Mg^{2+} and Ca^{2+} and anion Cl^- using adsorption columns. They performed detailed characterization experiments to understand the adsorption behavior in multiple combinations of binary systems. They further performed a series of transport experiments

for the ternary system using a mixture of electrolytes NaCl, $MgCl_2$ and $CaCl_2$ at constant pH. These well characterized experiments provide an optimal test for the analytical theory.

8.4.1.1 Summary of experiments

In the original paper, Voegelin et al. (2000) obtained the binary interaction coefficients for different isotherm models as best fits to multiple combinations of binary adsorption experimental data. These isotherm models differ in their use of an additional emperical parameter n_{ij} in the mass action law,

$$K_{ij} = \frac{\hat{c}_j^{\nu_i}}{\hat{c}_i^{\nu_j}} \left(\frac{c_i^{\nu_j}}{c_j^{\nu_i}} \right)^{n_{ij}} . \tag{8.30}$$

This emperical parameter n_{ij} helps account for nonidealities of the phases and the heterogenieties in the solid phase. The emperical parameter and the binary interaction coefficients are estimated using the experimental data.

All phases are assumed ideal for the development of the analytical solutions and use the mass action without any emperical constants. This is equivalent to the 1-site Gaines-Thomas isotherm Voegelin et al. (2000) . The binary interaction coefficients along with the cation exchange capacity, used for the development of analytical solutions, are listed in Table 8.4.

In the ternary experiments, varying concentration of electrolyte mixtures were injected sequentially for a fixed interval of time. The effluent solution was sampled at regular intervals and the cation concentrations were determined using atomic absorption spectroscopy. While results from a nu-

Table 8.4: Constants used for Development of Analytical Solution.

Parameter	Laboratory scale (Voegelin et al., 2000)	Field scale (Valocchi et al., 1981b)
K_{21}	46.933	1.7 eq/litre
K_{31}	67.839	3.0 eq/litre
Z_v	0.1171 (mol/litre)	0.1 meq/litre
Pore volume	Column 1 = 2.11 ml Column 2 = 3.87 ml	401.9 m^3

merical model were compared with experiments in Voegelin et al. (2000), analytical solutions have been developed and compared them with effluent cation concentrations reported in the ternary experiments.

The ternary experiments chosen for comparison with the analytical solution are listed in Table 8.5. Within each experiment, sufficient pore volumes were injected and the injected concentration was changed only after the effluent cation concentrations stabilized. Hence, each experiment in Voegelin et al. (2000) corresponds to multiple solutions of different Riemann problems as the waves do not interfere. Experiments 4 and 5 have been excluded from the analysis because it is not clear if all waves eluted before the injected concentration was changed. In Table 8.5, three parts each for Experiment 1 and 3 and two parts in Experiment 6 that constitute eight separate Riemann problems have been identified. Analytical solutions have been developed for each of these Riemann problems.

Table 8.5: Ternary Transport Experiments in Voegelin et al. (2000). Eq in the table stands for equivalent concentration.

No	Influent (pore volumes)	$CaCl_2$ (mM)	$MgCl_2$ (mM)	NaCl (mM)	Eq Ca c_2(mM)	Eq Mg c_1(mM)	Eq Na c_3(mM)	Eq Cl c_a(mM)
1	< 0	5.2	4.55	4.65	10.4	9.1	4.65	24.15
	0	5.3	-	-	10.6	-	-	10.6
	20	-	2.4	4.6	-	4.8	4.6	9.4
	65	5.2	4.55	4.65	10.4	9.1	4.65	24.15
3	< 0	5.4	5	95	10.8	10	95	115.8
	0	5	-	-	10	-	-	10
	20	-	2.6	95	-	5.2	95	100.2
	65	5.7	5.4	95	11.4	10.8	95	117.2
6	< 0	11.5	49	470	23	98	470	591
	0	3.1	0.62	1.7	6.2	1.24	1.7	9.14
	20	11.5	49	470	23	98	470	591

8.4.1.2 Analytical solution and experimental data

Figure 8.2 shows the adsorption isotherms resulting from the constant anion plane (c_3=0.0091 M) in the analytical solution for Experiment 6.1. The eigenvalues for this system were observed to be real, distinct and positive. The eigenvalues σ_2 and σ_3 were also monotonic and hence the fields are genuinely nonlinear. The solution to the Riemann problem can therefore be constructed using the theory described in the previous section.

The complete analytical solution obtained for the experiments are summarized in Tables 8.6- 8.8. The first intermediate point $\mathbf{c}_{M_1}$ is obtained (eqs G.2 and G.3) using the inference that the adsorbed concentrations are constant along wave $\mathcal{W}_1$. The other intermediate point $\mathbf{c}_{M_2}$ is obtained by the intersection of waves $\mathcal{W}_3$ and $\mathcal{W}_2$ from points $\mathbf{c}_J$ from $\mathbf{c}_{M_1}$ respectively. The Hugoniot

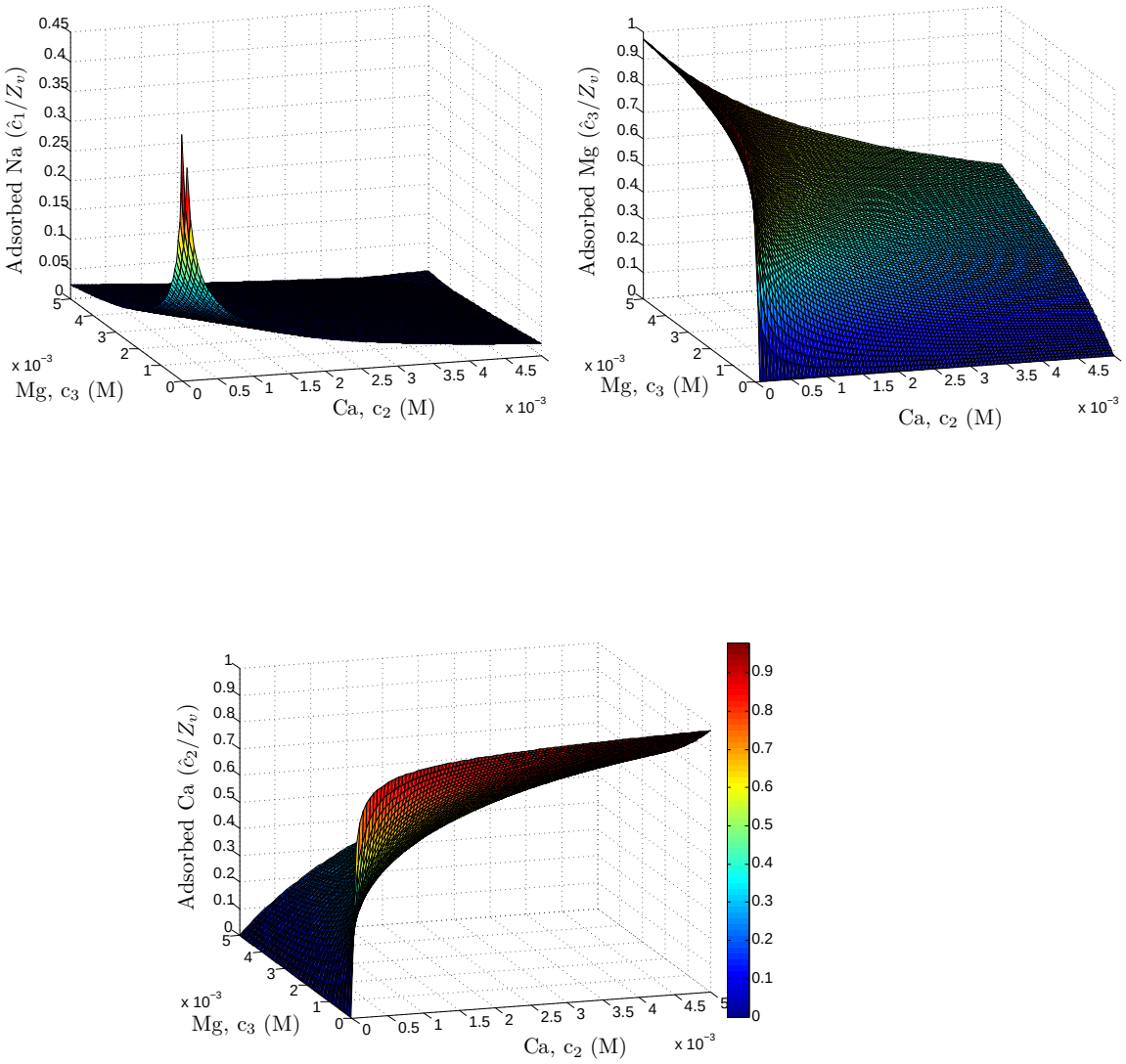

Figure 8.2: Adsorption isotherm for constant anion plane of $c_3 = 0.0091$ M in for Experiment 6 in Voegelin et al. (2000)

Table 8.6: Analytical Solution for Experiments 1 and 2 in Voegelin et al. (2000).

Part	Equivalent concentration ($\mathbf{c}$)	$\mathbf{c}_I$ (moles/ litre)	$\mathbf{c}_J$ (moles/ litre)	$\mathbf{c}_{M_1}$ (moles/ litre)	$\mathbf{c}_{M_2}$ (moles/ litre)	$\mathcal{W}_1$- $\mathcal{W}_2$- $\mathcal{W}_3$
1	Na, c_1	0.0046	-	0.0029	-	$\mathcal{D}_1 - \mathcal{S}_2 - \mathcal{S}_3$
	Mg, c_2	0.0091	-	0.0036	0.00496	
	Ca, c_3	0.0104	0.0106	0.0041	0.00564	
	Cl, c_a	0.0241	0.0106	0.0106	0.0106	
2	Na, c_1	-	0.0046	-	0.00458	$\mathcal{D}_1 - \mathcal{R}_2 - \mathcal{R}_3$
	Mg, c_2	-	0.0048	-	-	
	Ca, c_3	0.0106	-	0.0094	0.00482	
	Cl, c_a	0.0106	0.0094	0.0094	0.0094	
3	Na, c_1	0.0046	0.0046	0.0083	0.0047	$\mathcal{D}_1 - \mathcal{S}_2 - \mathcal{S}_3$
	Mg, c_2	0.0048	0.0091	0.0158	0.0195	
	Ca, c_3	-	0.0104	-	-	
	Cl, c_a	0.0094	0.0241	0.0241	0.0242	

loci and integral curves are constructed using the procedure explained in section 8.3.2. The appropriate waves in the solution are identified based on the criteria listed in Table 8.3.

The analytical solution for Experiments 6.1 and 3.2 compare well with the experimental data in the composition space (Figures 8.3 and 8.5). A contrast in the nature of waves is observed during the displacement for these experiments. Because points $\mathbf{c}_{M_1}$ and $\mathbf{c}_J$ lie on the same plane, one can characterize these waves based on their relative position and divide the composition space into four regions. Each region shows a different displacement behavior. The intermediate point $\mathbf{c}_{M_1}$ in Experiment 6.1 lies in the region of only shocks (region 1 in Figure 8.3) so that $\mathbf{c}_{M_2}$ lies at the intersection of Hugoniot loci

Table 8.7: Analytical Solution for Experiment 3 in Voegelin et al. (2000).

Part	Equivalent concentration ($\mathbf{c}$)	$\mathbf{c}_I$ (moles/ litre)	$\mathbf{c}_J$ (moles/ litre)	$\mathbf{c}_{M_1}$ (moles/ litre)	$\mathbf{c}_{M_2}$ (moles/ litre)	$\mathcal{W}_1$- $\mathcal{W}_2$- $\mathcal{W}_3$
1	Na, c_1	0.095	-	0.0098	0	$\mathcal{D}_1 - \mathcal{S}_2 - \mathcal{S}_3$
	Mg, c_2	0.01	-	0.0001	0.005268	
	Ca, c_3	0.0108	0.01	0.0001	0.004731	
	Cl, c_a	0.1158	0.01	0.01	0.01	
2	Na, c_1	-	0.095	-	0.0943	$\mathcal{D}_1 - \mathcal{R}_2 - \mathcal{R}_3$
	Mg, c_2	-	0.0052	-	-	
	Ca, c_3	0.01	-	0.1002	0.0059	
	Cl, c_a	0.01	0.1002	0.1002	0.1002	
3	Na, c_1	0.095	0.095	0.1102	0.0956	$\mathcal{D}_1 - \mathcal{S}_2 - \mathcal{S}_3$
	Mg, c_2	0.0052	0.0108	0.007	0.0216	
	Ca, c_3	-	0.0114	-	-	
	Cl, c_a	0.1002	0.1172	0.1172	0.1172	

Table 8.8: Analytical Solution for Experiment 6 in Voegelin et al. (2000).

Part	Equivalent concentration ($\mathbf{c}$)	$\mathbf{c}_I$ (moles/ litre)	$\mathbf{c}_J$ (moles/ litre)	$\mathbf{c}_{M_1}$ (moles/ litre)	$\mathbf{c}_{M_2}$ (moles/ litre)	$\mathcal{W}_1$- $\mathcal{W}_2$- $\mathcal{W}_3$
1	Na, c_1	0.47	0.0017	0.0091	0.0017	$\mathcal{D}_1 - \mathcal{S}_2 - \mathcal{S}_3$
	Mg, c_2	0.098	0.00124	3.67E-005	0.0062	
	Ca, c_3	0.023	0.0062	8.61E-006	0.0012	
	Cl, c_a	0.591	0.0091	0.0091	0.0091	
2	Na, c_1	0.0017	0.47	0.015	0.457	$\mathcal{D}_1 - \mathcal{R}_2 - \mathcal{R}_3$
	Mg, c_2	0.00124	0.098	0.096	0.0171	
	Ca, c_3	0.0062	0.023	0.48	0.117	
	Cl, c_a	0.0091	0.591	0.591	0.591	

from points $\mathbf{c}_J$ and $\mathbf{c}_{M_1}$ ($\mathcal{S}_2$ and $\mathcal{S}_3$). The intermediate point $\mathbf{c}_{M_1}$ in Experiment 3.2 lies in the two rarefaction region (region 3 in Figure 8.5) so that $\mathbf{c}_{M_2}$ lies at the intersection of integral curves from points $\mathbf{c}_J$ and $\mathbf{c}_{M_1}$ ($\mathcal{R}_2$ and $\mathcal{R}_3$). The effluent profile is captured well by the analytical solution (Figures 8.4 and 8.6).

The analytical solution predicts the intermediate constant states $\mathbf{c}_{M_1}$ and $\mathbf{c}_{M_2}$ to a reasonable accuracy. The analytical solution is also able to predict the trend of concentration changes and compares well with laboratory experiments. The sharp Ca concentration peak in Figure 8.6, not easily identifiable during experiments, is also captured well by the analytical solution.

Predictions from the numerical model using finite differences, presented in chapter 7, is used to verify the analytical solution predictions. The numerical model using the Gibbs free energy minimization approach was used to make predictions for this case of three cations. The values of the variables used in the numerical model are $Pe = 10^9$, $\Delta\tau = 0.004$ and $\Delta\xi = 0.005$ for laboratory experiments and $\Delta\xi = 0.004$ for the field case. A large value of Pe has been chosen to represent the hyperbolic equation. Also, a smaller value of $\Delta\xi$ was chosen to minimize numerical dispersion. The predictions from the numerical model are compared with the analytical solutions and the measured effluent concentrations in Figures 8.4 and 8.6. The numerical solution matches well with analytical solutions, further increasing our confidence in analytical solutions.

For the laboratory case, the prediction of wave $\mathcal{W}_2$ as a shock is earlier

than that observed in the experiments (Figures 8.4 and 8.6). One likely explanation is the binary interaction coefficients, estimated using experiments, have been observed to be a function of concentration (Voegelin et al., 2000). However, these coefficients are assumed to be constants over the entire range of concentrations. The analytical solution predicts a shock (sharp discontinuity) for both waves $\mathcal{W}_2$ and $\mathcal{W}_3$ while a smooth concentration profile was observed in experiments. Hydrodynamic dispersion and slow reaction kinetics could lead to a broadening of the shock fronts to a finite width (Rhee et al., 1971).

8.4.2 Field Scale

The field case study described in chapter 7 fits the description of a Riemann problem with a constant initial and a constant injected concentration. The native groundwater composition at the monitoring well and the injected water composition are listed in Table 8.9.

However, the initial and the injected equivalent concentrations of the cations do not add up to the anion concentration in Table 8.9. In addition to K^+, that constitutes a minor portion of the initial concentration observed in the field Valocchi et al. (1981a), there could also be other cations and anions. The analytical solutions have been constructed by neglecting the presence of these other cations and an equivalent anion concentration, obtained from charge balance (Table 8.9), has been used. The binary interaction coefficients, determined in the laboratory, and reported in the original paper (Valocchi

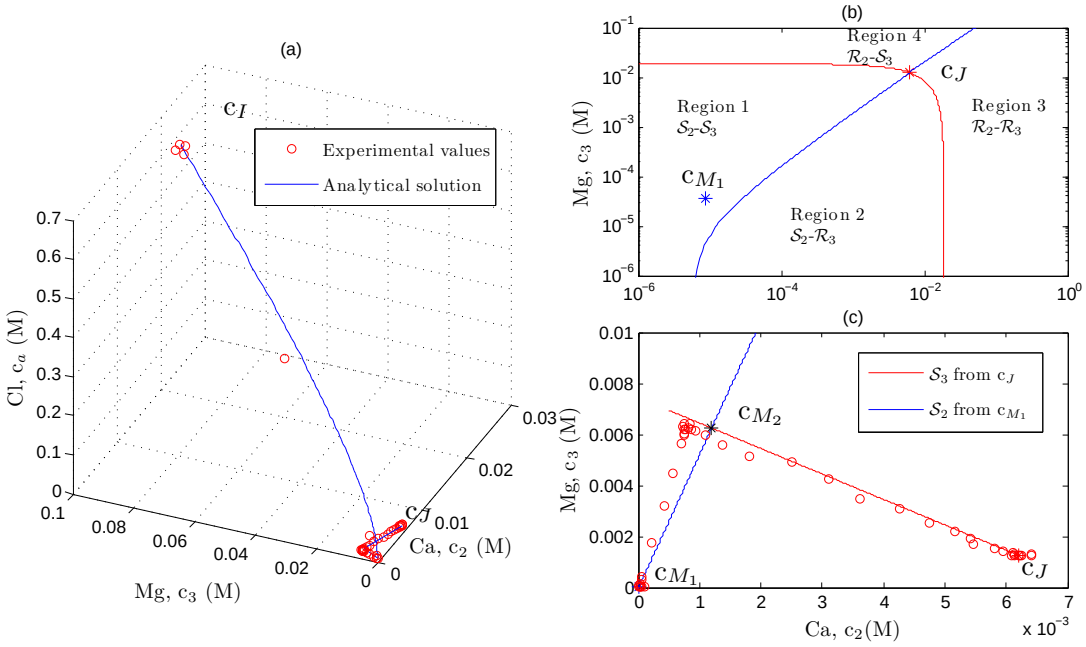

Figure 8.3: Clockwise (a) Comparison of analytical solution and experimental data in the composition space for Experiment 6.1 in Voegelin et al. (2000) (b) Wave classification based on relative positions of injection point c_J and first intermediate point c_{M1} (c) Intersection of Hugoniot curves to find second intermediate point c_{M2} and comparison with experimental data at the constant anion plane c_{3J}.

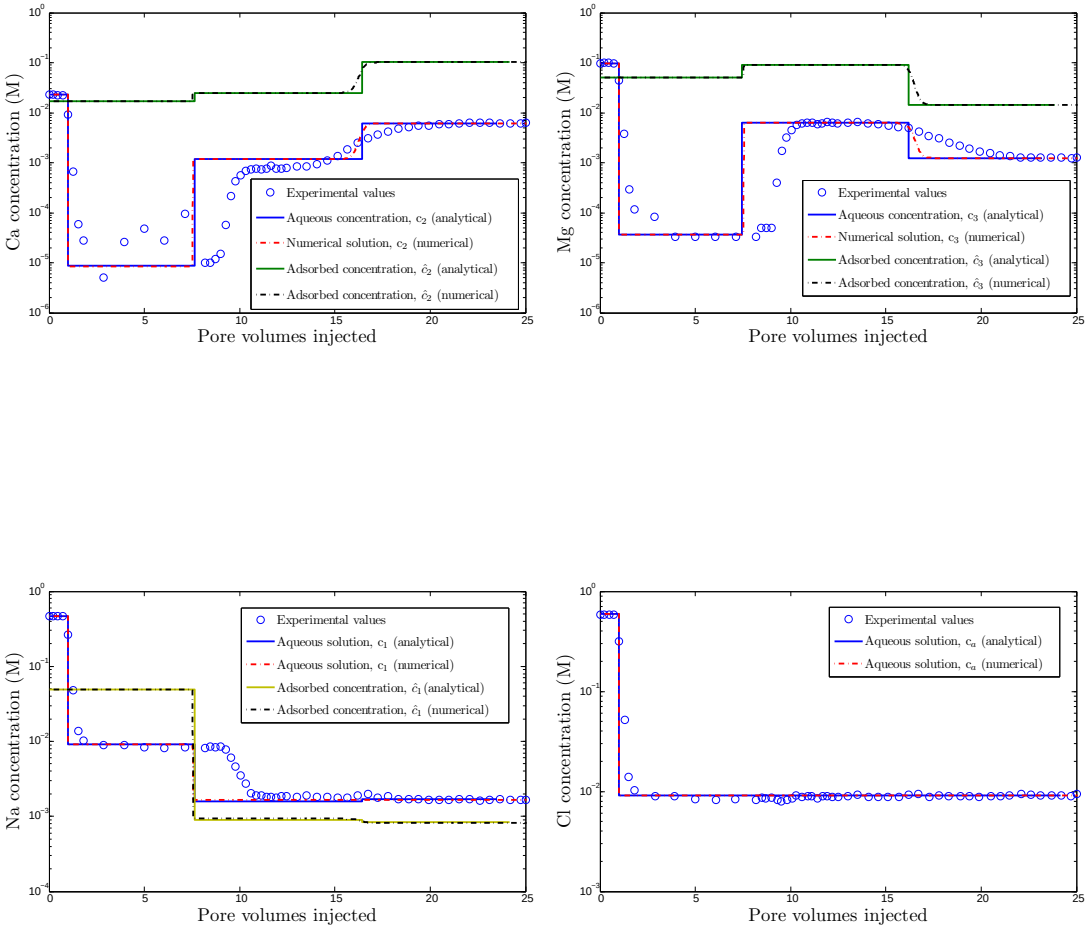

Figure 8.4: Concentration comparison for Experiment 6.1 in Voegelin et al. (2000)

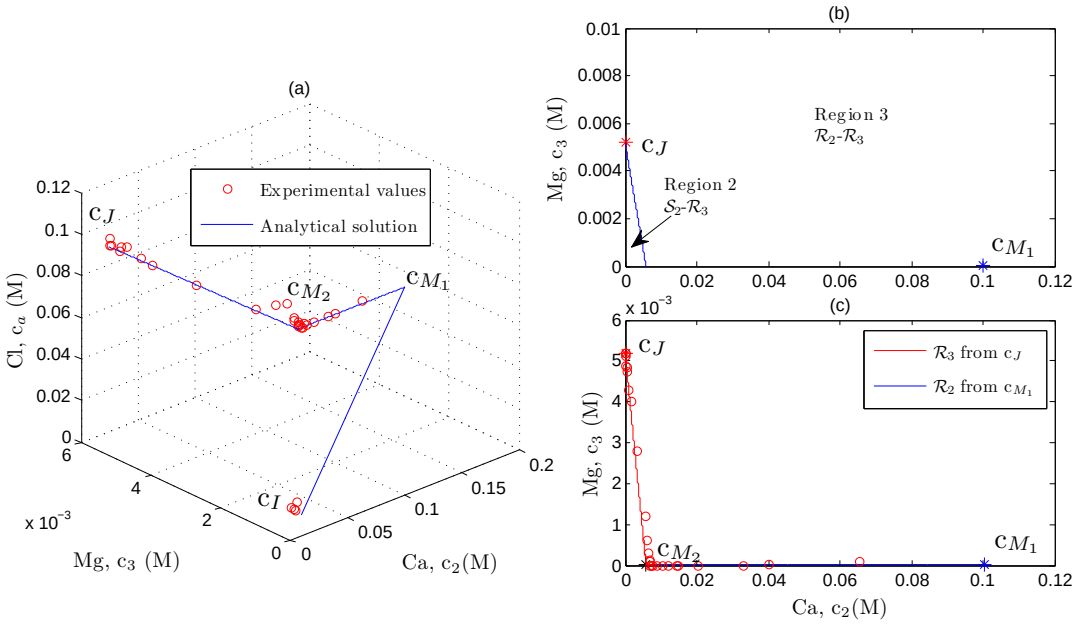

Figure 8.5: Clockwise (a)Comparison of analytical solution and experimental data in the composition space for Experiment 3.2 in Voegelin et al. (2000). (b) Wave classification based on relative positions of injection point c_J and first intermediate point c_{M1} (c) Intersection of integral curves to find second intermediate point c_{M2} and comparison with experimental data at the constant anion plane c_{3J}.

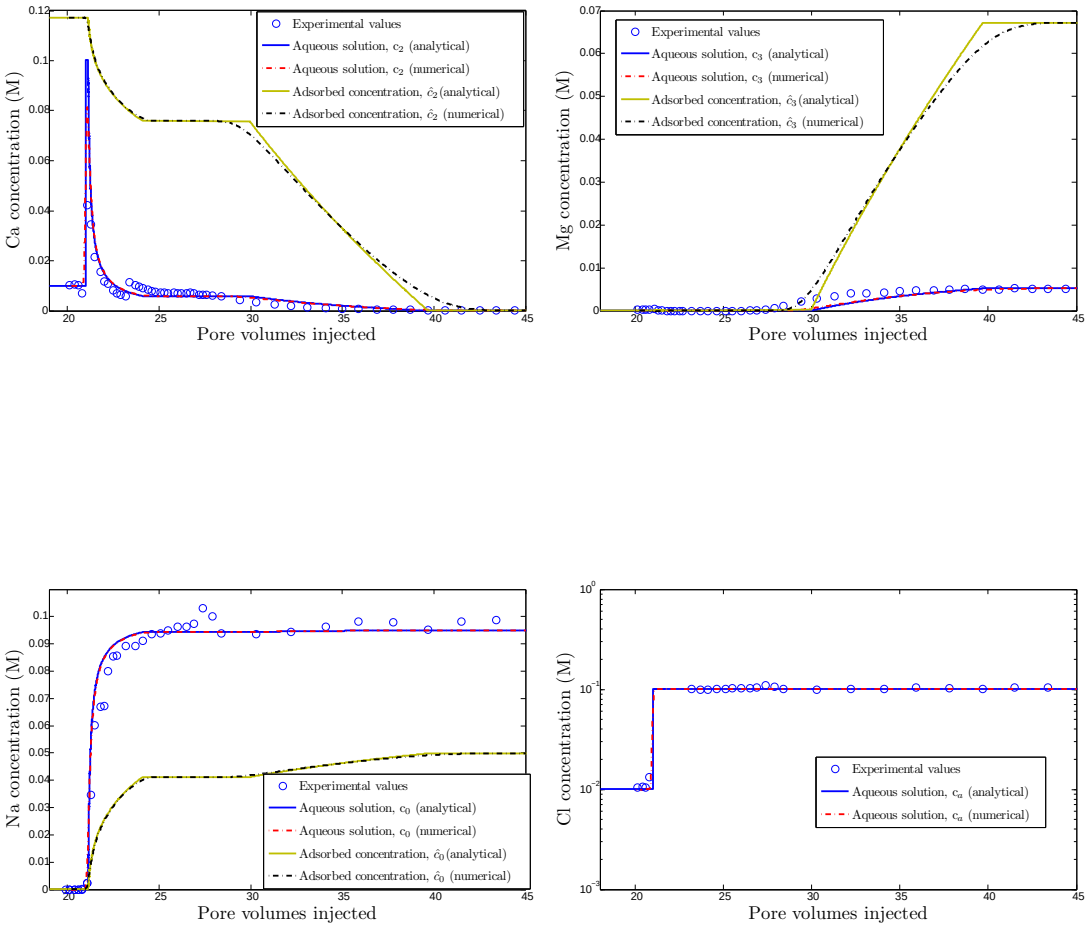

Figure 8.6: Concentration comparison for Experiment 3.2 in Voegelin et al. (2000)

Table 8.9: Field Scale Effluent Concentration Measurements at Producing Well S23 Described in (Valocchi et al., 1981b).* is the equivalent concentration (Eq) calculated using charge balance and used to construct the analytical solution.

Component	Well initial composition (mg/l)	Standard deviation (mg/l)	Injection composition (mg/l)	Eq initial (mM)	Eq injected (mM)
Cl^-	5700	54	320	160.6 (144.62*)	9 (14.7*)
Na^+	1990	30	216	86.52	9.4
Mg^{2+}	436	5.6	12	35.9	1
Ca^{2+}	444	12	85	22.2	4.3

Table 8.10: Analytical Solution for Ternary Transport Data in Producing Well S23 in Valocchi et al. (1981b)

Equivalent concentration ($\mathbf{c}$)	$\mathbf{c}_I$ (moles/ litre)	$\mathbf{c}_J$ (moles/ litre)	$\mathbf{c}_{M_1}$ (moles/ litre)	$\mathbf{c}_{M_2}$ (moles/ litre)	$\mathcal{W}_1$- $\mathcal{W}_2$- $\mathcal{W}_3$
Na^+, c_1	0.08652	0.0094	0.0133	0.0095	$\mathcal{D}_1 - \mathcal{S}_2 - \mathcal{S}_3$
Mg^{2+}, c_2	0.0359	0.001	0.0009	0.0033	
Ca^{2+}, c_3	0.0222	0.0043	0.0005	0.0019	
Cl^-, c_a	0.14462	0.0147	0.0147	0.0147	

et al., 1981b) are used for the development of this analytical solution (Table 8.4).

The eigenvalues for the field case were also observed to be real, distinct and positive along with monotonic σ_2 and σ_3. The analytical solution to get the intermediate compositions and the nature of the waves is similar to the laboratory case in Experient 6.1. Figure 8.7 shows the comparison in the composition space. The intermediate point $\mathbf{c}_{M_2}$ is obtained by the intersection of the Hugoniot curves ($\mathcal{S}_2$ and $\mathcal{S}_3$) from points $\mathbf{c}_{M_1}$ and $\mathbf{c}_J$ (Table 8.10). The analytical predictions, along with the numerical solution compare well with

the effluent cation measured at the observation well S23 (Figure 8.8).

As in the laboratory case, the analytical solution predicts the trend of concentration changes at the field scale. Dispersion increases at the field scale and hence both the waves $\mathcal{W}_2$ and $\mathcal{W}_3$ are more disperse at the field scale (Figure 8.8). Ca^{2+}, Mg^{2+}, Na^{+} and Cl^{-} are only the major ions present in groundwater Valocchi et al. (1981a). The other ions, also present in the native ground water, may form complexes. This could account for the deviation between experimental and analytical results, especially for the anion concentration. Though radial flow occurs in the field, linear flow has been assumed for the development of analytical solutions. The heterogeneities at the field scale and our assumption of constant porosity and constant exchange capacity could also contribute to the deviation.

8.5 Conclusions

Analytical solutions for 1D heterovalent cation exchange for a ternary system in a uniformly porous medium have been developed in the limit of local equilibrium and no dispersion. The predictions from the analytical solution for Riemann problems with constant initial and injection composition compare well with experimental data obtained at two different scales - laboratory scale and field scale. A numerical solution has also been developed that shows good agreement with the analytical solution.

The theory developed here allows the inspection of all possible solutions as a set of admissible paths in composition space for any set of initial and in-

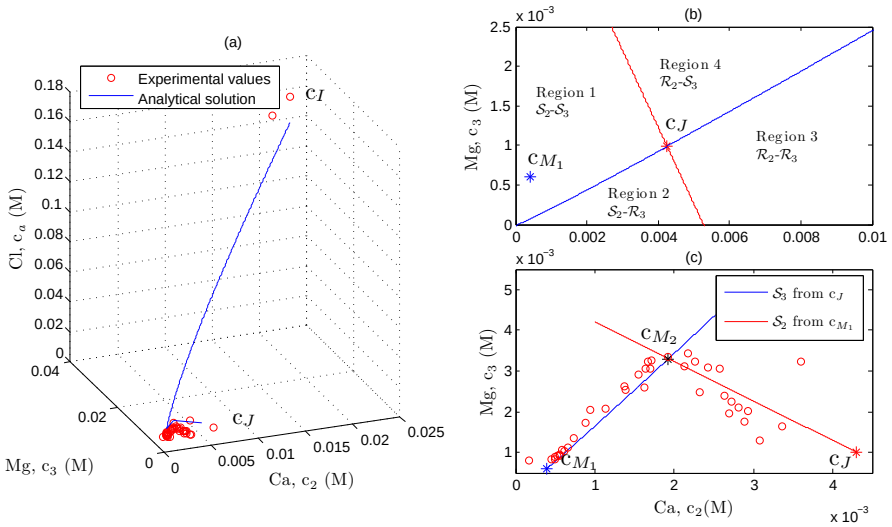

Figure 8.7: Clockwise (a)Comparison of analytical solution and experimental data in the composition space for field measurements in Valocchi et al. (1981b). (b) Wave classification based on relative positions of injection point c_J and first intermediate point c_{M1} (c) Intersection of integral curves to find second intermediate point c_{M2} and comparison with experimental data at the constant anion plane c_{3J}.

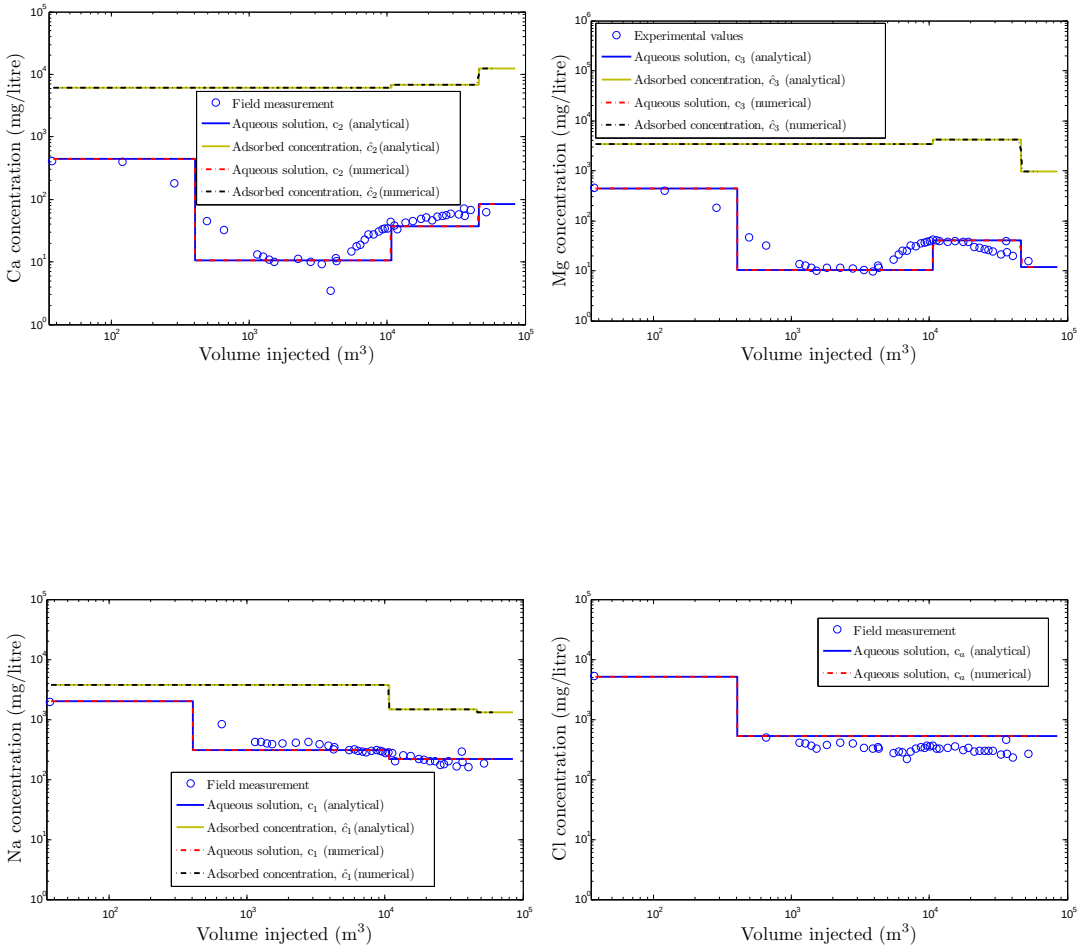

Figure 8.8: Concentration comparison for field measurements in Valocchi et al. (1981b)

jected concentrations. The theory clearly delineates regions in the composition space that realize four types of displacements in ternary cation exchange systems.

The theory predicts the first order structure of the reaction fronts at both field and laboratory scales and hence provides a good estimate at either scales. This can further help in designing experiments as well as validate field remediation processes in a laboratory.

Chapter 9

Conclusions and Recommendations

In this chapter, a summary of conclusions is presented along with recommendations for future research.

9.1 Conclusions

A framework for integrating phase behavior and geochemical reactions was developed using the Gibbs free energy function in this research. The presented Gibbs free energy model is capable of combining different phase descriptions (EOS and activity coefficient models) to estimate equilibrium compositions at different temperatures and pressures. The Gibbs free energy model can be used to predict equilibrium concentrations for not just phase equilibrium (no reactions) but also phase and chemical reactions (with geochemical reactions) using the standard state of all components.

The use of Gibbs free energy model in batch calculations were demonstrated for two applications. In the first application, acid gas solubility models in pure water as well as brine with ions were developed that give better predictions at high pressures than the Henry's law model with fugacity correactions. The solubility models have applications in CO_2 sequestration as well as for de-

signing acid gas reinjection schemes to produce from contaminated gas fields.

In the second application, the Gibbs free energy model was used for predicting phase equilibrium of hydrocarbon mixtures- CO_2-$nC_{14}H_{30}$ and CH_4-CO_2. The model was also used to predict the impact of geochemical reactions, occuring because of ions in the brine as well as solid $CaCO_3$, on the hydrocarbon phase behavior during CO_2 injection for enhancing oil recovery.

The Gibbs free energy model was integrated with 1D flow using the operator splitting approach for a case of cation exchange reactions with three cations. A similar integration with the stochiometric approach was also presented. The Gibbs free energy approach was observed to be faster than the stochiometric approach and hence, preferable for integration in compositional simulators.

The Gibbs free energy model can be adapted for different reservoir brines. The major components present in the brine can be identified and the Gibbs free energy model can be used to predict the change in phase behavior of hydrocarbons, and hence oil recovery, if CO_2 is injected especially in a carbonate reservoir.

Analytical solutions were developed for this case of three cation exchange reactions with 1D flow. The analytical solutions were compared with a numerical model developed using the Gibbs free energy model as well as with experimental data that was available at both laboratory and field scales.

9.2 Recommendations

The recommendations for improving the Gibbs free energy model and using the Gibbs free energy function as a unifying function for different applications as listed below -

1. One of the limitations of the model is the need to define all components present in the system. The field brine composition along with the hydrocarbon composition can help define all the components in the system. If some components that are present in the system are not included in the computations, the equilibrium compositions can be different. A future research project can investigate which components (from those typically present in a carbonate system), when included or excluded in computations, impact the equilibrium compositions drastically.

2. The tangent plane criteria for a system where all components are not present in all phases, derived in section 4.4, can be validated for cases of hydrocarbons with brine where there are no reactions. The tangent plane criteria can be extended to cases with reactions and hence identify the global from the local minimia for use in compositional simulations.

3. The current method of finding equilibrium compositions presented in this research involves finding the Gibbs free energy value of the system at different local minima to identify the global minima. While a simple Newton algorithm is used to find a minimum in the Gibbs free energy function of the system, more sophisticated algorithms for minimization

can be used to identify global minimia from the local minima. This is especially pertinent for cases when the number of hydrocarbon phases and the components increase. These algorithms can help reduce the time required to estimate equilibrium composition and help integration of the Gibbs free energy model in numerical simulators.

4. One of the challenges associated with current approach of integrating the geochemical package *PHREEQC* with *UTCOMP* (Kazemi Nia Korrani et al., 2014, 2013) is the time taken for simulations. The Gibbs free energy model, presented in this research, provides a potential way to integrate the extensive set of reactions, included in the *PHREEQC* package, in compositional simulators and reduce computational times. This integration can help quantify the impact of reactions on oil recovery predictions.

5. Experimental results are not available for the entire system consisting of CO_2, hydrocarbons, solid phase and the aqueous phase with ions. These results can help validate the model predictions.

6. Researchers have proposed that geochemical reactions are responsible for the increase in oil recovery observed during the low salinity waterflood process in laboratory as well as field scales. The ability of the Gibbs free energy model to include geochemical reactions can help model and explain these observations and make predictions.

7. The Gibbs free energy model can be used to develop macroscopic thermodynamic models for methane hydrates. One proposed recovery scheme involves injecting CO_2 and recovering CH_4 while sequestering CO_2. Thermodynamic models can be developed by modeling the hydrate formation and dissociation as a precipitation/dissolution reaction and find optimum pressure and temperature conditions for recovery.

8. The Gibbs free energy model can be also used to find equilibrium compositions at different scales by adding the appropriate energy function relevant at that scale. As an example, energy because of capillarity can be appropriately added for finding the equilibrium composition at the microscopic scale of shale rocks. This can be used for developing phase behavior models of hydrocarbons trapped in narrow pores of shale gas.

9. In addition to chemical compositions, the Gibbs free energy function can also be used to compute the equilibrium state of a system under deformation by addition of strain energy to the Gibbs free energy function. The Gibbs free energy function along with the strain energy can be further used to predict fracture propogation in reservoirs.

Appendices

Appendix A

Gibbs Free Energy Expressions

In this appendix, the Gibbs free energy expressions for components in different phases are presented.

A.1 Gas Phase Components

The expression for Gibbs free energy for a component present as a pure component is different than if the component were present in a mixture.

A.1.0.1 Pure component

The reference state for Gibbs free energy for an ideal gas single component system is the value of the molar Gibbs free energy at standard conditions of unit atmosphere pressure ($P^r = P_0 = 1$ atm) and temperature, $T^r = T_0 = 25°C$. Thus, eq 4.9 for an ideal gas can be written as,

$$\underline{G}^{IG}(T_0, P) = \underline{G}^{IG}(T_0, P_0) + RTln\frac{P}{P_0} \tag{A.1}$$

For a real gas (non-ideal gas), the corresponding equation for the molar Gibbs free energy, $\underline{G}$, is written in terms of the fugacity f,

$$\underline{G}(T_0, P) = \underline{G}^{IG}(T_0, P_0) + RTln\frac{f}{P_0} \tag{A.2}$$

The fugacity of any real fluid is also a measure of the deviation of the Gibbs free energy of that fluid from the ideal gas state. This is explained by considering the Gibbs free energy of an ideal gas at temperature (T) and pressure (P) as the reference state instead of standard conditions (T_0 and P_0). This results in,

$$\begin{aligned} \underline{G}(T_0, P) &= \underline{G}^{IG}(T_0, P) + RTln\frac{f}{P} \\ \implies f &= Pexp\left[\frac{\underline{G}(T_0, P) - \underline{G}^{IG}(T_0, P)}{RT}\right] \end{aligned} \tag{A.3}$$

Eqn A.3 is also used to define fugacity (Sandler, 2006) as a psuedo measure of pressure for a real fluid. Also, fugacity coefficient is defined as $\phi = f/P$. Further, it is possible to evaluate this deviation by integrating eq 4.2 for ideal and real gas between any two pressures,

$$\underline{G}^{IG}(T_0, P_2) - \underline{G}^{IG}(T_0, P_1) = \int_{P_1}^{P_2} \underline{V}^{IG} dP = \int_{P_1}^{P_2} \frac{RT}{P} dP \tag{A.4}$$

$$\underline{G}(T_0, P_2) - \underline{G}(T_0, P_1) = \int_{P_1}^{P_2} \underline{V} dP \tag{A.5}$$

Subtracting eqns A.4 from A.5, setting $P_1 = 0$ along with recognition that all fluids are ideal at $P = 0$ (Sandler, 2006) results in,

$$\underline{G}(T_0, P) - \underline{G}^{IG}(T_0, P) = \int_0^P \left(\underline{V} - \frac{RT}{P}\right) dP \tag{A.6}$$

Eqn A.6 is a general expression of the deviation in the Gibbs free energy from ideal gas state for any fluid. The fugacity as well as fugacity coefficient at different pressures can be estimated using this expression if experimental measurements of molar volume are available. These values of fugacities are

subsequently used in the Gibbs free energy expressions in eq A.2. Also, the expressions of molar volume available for fluids described using different Equation of State (EOS) (Sandler, 2006) like Peng Robinson, Virial, SRK etc. can be used to evaluate the integral in eq A.6.

A.1.0.2 Component in a mixture

The corresponding equation for the partial molar Gibbs free energy of component i in an ideal gas mixture ($\bar{G}_{ig}^{IGM}$) using eq 4.6 is,

$$\bar{G}_{ig}^{IGM}(T_0, P) = \underline{G}_i^{IG}(T_0, P_0) + RTln\frac{P_i}{P_0} = \underline{G}_i^{IG}(T_0, P_0) + RTln\frac{y_i P}{P_0} \quad \text{(A.7)}$$

For real gas mixtures, the partial molar Gibbs free energy of component i having mole fraction y_i in the mixture, can be given in terms of fugacity of component, $\bar{f}_i$, or fugacity coefficient, $\hat{\phi}_i$, as,

$$\bar{G}_{ig}(T_0, P) = \underline{G}_i^{IG}(T_0, P_0) + RTln\frac{\bar{f}_i}{P_0} = \underline{G}_i^{IG}(T_0, P_0) + RTln\frac{y_i\hat{\phi}_i P}{P_0} \quad \text{(A.8)}$$

Eqns A.7 and A.8 relate the partial molar Gibbs free energy of a component in a gas mixture ($\bar{G}_{ig}$) with the Gibbs free energy of the pure component as an ideal gas ($\underline{G}_i^{IG}$). The expressions for fugacity coefficient of a component in a mixture, described using different Equation of States (EOS), is also available (Sandler, 2006) for use in eq A.8 directly.

A.2 Hydrocarbon Phase Components

An equation of state description, especially PR EOS, is commonly used for hydrocarbon phase components. The reference state for components in the

hydrocarbon phase is the hypothetical pure component ideal gas property at standard conditions. All the equations developed for real gas phase components (pure fluids in eq A.2 and mixtures in eq A.8) in the previous section hold good for components in the hydrocarbon phase.

A.3 Aqueous Phase Components

An activity coefficient model is generally used to describe components present as solutes in the aqueous phase. In the Lewis-Randall convention (Table 4.1), the reference state for solute is different than that for the solvent H_2O. The reference state for solutes is the Gibbs free energy value, $\bar{G}_i^*$, at unit molality at standard conditions (T_0 and P_0). For consistency, we convert this reference state value of Gibbs free energy from unit molality of solute in the Lewis-Randall convention ($\bar{G}_i^*$) to unit molarity of the solute ($\bar{G}_s^0$) using the molecular weight M_0 of water to obtain,

$$\bar{G}_i^0 = \bar{G}_i^* + RTln\left(\frac{1000}{M_0}\right). \tag{A.9}$$

The expression for partial molar Gibbs free energy of a solute component i in water ($\bar{G}_{iw}$) at any pressure (P) having molality m_i (or molarity x_i) and described using an activity coefficient γ_i is given as,

$$\bar{G}_{iw}(T_o, P) = \bar{G}_i^*(T_o, P_o) + RTln\frac{m_i\gamma_i f_i}{f_i^0} = \bar{G}_i^0(T_o, P_o) + RTln\frac{x_i\gamma_i f_i}{f_i^0}. \tag{A.10}$$

Here, f_i is the pure component fugacity at the desired pressure P while f_i^0 is the fugacity of the pure component at standard pressure, P_0. Both these fugacities are at the same temperature T_0.

However, the Gibbs free energy of pure water at standard conditions ($\underset{\_}{G}^0_w$) is the reference state for the solvent, H_2O, in the Lewis-Randall convention. Using this reference state, the Gibbs free energy expression for the solvent at any pressure P is,

$$\bar{G}_w(T_o, P) = \underset{\_}{G}^0_w(T_o, P_o) + RTln\left(\frac{x_w \gamma_w f_w}{f^0_w}\right). \tag{A.11}$$

In this equation, x_w is the mole fraction of water in the solution, γ_w is the activity coefficient for water, f_w is the fugacity of pure component water at mixture pressure P while f^0_w is the fugacity of pure water at standard conditions (P_0 and T_0).

A.4 Solid Phase Components

The reference state used for components in a solid phase is the pure component property at standard conditions. This is the same as the reference state for pure water. The partial molar Gibbs free energy for component i in the solid phase ($\bar{G}_{is}$) is,

$$\bar{G}_{is}(T_o, P) = \underset{\_}{G}_i^{\,0}(T_o, P_o) + RTln\left(\frac{z_i \delta_i f_s}{f^0_s}\right) \tag{A.12}$$

Here, $\underset{\_}{G}_i^{\,0}$ is the Gibbs free energy of the pure component at standard pressure P_0, f_s is the fugacity of pure solid component at pressure P, f^0_s is fugacity of pure component at standard pressure P_0, z_i is the mole fraction of the solid component in the solid phase and δ_i is the activity coefficient in the solid phase.

In this dissertation, for all applications involving solid components, each component is taken as a separate phase. The Gibbs free energy expression for any solid component with this assumption is,

$$\underset{\_}{G}_i^0(T_o, P) = \underset{\_}{G}_i^0(T_o, P_o) + RTln\left(\frac{f_s}{f_s^0}\right) \tag{A.13}$$

The Gibbs free energy expressions presented in this appendix are used in the Gibbs free energy function for the entire system.

Appendix B

Pitzer Activity Coefficient Model

The Pitzers activity coefficient is extensively used to model the impact of ions in geochemistry in high salinity brines. It is used for solutions when the ionic strength I is greater than 0.02. The ionic strength measures ionic activity where m_i and z_i as molality and charge of component i, respectively and given as $I = 0.5 \sum_i z_i m_i^2$. The more popular Debye-Huckel activity coefficients and their extensions, are only used for solutions with ionic strengths less than 1.

For solutions with even higher ionic strengths, Mayer (1950) proposed a theoritically consistent virial expansion of the activity coefficient for high ionic concentrations that also accurately represents the experimental data. The expansion can be given as,

$$ln\gamma_i = ln\gamma_{DH} + \sum_j B_{ij}(I)m_j + \sum_{jk} C_{ijk}(I)m_j m_k + \ldots \tag{B.1}$$

Here, γ_{DH} is the Dubye-Huckel activity coefficient, m_i is the molality of species i while B_{ij} and C_{ijk} are the second and third virial activity coefficients respectively.

Harvie and Weare (1980) have adapted the Pitzer activity coefficient model for geochemical reactions. They have shown that it is sufficient to use

Table B.1: Interaction parameter data range and reference

Temperature Range	System	Reference
-60°C - 25°C	Na-K-Ca-Mg-Cl-SO_4-H_2O	Spencer et al. (1990)
25°C	Na-K-Mg-Ca-Cl-SO_4-H_2O	Harvie and Weare (1980)
25°C - 250°C	Na-Ca-Cl-SO_4-H_2O	Møller (1988)

the second (B_{ij}) and the third (C_{ijk}) virial coefficients to accurately describe mineral solubility data. These coefficients account for effects between like-charged ions at high ionic activity as well as the solvent structure and use the same parametrization as interaction coefficients used by Pitzer (Pitzer and Kim, 1974; Pitzer and Mayorga, 1974, 1973). The mineral solubility data at different temperatures were used to find temperature dependent expressions for the interaction parameters (See Table B.1).

In this appendix, the equations as well as the interaction coefficients for the Pitzer activity coefficient model are presented. The interaction coefficients, originally defined for a system of aqueous ions and minerals (listed in Harvie and Weare (1980)) are assumed to hold for a system that includes hydrocarbons in addition to aqueous ions and rock (for cases discussed in chapter 6 this dissertation). Although the interaction parameters are functions of temperature and pressure, the values at 25°C are used in all models developed at other temperatures and pressures.

In the Pitzer activity coefficient model, m_i is the molality of species i (m_c for cation with charge z_c and m_a for anion with charge z_a). Also, M, c and c' represent cations while X, a and a' represent anions. The underlying

equation for excess Gibbs free energy (G^E in the Pitzer activity coefficient model is,

$$\begin{aligned} G^E/RT &= n_w \left[f(I) + \sum_i \sum_j \lambda_{ij}(I) m_i m_j \right. \\ &\quad \left. + \sum_i \sum_j \sum_k \mu_{ijk} m_i m_j m_k \right] \end{aligned} \tag{B.2}$$

Here, both the first term $f(I)$ is the Debye-Huckel coefficient and the second coefficient in the virial expansion $\lambda_{ij}(I)$ are functions of the ionic strength, I, while the third coefficient μ_{ijk} is independent of I.

B.1 Solvent

The expression for G^E is used to derive expressions for osmotic coefficient and the activity coefficients of components. The osmotic coefficient measures the deviation of the solvent (water) from ideal behavior. The expression for osmotic coefficient (ϕ) for the Pitzer activity coefficient model is,

$$\begin{aligned} \phi - 1 &= \frac{2}{\sum_i m_i} \left[-\frac{A^\phi I^{3/2}}{1 + bI^{1/2}} + \sum_c \sum_a m_c m_a (B^\phi_{ca} + Z C_{ca}) \right. \\ &\quad + \sum_c \sum_{c'} m_c m_{c'} (\phi^\phi_{cc'} + \sum_a m_a \psi_{cc'a}) \\ &\quad \left. + \sum_a \sum_{a'} m_a m_{a'} (\phi^\phi_{aa'} + \sum_c m_c \psi_{aa'c}) \right]. \end{aligned} \tag{B.3}$$

At 25°C, $A^\phi = 0.392$ and $b = 1.2$. In the above equation, $Z = \sum_i m_i z_i$. The activity of water (a_{H_2O}) is obtained from the osmotic coefficient (ϕ) and given

as (Møller et al., 1998),

$$lna_{H_2O} = -0.0018(\sum_i m_i)\phi. \tag{B.4}$$

The other elements in eq B.3 are defined below.

B.2 Ionic Species

The activity coefficient expressions for cations (γ_M)and anions (γ_X) in the aqueous phase are,

$$\begin{aligned} ln\gamma_M &= z_M^2 F + \sum_a m_a(2B_{Ma} + ZC_{Ma}) + \sum_c m_c(2\phi_{Mc} + \sum_a m_a\psi_{Mca}) \\ &+ \sum_a \sum_{a'} m_c m_{a'} \psi_{aa'M} + z_M \sum_c \sum_a m_c m_a C_{ca} \end{aligned} \tag{B.5}$$

$$\begin{aligned} ln\gamma_X &= z_X^2 F + \sum_c m_c(2B_{cX} + ZC_{cX}) + \sum_a m_a(2\phi_{Xa} + \sum_c m_c\psi_{Xac}) \\ &+ \sum_c \sum_{c'} m_a m_{c'} \psi_{cc'X} + z_X \sum_c \sum_a m_c m_a C_{ca} \end{aligned} \tag{B.6}$$

In eqns B.5 and B.6, F represents the Debye-Huckel term and the derivatives of the second coefficient with respect to ionic strength (I), and is given as,

$$\begin{aligned} F &= -A^\phi \left[\frac{\sqrt{I}}{I + b\sqrt{I}} + \frac{2}{b} ln(1 + b\sqrt{I}) \right] + \sum_c \sum_a m_c m_a B'_{ca} \\ &+ \sum_c \sum_{c'} m_c m_{c'} \phi'_{cc'} + \sum_a \sum_{a'} m_a m_{a'} \phi'_{aa'} \end{aligned} \tag{B.7}$$

As mentioned earlier, A^ϕ and b are considered constants with values 0.392 and 1.2 respectively. Also, B', B, ϕ_{ij}, ϕ'_{ij} are coefficients of the binary interaction parameter and ψ_{ijk} is the coefficient for ternary interaction parameter.

The expressions for coefficients B^{ϕ}_{MX}, B_{MX} and B'_{MX} in eqns B.3-B.7 for 1-1 valence type ions are,

$$B^{\phi}_{MX} = \beta^0_{MX} + \beta^1_{MX} e^{-\alpha\sqrt{I}} \tag{B.8}$$

$$B_{MX} = \beta^0_{MX} + \beta^1_{MX} g(\alpha\sqrt{I}) \tag{B.9}$$

$$B'_{MX} = \beta^1_{MX} g'(\alpha\sqrt{I})/I \tag{B.10}$$

In eqns B.8-B.10, $\alpha = 2$ has been emperically found by Pitzer and $x = \alpha\sqrt{I}$. Besides, $g(x)$ and $g'(x)$ are functions defined as,

$$g(x) = \frac{2[1-(1+x)e^{-x}]}{x^2} \tag{B.11}$$

$$g'(x) = -\frac{[1-(1+x+\frac{1}{2}x^2)e^{-x}]}{x^2} \tag{B.12}$$

The constants B^{ϕ}_{MX}, B_{MX} and B'_{MX} for 2-2 valence type ions ($\alpha_1 = 2$ and $\alpha_2 = 12$) are given by,

$$B^{\phi}_{MX} = \beta^0_{MX} + \beta^1_{MX} e^{-\alpha_1\sqrt{I}} + \beta^2_{MX} e^{-\alpha_2\sqrt{I}} \tag{B.13}$$

$$B_{MX} = \beta^0_{MX} + \beta^1_{MX} g(\alpha_1\sqrt{I}) + \beta^2_{MX} g(\alpha_2\sqrt{I}) \tag{B.14}$$

$$B'_{MX} = \beta^1_{MX} \left(\frac{g'(\alpha_1\sqrt{I})}{I}\right) + \beta^2_{MX} \left(\frac{g'(\alpha_2\sqrt{I})}{I}\right) \tag{B.15}$$

The constants C_{MX}, ϕ^{ϕ}_{ij} and ϕ'_{ij} in eqns B.3-B.7 are,

$$C_{MX} = \frac{C^{\phi}_{MX}}{2\sqrt{z_M z_X}} \tag{B.16}$$

$$\phi^{\phi}_{ij} = \theta_{ij} + {}^{E}\theta_{ij}(I) + I\,{}^{E}\theta'_{ij}(I) \tag{B.17}$$

$$\phi_{ij} = \theta_{ij} + {}^{E}\theta_{ij}(I) \tag{B.18}$$

$$\phi'_{ij} = {}^{E}\theta'_{ij}(I) \tag{B.19}$$

Here, ${}^{E}\theta_{ij}$ and ${}^{E}\theta'_{ij}$ account for electrostatic unsymmetrical mixing effects and depend only on charges of ions i and j and the total ionic strength I. They are both zero if i and j are of the same charge. A complete list of binary interaction parameters for any two paris of cations/anions ($\phi^{\phi}_{cc'}/\phi^{\phi}_{aa'}$) as well as ternary interaction parameters between two cations and one anion ($\psi_{cc'a}$) or two anions and one cation ($\psi_{aa'c}$)are listed in Tables B.2 and B.4.

B.3 Neutral Components

The neutral species considered in our aqueous system for applications discussed in chapter 6 is CO_2 (aq). The Pitzer equations for activity coefficient for CO_2 (γ) to include its interaction with other ions is given as,

$$\log\gamma = \sum_{c} 2m_c\lambda_{CO_2-c} + \sum_{a} 2m_a\lambda_{CO_2-a} + \sum_{c}\sum_{a} m_c m_a \xi_{CO_2-c-a}. \quad \text{(B.20)}$$

The binary interaction parameter (λ) and the ternary interaction parameter (ξ) between CO_2 and different anions and cations at 25°C (He and Morse, 1993) are given in Tables B.3 and B.5 respectively. The interaction coefficients are functions of temperature and pressure. However, for all applications discussed in this dissertation, the values at 25°C are used for models at different temperatures and pressures.

Table B.2: Pitzer binary interaction parameters between different cations and anions (Harvie and Weare, 1980; He and Morse, 1993)

Component (i)	Component (j)	β^0_{MX}	β^1_{MX}	β^2_{MX}	C^ϕ_{MX}
Na^+	Cl^-	0.0765	0.2664	-	0.00127
Na^+	SO_4^{2-}	0.01958	1.113	-	0.00497
Na^+	HCO_3^-	0.028	0.044	-	-
Na^+	CO_3^{2-}	0.036	1.512	-	0.0052
K^+	Cl^-	0.04835	0.2122	-	0.00084
K^+	SO_4^{2-}	0.04995	0.7793	-	-
K^+	HCO_3^-	-0.0107	0.048	-	-
K^+	CO_3^{2-}	0.129	1.433	-	0.0005
Mg^{2+}	Cl^-	0.35235	1.6815	-	0.00519
Mg^{2+}	SO_4^{2-}	0.221	3.343	-37.25	0.025
Mg^{2+}	HCO_3^-	0.03	0.8	-	-
Mg^{2+}	CO_3^{2-}	-	-	-	-
Ca^{2+}	Cl^-	0.3159	1.614	-	-0.00034
Ca^{2+}	SO_4^{2-}	0.2	2.65	-57.7	0
Ca^{2+}	HCO_3^-	0.2	0.3	-	-
Ca^{2+}	CO_3^{2-}	-	-	-	-

Table B.3: Binary interaction coefficient between CO_2 and ionic component (He and Morse, 1993).

Component (j)	$\lambda_{CO_2} - j$
H+	-
Na^+	0.07748
K^+	0.04583
Ca^{2+}	0.19775
Mg^{2+}	0.1946
Cl^-	0.02021
SO_4^{2-}	0.1392

Table B.4: Pitzer binary (θ_{ij}) and ternary (ψ_{ijk}) interaction parameters for dirrerent cations and anions at 25°C (Harvie and Weare, 1980; He and Morse, 1993)

Component (i)	Component (j)	Component (k)	θ_{ij}	ψ_{ijk}
Na^+	K^+	Cl^-	-0.012	-0.0018
Na^+	K^+	SO_4^{2-}	-	-0.01
Na^+	Mg^{2+}	Cl^-	0.07	-0.012
Na^+	Mg^{2+}	SO_4^{2-}	-	-0.015
Na^+	Ca^{2+}	Cl^-	0.07	-0.014
Na^+	Ca^{2+}	SO_4^{2-}	-	-0.023
K^+	Mg^{2+}	Cl^-	-	-0.022
K^+	Mg^{2+}	SO_4^{2-}	-	-0.048
K^+	Ca^{2+}	Cl^-	0.032	-0.025
K^+	Ca^{2+}	SO_4^{2-}	-	-
Mg^{2+}	Ca^{2+}	Cl^-	0.007	-0.012
Mg^{2+}	Ca^{2+}	SO_4^{2-}	-	0.05
Cl^-	SO_4^{2-}	Na^+	0.02	0.0014
Cl^-	SO_4^{2-}	K^+	-	-
Cl^-	SO_4^{2-}	Mg^{2+}	-	-0.004
Cl^-	SO_4^{2-}	Ca^{2+}	-	-

Table B.5: Ternary interaction coefficient between CO_2 and ionic components (He and Morse, 1993)

Component (i)	Component (j)	ξ_{CO_2-ij}
H+	Cl^-	-0.00465
Na^+	Cl^-	-0.00055
K^+	Cl^-	-0.01273
Ca^{2+}	Cl^-	-0.01607
Mg^{2+}	Cl^-	-0.01529
Na^+	SO_4^{2-}	-0.0373
K^+	SO_4^{2-}	-0.00041
Mg^{2+}	SO_4^{2-}	-0.09277

Appendix C

Gibbs Free Energy Values at Reference State from Equilibrium Constants

The standard state values of components are needed for obtaining equilibrium composition using the Gibbs free energy minimization approach. The experimental values of equilibrium reaction constants are, however, more extensively reported especially, for ionic reactions. While equilibrium constant data lends itself naturally to the stochiometric approach, it can also be used to find a set of consistent reference state values of components for use in the Gibbs free energy minimization approach to find equilibrium composition.

Cheluget et al. (1987) have shown the general approach to obtain Gibbs free energy values for a system with reactive components when the equilbrium constant data is available. This approach has been adapted for a system of cations with exchange reactions between the aqueous phase and the solid phase. There are two independent reactions for this system,

$$Mg^{2+} + 2\hat{N}a \rightleftharpoons 2Na^{+} + \hat{M}g. \qquad K_{10} = \frac{\hat{\varsigma}_2 \varsigma_1^2}{\hat{\varsigma}_1^2 \varsigma_2}; \tag{C.1}$$

$$Ca^{2+} + 2\hat{N}a \rightleftharpoons 2Na^{+} + \hat{C}a. \qquad K_{20} = \frac{\hat{\varsigma}_3 \varsigma_1^2}{\hat{\varsigma}_1^2 \varsigma_3}. \tag{C.2}$$

The values of equilibrium constants K_{10} and K_{20} are available as they have been experimentally measured. These values are used to obtain the Gibbs

Free Energy values at reference states ($\bar{G}_i^r$) for all the six components - Na^+, Ca^{2+}, Mg^{2+}, $\hat{N}a$, $\hat{C}a$ and $\hat{M}g$. The aqueous and the solid phase are assumed to be ideal. The partial molar Gibbs free energy ($\bar{G}_{iw}$) of a component i with mole fraction x_i in an ideal aqueous phase ($\gamma_i = 1$ in eq 4.20) is given as,

$$\bar{G}_{iw}(T,P) = \bar{G}_i^r(T,P) + RTlnx_i \qquad \forall\, i = 1,2,3. \tag{C.3}$$

The partial molar Gibbs free energy ($\bar{G}_{ps}$) of a component p with mole fraction z_p in the ideal solid phase ($\delta_i = 1$ in eq 4.21) is given as,

$$\bar{G}_{ps}(T,P) = \bar{G}_p^r(T,P) + RTlnz_p \qquad \forall\, p = 1,2,3. \tag{C.4}$$

The six reference state values ($\bar{G}_j^r$ and $\bar{G}_p^r$) are required values input to the Gibbs free energy minimization approach for obtaining equilibrium compositions using eq 7.16. These can be found from the equilibrium constants K_{10} and K_{20}.

The necessary condition for a minimum in Gibbs free energy at equilibrium for a system with N components and R reactions is,

$$\sum_{i=1}^{N} \nu_{ij}\bar{G}_i = 0 \qquad \forall j = 1\,2,\ldots,R. \tag{C.5}$$

Here, $N = 6$, including cation components in both the aqueous and the solid phase and $R = 2$. Using eqs C.3-C.5,

$$\bar{G}^r_{Ca^{2+}} + 2\bar{G}^r_{\hat{N}a} - \bar{G}^r_{\hat{C}a} - 2\bar{G}^r_{Na^+} = RTln\frac{x^2_{Na^+}z_{\hat{C}a}}{z^2_{\hat{N}a}x_{Ca^{2+}}} \tag{C.6}$$

$$\bar{G}^r_{Mg^{2+}} + 2\bar{G}^r_{\hat{N}a} - \bar{G}^r_{\hat{M}g} - 2\bar{G}^r_{Na^+} = RTln\frac{x^2_{Na^+}z_{\hat{M}g}}{z^2_{\hat{N}a}x_{Mg^{2+}}} \tag{C.7}$$

The charge balance equation holds for aqueous phase components while the cation exchange capacity equation is valid for solid phase components. This results in,

$$x_i = \frac{\varsigma_i}{\sum_i \varsigma_i} = \frac{\varsigma_i}{\varsigma_a}; \qquad z_p = \frac{\hat{\varsigma}_p}{\sum_p \hat{\varsigma}_p} = \frac{\hat{\varsigma}_p}{Z_v} \qquad \forall\, i, p = 1, 2, 3. \tag{C.8}$$

Eqns C.6 and C.7 can be further simplified in terms of known quantities to obtain,

$$\bar{G}^r_{Ca^{2+}} + 2\bar{G}^r_{\hat{Na}} - \bar{G}^r_{\hat{Ca}} - 2\bar{G}^r_{Na^+} = RTlnK_{10} + RTln\frac{Z_v}{\varsigma_a} \tag{C.9}$$

$$\bar{G}^r_{Mg^{2+}} + 2\bar{G}^r_{\hat{Na}} - \bar{G}^r_{\hat{Mg}} - 2\bar{G}^r_{Na^+} = RTlnK_{20} + RTln\frac{Z_v}{\varsigma_a} \tag{C.10}$$

The anion concentrations ς_a are already known, as they are obtained independently (section 7.2.3). The solution set comprising of the Gibbs free energy reference state values for components is not unique as there are six unknowns and two equations. The four independent variables are chosen as zero and a compatible list of reference state values for the Gibbs free energy minimization method is presented in Table C.1. These values are used in the numerical model constructed using the Gibbs free energy minimization approach described in section 7.2.3.

Table C.1: Gibbs free energy reference state values for Gibbs free energy minimization approach

Component	Value
$\bar{G}^r_{Na^+}$	0
$\bar{G}^r_{Ca^{2+}}$	$RTlnK_{10} + RTln\frac{Zv}{\varsigma_a}$
$\bar{G}^r_{Mg^{2+}}$	$RTlnK_{20} + RTln\frac{Zv}{\varsigma_a}$
$\bar{G}^r_{\hat{Na}}$	0
$\bar{G}^r_{\hat{Ca}}$	0
$\bar{G}^r_{\hat{Mg}}$	0

Appendix D

Minimization Algorithm

The minimization algorithm used in the Gibbs free energy minimization approach to find equilibrium compositions is presented in this appendix. The RAND algorithm variation has been used for all the minimization cases discussed in this dissertation. The equations presented and the subsequent simplifications for ideal case are from Smith and Missen (1982b).

The minimization problem can be given as,

$$\begin{aligned} Minimize \quad G^T &= \sum_{i=1}^{N_c}\sum_{j=1}^{N_p} n_{ij}\bar{G}_{ij} \\ Subject \quad to \quad \sum_{i=1}^{N_c}\sum_{j=1}^{N_p} a_{ki}n_{ij} &= b_k \quad \forall\, k = 1, 2 \ldots M \,\text{and}\, n_{ij} \geq 0. \end{aligned} \tag{D.1}$$

Here, G^T is the total Gibbs free energy of the system consisting N_c components in N_p phases, M is the number of elements in the system, a_{ki} is the coefficient of moles of element k in the molecular formula of component i, b_k is the total number of moles of element k that is obtained by summing over all the components present in the system, n_{ij} is the numbers of moles and $\bar{G}_{ij}$ is the partial molar Gibbs free energy of component i in phase j. As described in chapter 4, there are different expressions for $\bar{G}_{ij}$ depending on whether the component is described using the EOS (hydrocarbon phase or gas phase

component) or described using the activity coefficient model (aqueous phase component).

D.1 Nonideal System

A Lagrangian approach is used to convert the constrained minimization problem to an unconstrained minimization problem. The Lagrangian function using Lagrangian parameters, λ_k, that is minimized can be given as,

$$\mathcal{L} = \sum_{i=1}^{N_c}\sum_{j=1}^{N_p} n_{ij}\bar{G}_{ij} + \sum_{k=1}^{M}\lambda_k(b_k - \sum_{i=1}^{N_c}\sum_{j=1}^{N_p} a_{ki}n_{ij}). \tag{D.2}$$

The necessary conditions for minimum of the Lagrangian function $\mathcal{L}$ are,

$$\frac{\partial\mathcal{L}}{\partial n_{ij}} = 0 \quad \Longrightarrow \quad \bar{G}_{ij} - \sum_{k=1}^{M}\lambda_k a_{ki} = 0. \,\forall\, i = 1, 2, \ldots N_c;\, \forall\, j = 1, 2, \ldots N_p. \tag{D.3}$$

$$\frac{\partial\mathcal{L}}{\partial \lambda_k} = 0 \quad \Longrightarrow \quad b_k - \sum_{i=1}^{N_c}\sum_{j=1}^{N_p} a_{ki}n_{ij} = 0. \,\forall k = 1, 2 \ldots M. \tag{D.4}$$

The unknowns are n_{ij} ($\forall\, i = 1, 2 \ldots N_c$ and $\forall\, j = 1, 2 \ldots N_p$) and λ_k ($\forall\, k = 1, 2 \ldots M$). The total number of unknowns are $N_cN_p + M$. Eqs D.3 and D.4, together, give a total of $N_cN_p + M$ equations that are solved to find the unknowns. Linearization about an arbitrary estimate of solution ($\mathbf{n^{(m)}}$, $\lambda^{(\mathbf{m})}$) of eq D.3 gives,

$$-\sum_{i=1}^{N_c}\sum_{j=1}^{N_p}\left(\frac{\partial\bar{G}_{ij}}{\partial n_{ij}}\right)_{\mathbf{n^{(m)}}}\delta n_j^{(m)} + RT\sum_{k=1}^{M} a_{ki}\delta\lambda_k^{(m)} = \bar{G}_{ij}^{(m)} - RT\sum_{k=1}^{M} a_{ki}\lambda_k^{(m)}$$
$$\forall\, i = 1, 2 \ldots N_c \,\text{and}\, \forall\, j = 1, 2 \ldots N_p. \tag{D.5}$$

Also,

$$\delta n_j^{(m)} = n_j - n_j^{(m)}. \tag{D.6}$$

$$\delta \lambda_k^{(m)} = \lambda_k - \lambda_k^{(m)}. \tag{D.7}$$

Eq D.4 is linearized around the solution ($\mathbf{n^{(m)}}$, $\lambda^{(\mathbf{m})}$) to obtain ,

$$\sum_{i=1}^{N_c} \sum_{j=1}^{N_p} a_{ki} \delta n_{ij}^{(m)} = b_k - b_k^{(m)}; \qquad k = 1, 2, \ldots, M. \tag{D.8}$$

where,

$$b_k^{(m)} = \sum_{i=1}^{N_c} \sum_{j=1}^{N_p} a_{ki} n_{ij}^{(m)}; \qquad k = 1, 2, \ldots, M. \tag{D.9}$$

Eqs D.7-D.9 form set of $N_c N_p + M$ nonlinear equations that can be solved to obtain the unknowns. These equations are also simplified by using appropriate expressions for $\bar{G}_{ij}$ presented in Appendix A. The number of equations can be reduced for a ideal system and this is discussed in the next section.

D.2 Ideal System

The number of nonlinear nonlinear equations can be reduced for ideal systems. This is illustrated for a single phase system. As explained in the previous section, for a single phase system, there are $N_c + M$ nonlinear equations.

$$\frac{1}{RT} \left(\frac{\partial \bar{G}_i}{\partial n_i} \right) = \frac{\delta_{ij}}{n_i} - \frac{1}{j_t} \tag{D.10}$$

$$\delta n_i^{(m)} = n_i^{(m)} \left(\sum_{k=1}^{M} \frac{a_{ki}}{RT} \lambda_k + u - \frac{\bar{G}_i^{(m)}}{RT} \right); \quad i = 1, 2, \ldots, N_c. \tag{D.11}$$

$$u = \frac{\sum_{i=1}^{N_c} \delta n_i^{(m)}}{n_t^{(m)}} \tag{D.12}$$

$$\sum_{s=1}^{M} \left(\sum_{k=1}^{N_c} a_{sk} a_{jk} n_k^{(m)} \right) \frac{\lambda_s}{RT} + b_j^{(m)} u = \sum_{k=1}^{N_c} a_{jk} n_k^{(m)} \frac{\bar{G}_k^{(m)}}{RT} + b_j - b_j^{(m)}; \quad \forall\, j = 1, 2, \ldots, M. \tag{D.13}$$

$$\sum_{i=1}^{M} b_i^{(m)} \frac{\lambda_i}{RT} - n_z u = \sum_{k=1}^{N_c} n_k^{(m)} \frac{\bar{G}_k}{RT} \tag{D.14}$$

Eqns D.13-D.14 are the *M+1* equations that are solved for ideal components (Smith and Missen, 1982b). The solution obtained by solving this minimization problem is the equilibrium compositions for all cases discussed in this dissertation.

In summary, only a list of components and their standard state values are required to determine the equilibrium composition for a system with or without reacting components.

Appendix E

Coherence Theory

Helfferich (1981) presented the coherence theory in the context of multicomponent and multiphase flow in porous media. He proposed that the concentration velocities of all components are equal irrespective of the nature of waves - shock or rarefaction waves and called it the coherence condition. We show how this is related to eigenvectors corresponding to the hyperbolic theory developed here. Walsh and Lake (1989) have derived this relationship for the case when the waves are rarefactions. We further extend it for cases where the waves are shocks.

Pope et al. (1978b) used the theory of coherence to derive their analytical solution. The coherence condition for spreading waves occuring in cation exchange (Pope et al., 1978b) can be given as,

$$d\hat{c}_i = \nu dc_i \qquad \forall\ i = 1, 2, \cdots, n. \tag{E.1}$$

Here, ν is the coherence velocity and is a constant for all n cation exchanging components. Using the chain rule, (E.1) can also be written as,

$$\sum_{j=1}^{j=n} \frac{\partial \hat{c}_i}{\partial c_j} dc_j = \nu dc_i \qquad \forall\ i = 1, 2, \cdots, n. \tag{E.2}$$

Using $\hat{c}_{ij} = \partial \hat{c}_i / \partial c_j$, we get,

$$\begin{bmatrix} \hat{c}_{11} & \hat{c}_{12} & \hat{c}_{13} \\ \hat{c}_{21} & \hat{c}_{22} & \hat{c}_{23} \\ \hat{c}_{31} & \hat{c}_{32} & \hat{c}_{33} \end{bmatrix} \begin{bmatrix} dc_1 \\ dc_2 \\ dc_3 \end{bmatrix} = \nu \begin{bmatrix} dc_1 \\ dc_2 \\ dc_3 \end{bmatrix}. \tag{E.3}$$

This eigenvalue-eigenvector equation has eigenvalues ν and can be directly compared with (8.17). The difference is the choice of independent variables - two cations and one anion in (8.17) whereas there are three cation concentrations present in (E.3). The system in (8.17) can also be developed using three cations as the linearly independent variables and one would obtain the same eigenvalues (σ_1, σ_2 and σ_3 in 8.18). We thus have,

$$\sigma = 1 + \nu. \tag{E.4}$$

An identical relationship exists when the wave is a shock. The coherence condition in such a case is called the integral coherence (Helfferich, 1981) and can be written as,

$$\Delta \hat{c}_i = \tilde{\nu} \Delta c_i \qquad \forall\ i = 1, 2, \cdots, n. \tag{E.5}$$

The Rankine-Hugoniot jump condition for a shock is given by (G.4) and can be written in scalar form for all components

$$\tilde{\sigma} = \frac{(\hat{c}_{i,L} + c_{i,L}) - (\hat{c}_{i,R} + c_{i,R})}{c_{i,L} - c_{i,R}} \quad \forall\ i = 1, 2, \cdots, n, \tag{E.6}$$

or equivalently,

$$\tilde{\sigma} = 1 + \frac{\Delta \hat{c}_i}{\Delta c_i} = 1 + \tilde{\nu} \qquad \forall\ i = 1, 2, \cdots, n. \tag{E.7}$$

The coherence condition itself, is a consequence of the hyperbolic theory and the Riemann boundary conditions (a step change at the origin).

Appendix F

Cation Exchange and Adsorption

The difference between modeling of cation exchange and solute adsorption processes is the presence of vacant sites in the latter case. We show equivalence between them and the special case for which they hold.

Glueckauf (1946) has stated the equations for equilibrium chromatography between two interacting solutes. Rhee et al. (2001) have also derived these expressions using kinetics. We use equilibrium arguments to derive the isotherm resulting from adsorption of a solute.

Consider two solutes, A and B, that are capable of adsorbing on surfaces with vacant sites. Let $\hat{c}_1$ and $\hat{c}_2$ be the adsorbed concentrations while c_1 and c_2 be the concentrations of A and B in the flowing phase respectively. Let X represent the free sites. This process depends on the amount of vacant sites available and let c_0 be a measure of concentration for the vacant sites. The adsorption process can be represented as an equilibrium reaction to give the following equations,

$$A + \hat{X} \rightleftharpoons \widehat{AX} \qquad K_1 = \frac{\hat{c}_1}{c_1 \hat{c}_0}; \tag{F.1}$$

$$B + \hat{X} \rightleftharpoons \widehat{BX} \qquad K_2 = \frac{\hat{c}_2}{c_2 \hat{c}_0}. \tag{F.2}$$

The total number of sites on the solid surface is the exchange capacity Z_v and corresponds to the sum of occupied and free sites,

$$c_1 + c_2 + c_0 = Z_v. \tag{F.3}$$

The isotherm expressions obtained using (F.2) and (F.3) are of the Langmuir type and given as,

$$\hat{c}_1 = \frac{K_1 c_1 Z_v}{1 + K_1 c_1 + K_2 c_2} \quad \hat{c}_2 = \frac{K_2 c_2 Z_v}{1 + K_1 c_1 + K_2 c_2}. \tag{F.4}$$

The isotherm expression obtained by using balance equations (charge and exchange capacity) and law of mass action for the case of cation exchange between three monovalent cations (Table B.4) is,

$$\hat{c}_1 = \frac{Z_v c_1 K_{10}}{c_0 + K_{10} c_1 + K_{20} c_2}. \tag{F.5}$$

Here, c_0, c_1 and c_2 are the concentration of the three cations in the flowing phase while $\hat{c}_1$ is the adsorbed concentration of cation *1* in the solid surface. The isotherm expressions (F.4 and F.5) developed for two solute adsorption and monovalent ternary cation exchange are equivalent when the following relationship holds,

$$K_1 = \frac{K_{10}}{c_0} \qquad \text{and} \qquad K_2 = \frac{K_{20}}{c_0}. \tag{F.6}$$

It is easy to extend the above relationship for a general case of adsorption of n solutes and cation exchange between $n+1$ cations. The only condition is that all cations should be monovalent.

Appendix G

Intermediate Points in Analytical Solution

The key to the analytical solution is the recognition that the adsorbed concentrations do not change along the anion wave $\mathcal{W}_1$. In the composition space, the intermediate point $\mathbf{c}_{M_1}$ is connected to the initial concentration (point $\mathbf{c}_I$) by the anion wave $\mathcal{W}_1$ and lies in the plane of injected anion concentration (c_{3M_1} =c_{3J}),

$$\hat{\mathbf{c}}_{M_1} = \hat{\mathbf{c}}_I. \tag{G.1}$$

At point $\mathbf{c}_{M_1}$, all the adsorbed concentrations are known. We use mass action equations and charge conservation at anion plane c_{3J} to obtain a quadratic equation. We choose the positive root to obtain,

$$c_{0M_1} = \frac{-1 + \sqrt{1 + 4c_{3J}\left(\frac{\hat{c}_{1I}}{\hat{c}_{0I}^2 K_{10}} + \frac{\hat{c}_{2I}}{\hat{c}_{0I}^2 K_{20}}\right)}}{2\left(\frac{\hat{c}_{1I}}{\hat{c}_{0I}^2 K_{10}} + \frac{\hat{c}_{2I}}{\hat{c}_{0I}^2 K_{20}}\right)}. \tag{G.2}$$

The other flowing concentrations are calculated using the law of mass action,

$$c_{1M_1} = \frac{\hat{c}_{1M_1} c_{0M_1}^2}{K_{10}\hat{c}_{0M_1}^2} \qquad \text{and} \qquad c_{2M_1} = \frac{\hat{c}_{2M_1} c_{0M_1}^2}{K_{20}\hat{c}_{0M_1}^2}. \tag{G.3}$$

The above equations can also be used to obtain the flowing concentrations at different planes of anion concentrations. This is used to plot the anion wave $\mathcal{W}_1$ in composition plots - Figures 8.3, 8.5 and 8.7. This wave is curved owing

to the heterovalent nature of the cations and the curvature depends on the concentration ranges involved (the curvature is more prominent in Figure 8.3 than Figure 8.5). The anion wave $\mathcal{W}_1$ for monovalent ternary cation system will be a straight line.

The other intermediate point $\mathbf{c}_{M_2}$ lies at the intersection of wave $\mathcal{W}_2$ from $\mathbf{c}_{M_1}$ and $\mathcal{W}_3$ from $\mathbf{c}_J$. These waves can be Hugoniot curves or integral curves. Hugoniot curves are constructed using the Rankine-Hugoniot jump condition. The jump condition connecting any two points, $\mathbf{c}_L$ as the left state and $\mathbf{c}_R$ as the right state can be given as,

$$\tilde{\sigma}_p = \frac{(\hat{\mathbf{c}}_R + \mathbf{c}_R) - (\hat{\mathbf{c}}_L + \mathbf{c}_L)}{\mathbf{c}_R - \mathbf{c}_L}. \tag{G.4}$$

The Hugoniot curve from point $\mathbf{c}_{M_1}$ (left state for wave $\mathcal{W}_2$) is the locus of all points $\mathbf{c}_R$, the right state, that satisfy this jump condition. The vector equation (G.4) results in the following scalar equation,

$$\frac{(\hat{c}_{1R} + c_{1R}) - (\hat{c}_{1M_1} + c_{1M_1})}{c_{1R} - c_{1M_1}} = \frac{(\hat{c}_{2R} + c_{2R}) - (\hat{c}_{2M_1} + c_{2M_1})}{c_{2R} - c_{2M_1}}. \tag{G.5}$$

Here, the adsorbed concentrations can be expressed as a function of aqueous concentrations using isotherm expressions available in Table 8.2. The Hugoniot curves from point $\mathbf{c}_{M_1}$ are obtained by solving for the root of this algebraic equation numerically in the plane of constant anion concentration c_{3J}. A similar algebraic equation for the Hugoniot curve from point $\mathbf{c}_J$, the right state for wave $\mathcal{W}_3$, can be obtained. In this case, we solve for unknown compositions $\mathbf{c}_L$, representing the left state, that satisfy the Rankine-Hugoniot condition.

The integral curves from any point in the composition space is the set of points obtained by integrating along the eigenvectors from that point. The two ODEs resulting from the two eigenvalues in (8.22) are,

$$\left(\frac{dc_1}{dc_2}\right)_{\sigma_2} = \left[\frac{2\hat{c}_{12}}{\hat{c}_{22} - \hat{c}_{11} - \sqrt{(\hat{c}_{11} - \hat{c}_{22})^2 + 4\hat{c}_{12}\hat{c}_{21}}}\right]; \tag{G.6}$$

$$\left(\frac{dc_1}{dc_2}\right)_{\sigma_3} = \left[\frac{2\hat{c}_{12}}{\hat{c}_{22} - \hat{c}_{11} + \sqrt{(\hat{c}_{11} - \hat{c}_{22})^2 + 4\hat{c}_{12}\hat{c}_{21}}}\right]. \tag{G.7}$$

The integral curves from $\mathbf{c}_J$ can be obtained by numerically integrating these ODEs and using the initial condition,

$$c_1(c_{2J}) = c_{1J}. \tag{G.8}$$

A similar set of equations are used to obtain the integral curve from $\mathbf{c}_{M_1}$. The derivatives of the adsorbed concentrations in (G.6) and (G.7) are obtained from the adsorption isotherm expressions in Table 8.2.

Bibliography

CAJ Appelo. Cation and proton exchange, ph variations, and carbonate reactions in a freshening aquifer. *Water Resources Research*, 30(10):2793–2805, 1994.

CAJ Appelo, JA Hendriks, and M Van Veldhuizen. Flushing factors and a sharp front solution for solute transport with multicomponent ion exchange. *Journal of Hydrology*, 146:89–113, 1993.

Todd Arbogast. User's guide to PARSSim1, The Parallel Subsurface Simulator, Single phase. Technical report, TICAM, The University of Texas at Austin, 1998.

David M Austgen, Gary T Rochelle, and Chau Chyun Chen. Model of vapor-liquid equilibria for aqueous acid gas-alkanolamine systems. 2. representation of hydrogen sulfide and carbon dioxide solubility in aqueous mdea and carbon dioxide solubility in aqueous mixtures of mdea with mea or dea. *Industrial & Engineering Chemistry Research*, 30(3):543–555, 1991.

S Bachu and JJ Adams. Sequestration of CO_2 in geological media in response to climate change: capacity of deep saline aquifers to sequester CO_2 in solution. *Energy Conversion and Management*, 44(20):3151–3175, 2003.

Stefan Bachu and William D Gunter. Acid-gas injection in the alberta basin, canada: a co_2-storage experience. *Geological Society, London, Special Publications*, 233(1):225–234, 2004a.

Stefan Bachu and William D Gunter. Overview of acid-gas injection operations in western canada. In *Greenhouse Gas Control Technologies, Proceedings of the 7th International Conference on Greenhouse Gas Control Technologies*, pages 5–9, 2004b.

Lee E Baker, Alan C Pierce, and Kraemer D Luks. Gibbs energy analysis of phase equilibria. *SPE Journal*, 22(5):731–742, 1982.

A Bamberger, G Sieder, and G Maurer. High-pressure (vapor+ liquid) equilibrium in binary mixtures of (carbon dioxide+ water or acetic acid) at temperatures from 313 to 353 k. *The Journal of Supercritical Fluids*, 17(2): 97–110, 2000.

Jacob Bear. *Dynamics of fluids in porous media*. Dover Publications, 2013.

Craig M Bethke and Pathick V Brady. How the kd approach undermines ground water cleanup. *Ground Water*, 38(3):435–443, 2000.

Debojit Bhuyan. *Development of an Alkaline/Surfactant/Polymer Flood Compositional Reservoir Simulator*. PhD thesis, The University of Texas at Austin, 1989.

Debojit Bhuyan, Larry W Lake, and Gary A Pope. Mathematical modeling of high-ph chemical flooding. *SPE reservoir engineering*, 5(2):213–220, 1990.

S.R. Brinkley. Calculation of the equilibrium composition of systems of many components. *J. Chem. Phys*, 15:107–110, 1947.

Christa S Buergisser, Andre M Scheidegger, Michal Borkovec, and Hans Sticher. Chromatographic charge density determination of materials with low surface area. *Langmuir*, 10(3):855–860, 1994.

Mitchell P Burgess and Raymond P Germann. Physical properties of hydrogen sulfide-water mixtures. *AIChE Journal*, 15(2):272–275, 1969.

J Carroll. Phase equilibria relevant to acid gas injection: Part 2-aqueous phase behaviour. *Journal of Canadian Petroleum Technology*, 41(7), 2002.

John J Carroll and Alan E Mather. The solubility of hydrogen sulphide in water from 0 to 90 c and pressures to 1 mpa. *Geochimica et Cosmochimica Acta*, 53(6):1163–1170, 1989.

Center for Subsurface Modeling. *IPARS: Integrated Parallel Reservoir Simulator, CVS distribution of IPARSv2*, 2000.

Yi-bor Chang. *Development and Application of an Equation of State Compositional Simulator*. PhD thesis, The University of Texas at Austin, 1990.

Yih-bor Chang, Gary A Pope, and Kamy Sepehrnoori. A higher-order finite-difference compositional simulator. *Journal of Petroleum Science and Engineering*, 5(1):35–50, 1990.

Randall J Charbeneau. Calculation of pollutant removal during groundwater restoration with adsorption and ion exchange. *Water Resources Research*, 18(4):1117–1125, 1982.

R.J. Charbeneau. Multicomponent exchange and subsurface solute transport: Characteristics, coherence, and the riemann problem. *Water Resources Research*, 24(1):57–64, 1988.

Eric L Cheluget, Ronald W Missen, and William R Smith. Computer calculation of ionic equilibria using species-or reaction-related thermodynamic data. *Journal of Physical Chemistry*, 91(9):2428–2432, 1987.

Rudolf Clausius. *The Mechanical Theory of Heat: with its applications to the steam-engine and to the physical properties of bodies*. J. van Voorst, 1867.

Computer Modeling Group. *STARS User's Guide: Advanced Process and Thermal Reservoir Simulator, Version 2010*, 2010.

Randall T Cygan, Caroline T Stevens, Robert W Puls, Steven B Yabusaki, Robert D Wauchope, Christian J McGrath, Gary P Curtis, Malcolm D Siegel, Linda A Veblen, and David R Turner. Research activities at us government agencies in subsurface reactive transport modeling. *Vadose Zone Journal*, 6(4):805–822, 2007.

Kenneth Denbigh. *The Principles of Chemical Equilibrium*. Cambridge University Press Cambridge, 1966.

WS Dodds, LF Stutzman, and BJ Sollami. Carbon dioxide solubility in water. *Industrial & Engineering Chemistry Chemical & Engineering Data Series*, 1(1):92–95, 1956.

Zhenhao Duan, Nancy Møller, and John H Weare. An equation of state for the ch$_4$-co$_2$-h$_2$o system: I. pure systems from 0 to 1000deg c and 0 to 8000 bar. *Geochimica et Cosmochimica Acta*, 56(7):2605–2617, 1992.

Zhenhao Duan, Nancy Møller, and John H Weare. Equation of state for the nacl-h$_2$o-co$_2$ system: prediction of phase equilibria and volumetric properties. *Geochimica et Cosmochimica Acta*, 59(14):2869–2882, 1995.

Zhenhao Duan, Rui Sun, Rong Liu, and Chen Zhu. Accurate thermodynamic model for the calculation of h$_2$s solubility in pure water and brines. *Energy & Fuels*, 21(4):2056–2065, 2007.

Robert M Enick and Scott M Klara. Co2 solubility in water and brine under reservoir conditions. *Chemical Engineering Communications*, 90(1):23–33, 1990.

Yaqing Fan. *Chemical Reaction Modeling in a Subsurface Flow Simulator with Application to In-Situ Upgrading and CO_2 mineralization.* PhD thesis, Stanford, 2010.

Robert Minard Garrels and Charles Louis Christ. *Solutions, Minerals, and Equilibria.* Jones and Bartlett Publishers, 1990.

Rajeev Gautam and Warren D. Seider. Computation of phase and chemical equilibrium: Part II. phase-splitting. *AIChE Journal*, 25(6):999–1006, 1979a.

Rajeev Gautam and Warren D Seider. Computation of phase and chemical equilibrium: Part ii. phase-splitting. *AIChE Journal*, 25(6):999–1006, 1979b.

J Willard Gibbs. *The Collected Works of J. Willard Gibbs, Volume I: Thermodynamics*. Yale University Press, 1928.

Josiah Willard Gibbs. *On the equilibrium of heterogeneous substances*. Connecticut Academy of Arts and Sciences, 1877.

E Glueckauf. Contributions to the theory of chromatography. *Proceedings of the Royal Society of London*, A186:35–57, 1946.

E Glueckauf. Theory of chromatography. vii. the general theory of two solutes following non-linear isotherms. *Discussions of the Faraday Society*, 7:12–25, 1949.

Charles E Harvie and John H Weare. The prediction of mineral solubilities in natural waters: the na-k-mg-ca-cl-so_4-h_2o system from zero to high concentration at 25°c. *Geochimica et Cosmochimica Acta*, 44(7):981–997, 1980.

Charles E Harvie, Hans P Eugster, and John H Weare. Mineral equilibria in the six-component seawater system, na-k-mg-ca-so_4-cl-h_2o at 25 c. ii: Compositions of the saturated solutions. *Geochimica et Cosmochimica Acta*, 46(9):1603–1618, 1982.

Charles E Harvie, Nancy Møller, and John H Weare. The prediction of mineral solubilities in natural waters: The na-k-mg-ca-h-cl-so_4-oh-hco_3-co_3-co_2-h_2o system to high ionic strengths at 25 c. *Geochimica et Cosmochimica Acta*, 48:723–751, 1984.

Charles E. Harvie, Jerry P. Greenberg, and John H. Weare. A chemical equilibrium algorithm for highly non-ideal multiphase systems: Free energy minimization. *Geochimica et Cosmochimica Acta*, 51(5):1045 – 1057, 1987a.

Charles E Harvie, Jerry P Greenberg, and John H Weare. A chemical equilibrium algorithm for highly non-ideal multiphase systems: free energy minimization. *Geochimica et Cosmochimica Acta*, 51(5):1045–1057, 1987b.

Shiliang He and John W Morse. The carbonic acid system and calcite solubility in aqueous na-k-ca-mg-cl-so_4 solutions from 0 to 90°c. *Geochimica et Cosmochimica Acta*, 57(15):3533–3554, 1993.

F. Helfferich. Theory of multicomponent, multiphase displacement in porous media. *SPE Journal*, 21(1):51–62, 1981.

F.G. Helfferich and G. Klein. *Multicomponent chromatography: theory of interference*, volume 4. M. Dekker, 1970.

Harold C Helgeson and David H Kirkham. Theoretical prediction of thermodynamic properties of aqueous electrolytes at high pressures and temperatures. iii. equation of state for aqueous species at infinite dilution. *American Journal of Science*, 276(2), 1976.

IEA. Energy technology perspectives: Fact sheet - the blue scenario. Technical report, Paris, France, 2008.

IHS. The international exploration and production (e & p) database. Technical report, http://www.ihs.com, May 2009.

F Jalali and JD Seader. Homotopy continuation method in multi-phase multi-reaction equilibrium systems. *Computers & Chemical Engineering*, 23(9): 1319 – 1331, 1999.

Farhang Jalali, J.D. Seader, and Saeed Khaleghi. Global solution approaches in equilibrium and stability analysis using homotopy continuation in the complex domain. *Computers & Chemical Engineering*, 32(10):2333 – 2345, 2008.

James W Johnson, Eric H Oelkers, and Harold C Helgeson. Supcrt92: A software package for calculating the standard molal thermodynamic properties of minerals, gases, aqueous species, and reactions from 1 to 5000 bar and 0 to 1000 c. *Computers & Geosciences*, 18(7):899–947, 1992.

Aboulghasem Kazemi Nia Korrani, Mojdeh Delshad, Kamy Sepehrnoori, et al. A novel mechanistic approach for modeling low salinity water injection. In *SPE Annual Technical Conference and Exhibition*. Society of Petroleum Engineers, 2013.

Aboulghasem Kazemi Nia Korrani, Gary Russell Jerauld, Kamy Sepehrnoori, et al. Coupled geochemical-based modeling of low salinity waterflooding.

In *SPE Improved Oil Recovery Symposium*. Society of Petroleum Engineers, 2014.

MB King, A Mubarak, JD Kim, and TR Bott. The mutual solubilities of water with supercritical and liquid carbon dioxides. *The Journal of Supercritical Fluids*, 5(4):296–302, 1992.

Theo Klaver and Eric Geers. Development of highly contaminated gas & oil fields, breakthrough co_2/h_2s separation technologies. In *Asia Pacific Oil and Gas Conference and Exhibition*, 2007.

Gerhard Klein, Daniel Tondeur, and Theodore Vermeulen. Multicomponent ion exchange in fixed beds. general properties of equilibrium systems. *Industrial & Engineering Chemistry Fundamentals*, 6(3):339–351, 1967.

Donald K. Knuth. *The TEXbook*. Addison-Wesley, 1984.

Diana Koschel, Jean-Yves Coxam, and Vladimir Majer. Enthalpy and solubility data of h_2s in water at conditions of interest for geological sequestration. *Industrial & Engineering Chemistry Research*, 46(4):1421–1430, 2007.

Larry W Lake. *Enhanced oil recovery*. Old Tappan, NJ; Prentice Hall Inc., 1989.

Larry W Lake, Steven L Bryant, and Aura N Araque-Martinez. *Geochemistry and fluid flow*, volume 7. Access Online via Elsevier, 2003.

Leslie Lamport. *LaTeX: A document preparation system*. Addison-Wesley, 2nd edition, 1994.

Peter D Lax. Hyperbolic systems of conservation laws ii. *Communications on Pure and Applied Mathematics*, 10(4):537–566, 1957.

Jong Ii Lee and Alan E Mather. Solubility of hydrogen sulfide in water. *Berichte der Bunsengesellschaft für physikalische Chemie*, 81(10):1020–1023, 1977.

Randall J LeVeque. *Numerical Methods for Conservation Laws.* Birkhäuser Verlag AG, 1994.

GN Lewis and Merle Randall. *Thermodynamics, revised by K.S. Pitzer and L. Brewer*. McGraw-Hill, New York, 1961.

Li Li, Catherine A Peters, and Michael A Celia. Upscaling geochemical reaction rates using pore-scale network modeling. *Advances in Water Resources*, 29(9):1351–1370, 2006a.

Li Li, Catherine A Peters, and Michael A Celia. Applicability of averaged concentrations in determining geochemical reaction rates in heterogeneous porous media. *American Journal of Science*, 307(10):1146–1166, 2007.

Shiguang Li, John L Falconer, and Richard D Noble. Improved sapo-34 membranes for co_2/ch_4 separations. *Advanced Materials*, 18(19):2601–2603, 2006b.

Yau-Kun Li and Long X Nghiem. Phase equilibria of oil, gas and water/brine mixtures from a cubic equation of state and henry's law. *The Canadian Journal of Chemical Engineering*, 64(3):486–496, 1986.

Peter C Lichtner, Steve Yabusaki, Karsten Pruess, and Carl I Steefel. Role of competitive cation exchange on chromatographic displacement of cesium in the vadose zone beneath the hanford s/sx tank farm. *Vadose Zone Journal*, 3(1):203–219, 2004.

Chan Lu and Peter C. Lichtner. PFLOTRAN Massively Parallel 3D simulator for CO_2 sequestration in geologic media. In *Fourth Annual Conference on Carbon Capture and Sequestration DOE/NETL*, 2005.

Michael Luckas, Klaus Lucas, and Hans Roth. Computation of phase and chemical equilibria in flue-gas/water systems. *AIChE Journal*, 40(11):1892–1900, 1994.

F Mittelbach M Goosens and A Samarin. *The LaTeXCompanion*. Addison-Wesley, 1994.

Dean Joseph Mangone. *Multiple phase behavior of carbon dioxide and hydrocarbon systems including the effects of water*. PhD thesis, University of Pittsburgh, 1985.

Maria Goeppert Mayer. Nuclear configurations in the spin-orbit coupling model. i. empirical evidence. *Physical Review*, 78(1):16, 1950.

Marco Mazzotti and Arvind Rajendran. Equilibrium theory-based analysis of nonlinear waves in separation processes. *Annual Review of Chemical and Biomolecular Engineering*, (0), 2013.

Conor M. Mcdonald and Christodoulos A. Floudas. Global optimization for the phase and chemical equilibrium problem: Application to the NRTL equation. *Comput. Chem. Eng*, 19:1111–1139, 1994.

Conor M McDonald and Christodoulos A Floudas. Global optimization and analysis for the gibbs free energy function using the unifac, wilson, and asog equations. *Industrial & Engineering Chemistry Research*, 34(5):1674–1687, 1995.

Conor M McDonald and Christodoulos A Floudas. Glopeq: A new computational tool for the phase and chemical equilibrium problem. *Computers & Chemical Engineering*, 21(1):1–23, 1996.

Michael L. Michelsen. The isothermal flash problem. part i. stability. *Fluid Phase Equilibria*, 9(1):1 – 19, 1982.

Richard Tran Mills, Chuan Lu, Peter C Lichtner, and Glenn E Hammond. Simulating subsurface flow and transport on ultrascale computers using PFLOTRAN. *Journal of Physics: Conference Series*, 78(1):012051, 2007.

Saeedeh Mohebbinia. *Advanced equation of state modeling for compositional simulation of gas floods*. PhD thesis, The University of Texas at Austin, 2013.

Nancy Møller. The prediction of mineral solubilities in natural waters: A chemical equilibrium model for the na-ca-cl-so¡ sub¿ 4¡/sub¿-h¡ sub¿ 2¡/sub¿ o system, to high temperature and concentration. *Geochimica et Cosmochimica Acta*, 52(4):821–837, 1988.

Nancy Møller, Jerry P Greenberg, and John H Weare. Computer modeling for geothermal systems: predicting carbonate and silica scale formation, co2 breakout and h2s exchange. *Transport in porous media*, 33(1-2):173–204, 1998.

L. Nghiem, V. Shrivastava, B. Kohse, M. Hassam, and C. Yang. Simulation and optimization of trapping processes for co_2 storage in saline aquifers. *Journal of Canadian Petroleum Technology*, 49(8):15–22, 2010.

Darrell Kirk Nordstorm and James L Munoz. *Geochemical Thermodynamics*. Blackwell Scientific Publications, 1986.

P Scott Northrop and Jaime A Valencia. The cfz^{TM} process: A cryogenic method for handling high co_2 and h_2s gas reserves and facilitating geosequestration of co_2 and acid gases. *Energy Procedia*, 1(1):171–177, 2009.

Ryosuke Okuno. *Modeling of Multiphase Behavior for Gas Flooding Simulation*. PhD thesis, The University of Texas at Austin, 2011.

Ryosuke Okuno, Russell T Johns, Kamy Sepehrnoori, et al. Application of a reduced method in compositional simulation. *SPE Journal*, 15(01):39–49, 2010.

Robin Ozah, Srivatsan Lakshminarasimhan, Gary Pope, Kamy Sepehrnoori, and Steven Bryant. Numerical simulation of the storage of pure co_2 and co_2-h_2s gas mixtures in deep saline aquifers. In *SPE Annual Technical Conference and Exhibition*, 2005.

Huanquan Pan, Abbas Firoozabadi, et al. Complex multiphase equilibrium calculations by direct minimization of gibbs free energy by use of simulated annealing. *SPE Reservoir Evaluation & Engineering*, 1(01):36–42, 1998.

AZ Panagiotopoulos and RC Reid. New mixing rule for cubic equations of state for highly polar, asymmetric systems. In *ACS Symp. Ser*, volume 300, pages 571–582. ACS Publications, 1986.

D.L. Parkhust and C.A.J. Appelo. *Description of input and examples for PHREEQC version 3 - A computer program for speciation, batch-reaction, one-dimensional transport, and inverse geochemical calculations*, volume 6. U.S. Geological Survey Techniques and Methods, 2013.

DY Peng and DB Robinson. *Two- and Three-Phase Equilibrium Calculations for Coal Gasification and Related Processes*, chapter 21, pages 393–414. ACS Publications, 1980. doi: 10.1021/bk-1980-0133.ch020. URL `http://pubs.acs.org/doi/abs/10.1021/bk-1980-0133.ch020`.

Yeow Peng Lee, Gade Pandu Rangaiah, and Rein Luus. Phase and chemical equilibrium calculations by direct search optimization. *Computers & Chemical Engineering*, 23(9):1183–1191, 1999.

M Peszynska and Shuyu Sun. Multiphase reactive transport module TRCHEM in IPARS. Technical report, TICAM, The University of Texas at Austin, 2001.

Kenneth S Pitzer. Thermodynamics of electrolytes. i. theoretical basis and general equations. *The Journal of Physical Chemistry*, 77(2):268–277, 1973.

Kenneth S Pitzer and Janice J Kim. Thermodynamics of electrolytes. iv. activity and osmotic coefficients for mixed electrolytes. *Journal of the American Chemical Society*, 96(18):5701–5707, 1974.

Kenneth S Pitzer and Guillermo Mayorga. Thermodynamics of electrolytes. ii. activity and osmotic coefficients for strong electrolytes with one or both ions univalent. *The Journal of Physical Chemistry*, 77(19):2300–2308, 1973.

Kenneth S Pitzer and Guillermo Mayorga. Thermodynamics of electrolytes. iii. activity and osmotic coefficients for 2–2 electrolytes. *Journal of Solution Chemistry*, 3(7):539–546, 1974.

G A Pope, L W Lake, and F G Helfferich. Cation exchange in chemical flooding: Part 1–basic theory without dispersion. *Society of Petroleum Engineers Journal*, 18(6):418–434, 1978a.

GA Pope, LW Lake, and FG Helfferich. Cation exchange in chemical flooding: Part 1–basic theory without dispersion. *SPE Journal*, 18(6):418–434, 1978b.

GA Pope, RC Nelson, et al. A chemical flooding compositional simulator. *Society of Petroleum Engineers Journal*, 18(05):339–354, 1978c.

John M Prausnitz and PL Chueh. *Computer Calculations for High-Pressure Vapor-Liquid Equilibria*. Prentice-Hall Englewood Cliffs, NJ, 1968.

John M Prausnitz, Rudiger N Lichtenthaler, and Edmundo Gomes de Azevedo. *Molecular Thermodynamics of Fluid-Phase Equilibria*. Prentice Hall, 1998.

CF Prutton and RL Savage. The solubility of carbon dioxide in calcium chloride-water solutions at 75, 100, 120 c and high pressures. *Journal of the American Chemical Society*, 67(9):1550–1554, 1945.

HH Rachford Jr and JD Rice. Procedure for use of electronic digital computers in calculating flash vaporization hydrocarbon equilibrium. *Journal of Petroleum Technology*, 4(10):327–328, 1952.

Henri Renon and John M Prausnitz. Local compositions in thermodynamic excess functions for liquid mixtures. *AIChE Journal*, 14(1):135–144, 1968.

H. K. Rhee and Neal R Amundson. An analysis of an adiabatic adsorption column: Part 1. theoretical development. *The Chemical Engineering Journal*, 1(3):241–254, 1970.

H. K. Rhee, BF Bodin, and NR Amundson. A study of the shock layer in equilibrium exchange systems. *Chemical Engineering Science*, 26(10):1571–1580, 1971.

H. K. Rhee, Edmund D Heerdt, and Neal R Amundson. An analysis of an adiabatic adsorption column: Part iii: Adiabatic adsorption of two solutes. *The Chemical Engineering Journal*, 3:22–34, 1972.

H. K. Rhee, R. Aris, and N.R. Amundson. *First-order partial differential equations*, volume 2. Dover Publications, 2001.

W. Rossen, A. Venkatraman, R. Johns, K. Kibodeaux, H. Lai, and N. Tehrani. Fractional flow theory applicable to non-newtonian behavior in eor processes. *Transport in Porous Media*, 89:213–236, 2011. ISSN 0169-3913.

Frederick Dominic Rossini, Donald D Wagman, and William H Evans. *Selected values of chemical thermodynamic properties*. US Government Printing Office Washington, DC, 1952.

Fredrik Saaf. *A Study of Reactive Transport Phenomena in Porous Media*. PhD thesis, Rice, 1996.

Stanley I Sandler. *Chemical, biochemical, and engineering thermodynamics*, volume 4. John Wiley & Sons Hoboken, NJ, 2006.

Véronique Savary, Gilles Berger, Michel Dubois, Jean-Claude Lacharpagne, Alain Pages, Sylvain Thibeau, and Marc Lescanne. The solubility of CO_2 + H_2S mixtures in water and 2M NaCl at 120 c and pressures up to 35 MPa. *International Journal of Greenhouse Gas Control*, 10:123–133, 2012.

FT Selleck, LT Carmichael, and BH Sage. Phase behavior in the hydrogen sulfide-water system. *Industrial & Engineering Chemistry*, 44(9):2219–2226, 1952.

Everett L Shock, Harold C Helgeson, and Dimitri A Sverjensky. Calculation of the thermodynamic and transport properties of aqueous species at high

pressures and temperatures: Standard partial molal properties of inorganic neutral species. *Geochimica et Cosmochimica Acta*, 53(9):2157–2183, 1989.

Jeffrey V. Smith, Ronald W. Missen, and William R. Smith. General optimality criteria for multiphase multireaction chemical equilibrium. *AIChE Journal*, 39(4):707–710, 1993a.

Jeffrey V Smith, Ronald W Missen, and William R Smith. General optimality criteria for multiphase multireaction chemical equilibrium. *AIChE Journal*, 39(4):707–710, 1993b.

William Robert Smith and Ronald William Missen. *Chemical Reaction Equilibrium Analysis: Theory and Algorithms*. Wiley New York, 1982a.

W.R. Smith and R.W. Missen. *Chemical reaction equilibrium analysis: theory and algorithms*. Wiley New York, 1982b.

Kyoo Y Song and Riki Kobayashi. The water content of ethane, propane and their mixtures in equilibrium with liquid water or hydrates. *Fluid phase equilibria*, 95:281–298, 1994.

Ingolf Soreide and Curtis H Whitson. Peng-robinson predictions for hydrocarbons, co_2, n_2 and h_2s with pure water and naci brine. *Fluid Phase Equilibria*, 77:217–240, 1992.

Ronald J Spencer, Nancy Møller, and John H Weare. The prediction of mineral solubilities in natural waters: A chemical equilibrium model for the

na-k-ca-mg- cl-so$_4$-h$_2$o system at temperatures below 25 c. *Geochimica et Cosmochimica Acta*, 54(3):575–590, 1990.

Carl I. Steefel and Kerry T. B. MacQuarrie. *Reactive transport in porous media*, volume 34. Reviews in Mineralogy, 1996.

Carl I Steefel and Kerry TB MacQuarrie. Approaches to modeling of reactive transport in porous media. *Reviews in Mineralogy and Geochemistry*, 34(1): 85–129, 1996.

Carl I Steefel, Donald J DePaolo, and Peter C Lichtner. Reactive transport modeling: An essential tool and a new research approach for the earth sciences. *Earth and Planetary Science Letters*, 240(3):539–558, 2005.

R Stryjek and JH Vera. Prsv: An improved peng-robinson equation of state for pure compounds and mixtures. *The Canadian Journal of Chemical Engineering*, 64(2):323–333, 1986.

Amy C. Sun and Warren D. Seider. Homotopy-continuation method for stability analysis in the global minimization of the gibbs free energy. *Fluid Phase Equilibria*, 103(2):213 – 249, 1995.

Sukune Takenouchi and George C Kennedy. The solubility of carbon dioxide in nacl solutions at high temperatures and pressures. *American Journal of Science*, 263(5):445–454, 1965.

Klaus Tödheide and EU Franck. Das zweiphasengebiet und die kritische kurve im system kohlendioxid–wasser bis zu drucken von 3500 bar. *Zeitschrift für Physikalische Chemie*, 37(5_6):387–401, 1963.

Daniel Tondeur and Gerhard Klein. Multicomponent ion exchange in fixed beds. constant-separation-factor equilibrium. *Industrial & Engineering Chemistry Fundamentals*, 6(3):351–361, 1967.

John A Trangenstein. Customized minimization techniques for phase equilibrium computations in reservoir simulation. *Chemical Engineering Science*, 42(12):2847–2863, 1987.

Albert J Valocchi, Paul V Roberts, George A Parks, and Robert L Street. Simulation of the transport of ion-exchanging solutes using laboratory-determined chemical parameter values. *Ground Water*, 19(6):600–607, 1981a.

Albert J Valocchi, Robert L Street, and Paul V Roberts. Transport of ion-exchanging solutes in groundwater: Chromatographic theory and field simulation. *Water Resources Research*, 17(5):1517–1527, 1981b.

Alf J. van der Poorten. Some problems of recurrent interest. Technical Report 81-0037, School of Mathematics and Physics, Macquarie University, North Ryde, Australia 2113, August 1981.

HP van Kemenade and JJH Brouwers. Hydrocarbon recovery by condensed

rotational separation. *Journal of Petroleum Exploration and Production Technology*, 2(1):49–56, 2012.

Andreas Voegelin, Vijay M Vulava, Florian Kuhnen, and Ruben Kretzschmar. Multicomponent transport of major cations predicted from binary adsorption experiments. *Journal of Contaminant Hydrology*, 46(3-4):319–338, 2000.

M.P. Walsh and L.W. Lake. Applying fractional flow theory to solvent flooding and chase fluids. *Journal of Petroleum Science and Engineering*, 2(4):281–303, 1989.

Stanislaw K. Wasylkiewicz, Lakshmi N. Sridhar, Michael F. Doherty, and Michael F. Malone. Global stability analysis and calculation of liquidliquid equilibrium in multicomponent mixtures. *Industrial & Engineering Chemistry Research*, 35(4):1395–1408, 1996.

William B White, Selmer Martin Johnson, and George Bernard Dantzig. Chemical equilibrium in complex mixtures. *The Journal of Chemical Physics*, 28(5):751, 1958.

R Wiebe. The binary system carbon dioxide-water under pressure. *Chemical Reviews*, 29(3):475–481, 1941.

Tianfu Xu, Nicolas Spycher, Eric Sonnenthal, Liange Zheng, and Karsten Pruess. *TOUGHREACT User's Guide: A Simulation Program for Non-*

isothermal Multiphase Reactive Geochemical Transport in Variably Saturated Geologic Media, Version 2.0. Lawrence Berkeley National Laboratory, 2012.

Vita

Ashwin Venkatraman was born in Melmangalam, Periyakulam, India. He grew up in the city of Bombay (now Mumbai) in India. He received a Dual Degree, both Bachelors and Masters of Technology, in Chemical Engineering from the Indian Institute of Technology (IIT), Bombay in 2004. Following graduation, he joined BG E & P at their offshore operations in the Panna-Mukta field off the coast of Bombay. He joined Shell in 2006 and worked in various field development roles of process design, concept engineering as well as upstream technology research in Rijswijk, The Netherlands. After working in the oil and gas industry for over five years, Ashwin decided to get back to academics and pursue a PhD. He married Dr. Neeraja Swaminathan in 2010.

Email address: ashwin.venkatraman@gmail.com;
ashwin.venkatraman@utexas.edu

This dissertation was typeset with LaTeX[†] by the author.

[†]LaTeX is a document preparation system developed by Leslie Lamport as a special version of Donald Knuth's TeX Program.